International Institute for
Applied Systems Analysis
IIASA www.iiasa.ac.at

Thousands of Data at a Glance: Shaded Contour Maps of Demographic Surfaces

Vaupel, J.W., Gambill, B.A. and Yashin, A.I.

IIASA Research Report
July 1987

Thousands of Data at a Glance: Shaded Contour Maps of Demographic Surfaces

James W. Vaupel, Bradley A. Gambill, and Anatoli I. Yashin
International Institute for Applied Systems Analysis

RR-87-16
July 1987

Please address correspondence concerning this report to:
Prof. James W. Vaupel, Humphrey Institute of Public Affairs,
University of Minnesota, 301 19th Avenue South,
Minneapolis, Minnesota 55455, USA

International Institute for Applied Systems Analysis
Laxenburg, Austria

International Standard Book Number 3-7045-0079-8

Cover design by Martin Schobel

Printed by Novographic, Vienna, Austria

Summary

Contour maps are useful for displaying demographic surfaces, including surfaces of population levels and fertility, marriage, and mortality rates. Most often the surfaces are defined over age and time, but other dimensions can be used such as life expectancy or population growth rate. This research report presents a bouquet of contour maps to suggest the broad potential of their use in demographic studies. The maps presented range from maps of Italian mortality, French population levels, and US birth rates, to maps of Coale and Demeny's and Brass's model life tables. The value of the maps lies in their substantive import: by giving demographers visual access to population surfaces, the maps can help demographers uncover and understand population patterns. The text of the research report adumbrates some of these patterns and discusses the use of contour maps in exploratory data analyses and model building, including the use of maps of residuals in fitting models to data.

Foreword

At one time the limits of demographic research were set by the data available. Some results could be obtained by analysis of birth and death registrations and censuses, but only for the few countries for which these were available and for the few breakdowns that were permitted by the tabulating equipment in existence. With so little data available, analysis by hand methods was perfectly feasible.

Now there are masses of data, so the problem has shifted: the due consideration and interpretation of data is a major difficulty. Under the guidance of James Vaupel and Anatoli Yashin methods have been developed that provide interpretation at a glance. In respect of Sweden, for instance, mortality data are available for some 85 ages for more than two centuries. To look at 20000 numbers and draw out their meaning is a major research enterprise in itself. Yet with the methods used in this research report all that information is contained in a single contour map.

Of course, the method has antecedents that go all the way back to Descartes' insight that mathematical functions are represented on a plane. From that it is only a step to showing empirical curves on a plane, and then to go on to three dimensions, as these contour maps do. Stages in this progression were diagrams by Perozzo and Lexis that show a population as lines on the age–time plane. Arthur and Vaupel (1984), building on Preston and Coale (1982), generalized the Lexis diagram to a Lexis surface.

The material that follows makes ingenious use of computation and takes advantage of many antecedent forms of diagram. It is presented in this research report neither for its originality as a method of representation, nor for the exhibition of programming skill by Bradley Gambill. The drawings here appeal by reason of their substantive interest. Whether mortality improvement takes place by cohorts or by periods; at what historical periods has the fall in mortality been most striking; was the baby boom after World War II due to more births to women in the prime ages, say the 20s, or was it due to longer continuance of childbearing by women in their 30s? These and many other issues are raised in the text, but that text is suggestive rather than exhaustive, and the maps can well be used as a basis for further research.

Nathan Keyfitz
Leader
Population Program
International Institute for Applied Systems Analysis

Acknowledgments

Four research assistants at IIASA, Alan J. Bernstein, Ann E. Gowan, Mark Harris, and John M. Owen, made substantial contributions to this paper, both by helping prepare the data bases used and by providing various useful suggestions. Martina Joestl-Segalla ably assisted us in producing the maps, and Margaret Kerr helped with some programming. We also thank Nathan Keyfitz, Graziella Caselli, W. Brian Arthur, Dianne Goodwin, Gustav Feichtinger, Jan Hoem, Wolfgang Lutz, Gun Stenflo, Michael A. Stoto, Waldo Tobler, Jacques Vallin, Andrew Foster, Nedka Gateva, Arno Kitts, Eva Lelievre, Lucky Tedrow, John Wilmoth, and Zeng Yi for their insightful comments and Susan Stock for her superb secretarial assistance.

Contents

List of Figures

(*a*) In color.
(*b*) In black and white.

Figure 6. US cohort fertility rates, with contour lines selectively placed from 0.001 to 0.25, and from age 14 to 49 and year of birth 1868 to 1966.

Figure 7. US fertility rates by current year and year of birth, with selected contour lines from 0.05 to 0.25, and from current year 1917 to 1980 and year of birth 1868 to 1966.

Figure 8. Chinese fertility rates, with contour lines selectively placed from 0.01 to 0.36, and from age 15 to 49 and year 1940 to 1981.

Figure 9. Finnish fertility rates, with contour lines selectively placed from 0.001 to 0.25, and from age 15 to 49 and year 1776 to 1978.

Figure 10. US birth rates:

(*a*) From year 1917 to 1980.
(*b*) From age 14 to 49.
(*c*) Three-dimensional perspective of US fertility rates for ages and years in *Figures 10*(*a*) and *10*(*b*).

Figure 11. High-quality three-dimensional plots of US fertility rates.

Figure 12. French population from age 0 to 79 and year 1851 to 1964:

(*a*) At each age and time, with contour lines from 100 000 to 800 000 at intervals of 50 000.
(b) Male relative to 1851 age-specific levels, with contour lines from 0.868 to 3.30 at multiples of 1.1.

Figure 13. Population of Sophia, Bulgaria, with contour lines from 9 000 to 121 000 at intervals of 8 000, and from age 0 to 85, projected from 1975 to 2049.

Figure 14. Italian male mortality rates relative to age-specific 1925 levels, with contour lines from 0.3 to 2.12 at multiples of 1.15, smoothed on a 5 × 5 square, and from age 0 to 79 and year 1870 to 1979.

Figure 15. US birth rates relative to age-specific 1980 levels, with contour lines from 0.8 to 5.66 at multiples of 1.15, and from age 14 to 49 and year 1917 to 1980.

Figure 16. Italian male mortality rates relative to infant mortality, with contour lines from 0.007 to 1.27 at multiples of 1.5, smoothed on a 5 × 5 square, and from age 0 to 79 and year 1870 to 1979.

(*a*) Male.
(*b*) Female.

Figure 24. Mortality rates relative to 1870 age-specific cohort levels, with contour lines from 0.1 to 1.283 at multiples of 1.2, smoothed on a 5 × 5 square, and from age 5 to 79 and year 1870 to 1978:

(*a*) Italian male.
(*b*) Italian female.
(*c*) Swedish male.
(*d*) Swedish female.
(*e*) English and Welsh male.
(*f*) English and Welsh female.

Figure 25. Italian female mortality rates divided by Italian male mortality rates, smoothed on a 5 × 5 square, and from age 0 to 79 and year 1870 to 1979:

(*a*) With contour lines at multiples of 1.1 from 0.513 to 1.95.
(*b*) With *selected* contour lines from 0.513 to 1.95.

Figure 26. French male mortality rates divided by Italian male mortality rates:

(*a*) With contour lines from 0.513 to 1.950 at multiples of 1.1, and from age 10 to 70 and year 1900 to 1960.
(*b*) As *Figure 26*(*a*), but smoothed on a weighted 5 × 5 square.

Figure 27. US fertility at parity 1 minus that at parity 2, with contour lines from −0.020 to 0.050 at intervals of 0.005, and from age 14 to 49 and year 1917 to 1980.

Figure 28. Belgian female population divided by Belgian male population, with contour lines selectively placed from 0.90 to 2.00, smoothed on a 5 × 5 square, with a grid, and from age 0 to 99 and year 1892 to 1977.

Figure 29. Chinese female first marriage rates:

(*a*) From age 15 to 35 and year 1950 to 1981.
(*b*) Smoothed and conditional.

Figure 30. English and Welsh male tuberculosis mortality rates, with contour lines from 0.000067 to 0.00385 at multiples of 1.5, and from age 0 to 79 and year 1861 to 1964.

Figure 31. Belgian female population for single year of age and time, with contour lines from 10 000 to 90 000 at intervals of 10 000, and from age 0 to 99 and year 1892 to 1977.

Thousands of Data at a Glance: Shaded Contour Maps of Demographic Surfaces

James W. Vaupel, Bradley A. Gambill, and Anatoli I. Yashin

1. Introduction

Shaded contour maps, which are widely used to depict spatial patterns, can be readily adapted to represent any surface that is defined over two dimensions. In particular, an array of demographic data can often be pictured in an intelligible and graphically striking way by a shaded contour map. The data might pertain to population levels or to rates of fertility, marriage, divorce, migration, morbidity, or mortality. Most often the data are structured by age and time—e.g., age-specific mortality rates over time—but in some cases other dimensions might be used, such as life expectancy or population growth rate.

Shaded contour maps permit visualization of population surfaces and offer a panoramic view impossible to obtain from the usual graphs of levels or rates at selected ages over time or at selected times over age. Furthermore, a contour map is often superior to a three-dimensional perspective plot in providing a clear, yet rich, representation of a demographic surface; it is usually difficult on a three-dimensional plot to discern the exact position of the surface above the age and time dimensions; also three-dimensional plots become confusing if made too detailed, especially when displayed on a moderately priced monitor or printer. Contour maps are particularly effective in highlighting patterns in the interaction of age, period, and cohort effects.

Shaded contour maps have been used only occasionally by demographers, in part because of the computational effort required, in part because of the lack of detailed data over long stretches of age and time, and in part because the advantages of working with population surfaces have not been fully appreciated. The use of shaded maps (without contour lines) is implicit in some of Lexis' (1875, 1880) original diagrams, as discussed by Dupaquier and Dupaquier (1985). In their influential study of changes in death rates over time, Kermack *et al.* (1934) superimpose on three of their tables some rough lines that are, in effect, contours of relative mortality. The pioneering study by Delaporte (1941) includes a set of contour maps that summarize mortality patterns in several European countries; Federici (1955) directs attention to Delaporte's contour maps in her survey of demographic methods.

Three recent developments should lead to greater use of demographic contour maps in the future. First, advances in computers, including the proliferation of inexpensive microcomputers, are providing demographers with convenient computational power. Second, extensive arrays of population statistics are being collected, published, and put on computer tapes and other storage devices; some of this data is by single year of age and time [e.g., Natale and Bernassola (1973), Vallin (1973), Heuser (1976, 1984), and Veys (1983)]. Finally, there is growing recognition among demographers of the usefulness of population surfaces. Demographers have drawn three-dimensional representations of population densities at least since Berg (1860), Perozzo (1880), and Lotka (1926, 1931), but it was only recently that an article by Arthur and Vaupel (1984), building on important research by Bennett and Horiuchi (1981) and Preston and Coale (1982), focused attention on the conceptual and analytical advantages of population surfaces.

Arthur and Vaupel (1984) introduced the phrase "Lexis surface" to describe a surface of demographic rates defined over age and time and we continue that usage here. Specific kinds of surfaces are called mortality surfaces, fertility surfaces, and so on, as appropriate, and we use interchangeably the equivalent phrases Lexis surface, population surface, and demographic surface as generic terms to describe any kind of surface pertaining to some population parameter. Because of this usage of Lexis surface and because, as noted above, the use of shaded contour maps of population surfaces is implicit in some of Lexis' diagrams, we use Lexis map as a synonym for shaded contour map.

This Report presents a bouquet of Lexis maps to suggest the broad potential of their use in population studies. The maps are of interest to demographers not because the computer programming required considerable virtuosity and creativity, especially to make it all work in 128K of memory on an ordinary IBM PC, nor because the technique of contour mapping is new [the technique is widely used in other applications and was systematically employed by Delaporte (1941) to analyze mortality patterns]. Rather, the value of the maps lies in their substantive import—they provide demographers with visual access to data that sheds light on significant patterns and trends in population levels, mortality rates, fertility rates, and other demographic parameters. In the following text we point to some of the more interesting substantive features of the maps, to suggest the worth of such maps in population studies.

Every picture presented deserves a thousand words or more of explanation and analysis and we hope that demographers will exploit the maps as a rich lode for research. Several steps in this direction have already been taken. Caselli *et al.* (1985a) analyzed Lexis maps of Italian mortality and Yi *et al.* (1985) analyzed Lexis maps of Chinese marriage and fertility rates. Gateva (1985) used Lexis maps to depict evolving trends in age-specific population levels in different regions of Bulgaria and Tremblay (1985) applied the maps in his study of linguistic mobility in Canada. In Wilmoth's (1985) study of age, period, and cohort effects in Italian female mortality, Lexis maps of various kinds of changes and residuals are intriguingly suggestive and revealing. Finally, in research just completed, Caselli *et al.* (1985b) compare patterns of French versus Italian mortality by using Lexis maps.

As a compilation of data, the demographic maps displayed in this research report might be compared with the demographic tables presented in Keyfitz and Flieger (1968) or Preston *et al.* (1972), and we hope that the maps will prove to be useful complements to such tabular compendiums. The typical map in this paper is based on more than 6000 data points, and some of the maps summarize considerably more data: *Figure 4* is based on 16 000 points and the small multiples in *Figure 22* present close to 50 000 data values. More than 80 distinct maps are included in this report, so that the maps collectively display roughly 500 000 values. Each page of tables in Keyfitz and Flieger (1968) contains about 625 statistics and there are about 650 pages of tables, amounting to roughly 400 000 values. Similarly, each page of tables in Preston *et al.* (1972) contains about 575 figures, on average, and there are more than 700 tables, for a grand total, once again, of roughly 400 000 values.

The maps presented here were produced by a computer program, dubbed LEXIS, that was developed by Gambill under Vaupel's direction at Duke University and at the International Institute for Applied Systems Analysis (IIASA). This program and a user's manual (Gambill *et al.*, 1985) can be obtained, at nominal charge, from the Population Program at IIASA. The program runs on an IBM PC or compatible personal computer with at least 128K of memory and with graphics capabilities. Available upon request to IIASA is a demonstration diskette that includes a sampling of Lexis maps; to use the diskette type DEMO at the DOS prompt >.

2. The Evolution of Italian Male Mortality

Figure 1 displays the contours of mortality for Italian males from age 0 to 79 and for years 1870–1979. The Lexis map is based on mortality rates, q, for single years of age and time assembled by Natale and Bernassola (1973) and Caselli *et al.* (1985a).* Thus the map, in the space of half a page or so, summarizes 80 × 110, or some 8800, mortality rates. For comparison, *Figure 1*(*a*) is in color and *Figure 1*(*b*) in black and white.

*These mortality rates are calculated on a cohort basis. That is, the data pertain to the probability that a person born in a particular calendar year and alive at exact age x will die before his or her x+1-st birthday. This type of probability refers to events that affect each single-year cohort at each age in two successive calendar years; for a discussion of this, see Vallin (1973) or Wunsch and Termote (1978). Standard calculations yield period life tables for two consecutive years from a diagonal reading of the cohort life tables. For our data, this allowed computation of period life tables from 1869–1870 to 1978–1979. For convenience in constructing mortality surfaces, we assumed that each simple-year mortality rate, ${}_1q$, calculated by this method described the height of the mortality surface at age x and at time y halfway through the two-year period, which we took to be January 1st, 1870 for the 1869–1870 period, and so on. Thus on our maps of Italian mortality, and on other maps that we based on cohort rates, the point on the horizontal axis labeled 1890, say, refers to January 1st, 1890. The mortality rate given at age 10, say, in 1890 is the mortality rate suffered by the cohort born not in 1880 but in 1879.

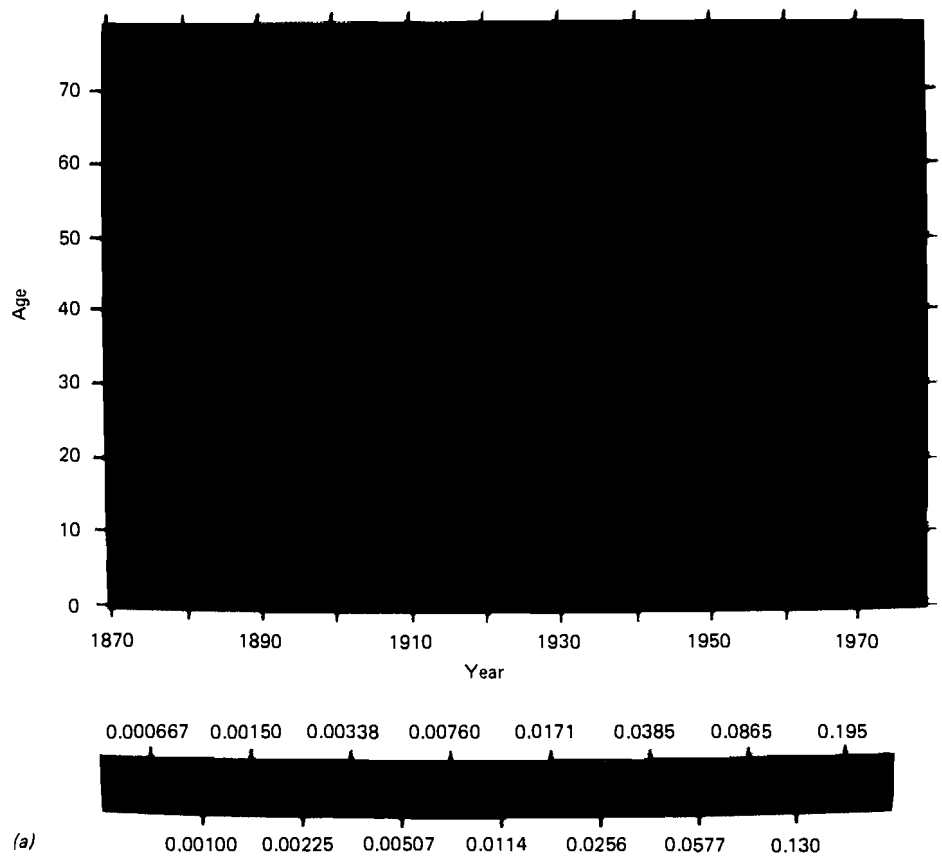

Figure 1(a). Italian male mortality rates (in color), with contour lines from 0.000667 to 0.195 at multiples of 1.5, and from age 0 to 79 and year 1870 to 1979.

Data are discrete, but a surface is continuous: the surface $q(x,y)$ can be defined by linearly interpolating between adjacent data points. The values of $q(x,y)$ give the height of the mortality surface over age x and time y. The lines on a contour map connect adjacent points on a surface that are of equal height; these lines are sometimes called level lines or isograms. In *Figure 1*, one of the level lines represents a mortality rate of about 11%: the line starts in 1870 at age 35 and ends in 1979 at age 56, indicating that 56-year-old Italian men in recent years faced the same chance of mortality as 35-year-olds faced about a century ago.

The major features of the evolution of Italian male mortality are apparent on the map. The devastation of World War I and the Spanish influenza epidemic appears as a sharp ridge of high mortality that interrupts the map around 1918. A lower ridge shows the effects of World War II. The general pattern over time is one of progress against mortality, rapid at younger ages and slow at advanced ages. The general pattern over age is equally clear: high mortality in infancy and again

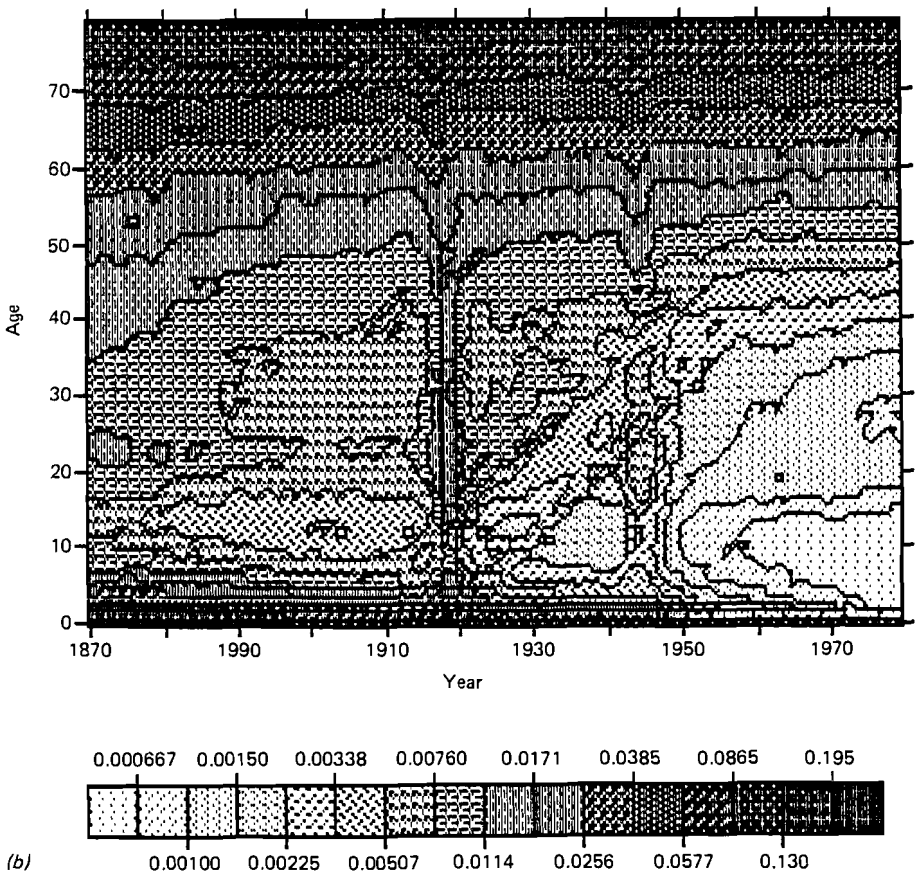

Figure 1(b). Italian male mortality rates (in black and white), with contour lines from 0.000667 to 0.195 at multiples of 1.5, and from age 0 to 79 and year 1870 to 1979.

among the elderly. The intriguing diagonal patterns suggest possible cohort effects, most notably during the 1920s and 1930s among the cohorts born around 1900: males in these cohorts, who were in their late teens and early 20s during World War I, may have been particularly debilitated by the war and its aftermath. Also notable are the various islands and peninsulas of high mortality that run across the map between ages 20 and 25: as discussed by Caselli *et al.* (1985a,b), these reflect various disruptive socioeconomic and political events in Italian history as well as the tendency for younger men to engage in reckless behavior.

3. Levels, Shades, and Grids

An important consideration when designing a contour map is how many different levels to use. The LEXIS computer program that we employed to draw the maps allows lines to be drawn at up to 15 levels, separating the surface into 16 tiers. Use of fewer lines sacrifices detail, whereas use of more lines tends to make the map less intelligible: 15 levels is a reasonable compromise, although the use of 10 or 20 levels might be considered. Delaporte (1941) draws lines at 19, 20, or 21 levels on his various maps of European mortality; a number of the figures in this research report, including *Figures 15* and *16*, use fewer than 15 levels. *Figure 1*(*c*) presents the contours of Italian male mortality using 10 levels rather than the 15 levels used in *Figure 1*(*b*).

Which specific elevations the contour lines should connect is a second important design decision. On mortality surfaces, where mortality rates might approach a minimum of the order of magnitude of 0.0001 and a maximum of 1, use of equally spaced lines—say at 0.01, 0.02, and so on up to 0.15—results in a map where the contours are clumped together at the youngest and oldest ages, with a largely empty expanse in-between. *Figure 1*(*d*) illustrates this for Italian male mortality. The map is far more informative when the lines are spread out at constant multiples—e.g., each line represents a level 50% higher than the previous line, as in *Figure 1*(*b*). Alternatively, a convenient scale can be used: Delaporte places his lines at levels of mortality of 1, 2, 3, ..., 9, 10, 12, 15, 20, 30, 50, 100, 150, 200, 250, 300, 350, and 400 per thousand, and in several figures in this paper, including *Figures 5* and *17*, contour lines are selectively placed at convenient levels.

Shifting the location of contour lines can make a difference in the appearance of a Lexis map, especially in the details. The map in *Figure 1*(*e*) provides an example. Compare, for instance, the region from 1920 to 1930 from age 20 to 30 on *Figure 1*(*b*) and (*e*).

Demographers often work with transformations, such as the log or logit, so it might seem reasonable to transform the surface $q(x,y)$ into the surface of, say, $\log q(x,y)$ and then to draw level lines at equal intervals on the transformed surface. If the transformation is monotonic, like the log or logit transformation, an identical contour map can be drawn by spacing the level lines at appropriately unequal intervals on the original surface. In the case of logarithms, the level lines should be at multiples of each other rather than being equally spaced. Thus, the map in *Figure 1*(*b*) can also be interpreted as depicting log mortality rates.

A key feature of the LEXIS computer program we developed is the shading of regions according to the height of the surface. The shading varies from light to dark as the surfaces rise from low to high levels of mortality. Such shading, which is time-consuming to do by hand but easy with the help of a computer, makes the overall pattern of a mortality surface more immediately comprehensible, especially if the map is viewed at a distance. At the same time, the details of small peaks and pits and of the twists and turns of the contour lines are still there to be scrutinized at close range. Literature, critics note, can be profitably read at different levels of understanding; we suggest the reader try viewing *Figure 1*(*b*) and perhaps some of the other figures in this paper at levels of 25 cm and 5 m.

Sometimes it is useful to draw a grid on a contour map so that the coordinates of various points can be conveniently located. In *Figure 1(f)* the map in *Figure 1(a)* is redrawn with a superimposed grid every 20 years of time and age. The grid detracts a bit from the underlying pattern—that is the price of adding additional information. Grids are also included in *Figures 2(a)* and *2(b)*, *18*, and *28*.

To see general trends it may be helpful to suppress the contour lines in a map of a population surface. In *Figure 1(g)* the map in *Figure 1(b)* is redrawn with shading but without lines. Alternatively, one could draw a traditional contour map with lines but without shading. *Figure 1(h)* displays such a map for Italian male mortality. The lines in this figure are not labeled, but they could be.

4. Smoothed Maps

It is useful to take a close look at the small blemishes isolated from contour lines on a Lexis map, because these spots indicate outliers—very localized peaks or pits—that might be due to erroneous data values. Consider, for instance, the spot in *Figure 1(b)* at about age 9 and year 1958: it turns out that this blemish was, indeed, produced by an error made in transcribing the Italian mortality data to a computer tape. (The error was corrected, but we have left the spot as an illustration.) On the other hand, the mark at about age 19 in 1962 represents a point where the mortality surface barely crosses a contour level, like the top of a sea mount that appears as a small island just rising above the level of the surrounding ocean.

In addition to these blemishes, some cluttered areas appear in *Figure 1(b)*. These represent virtual plateaus where the mortality surface is repeatedly crossing and recrossing a level line, or cliffs where mortality rates are rising or falling rapidly. To reduce this kind of noise and to suppress the details of local fluctuations so that the global patterns can be more clearly perceived, it may be useful to smooth a surface. Delaporte (1941) presented both raw and smoothed contour maps of mortality rates in various European countries: on his "adjusted" maps, he drew smooth contour lines based on his feeling for the data. We used a mechanistic, computer algorithm to produce the smoothed map shown in *Figure 1(i)*. In the smoothed map the height of the surface at age x in year y was replaced by the average of the 25 heights in the 5×5 square of points from $(x - 2)$ to $(x + 2)$ and from $(y - 2)$ to $(y + 2)$. On the edges of the map, where a full 5×5 array of data points is not available, the smoothing procedure averages the available data.

Instead of smoothing by averaging over a 5×5 square, a larger (or smaller) square might be used. In *Figure 1(j)* Italian male mortality is smoothed on an 11×11 square. Global patterns in this map are somewhat clearer than in *Figure 1(i)*, but some interesting local detail is lost and effects that are concentrated in time or age, such as infant mortality and mortality during the 1918 Spanish influenza epidemic, are smeared out.

A variety of alternative smoothing procedures might be used, including procedures that replace points by a weighted average of adjacent points, the weights diminishing with distance. *Figure 1(k)* presents a map of Italian male mortality smoothed by an algorithm in which the weights given to the points in a 5×5

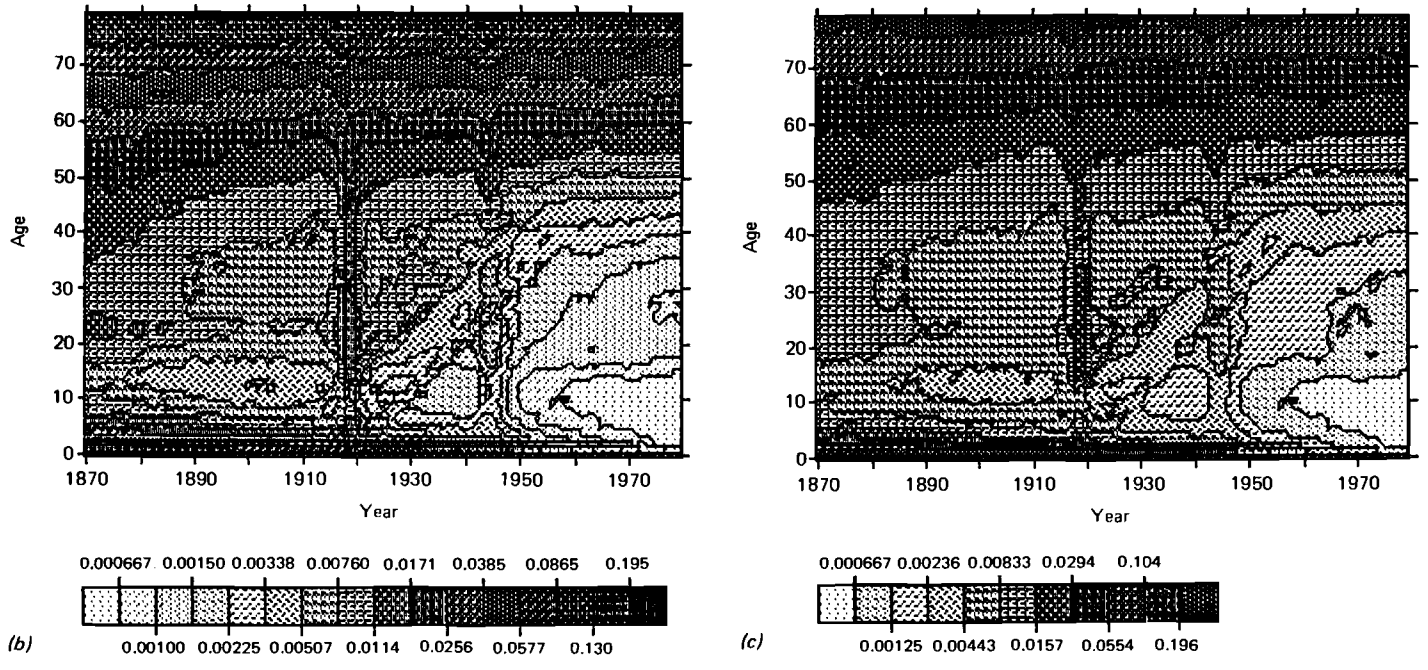

Figure 1. Italian male mortality rates: (*b*) (repeated) with contour lines from 0.000667 to 0.195 at multiples of 1.5, and from age 0 to 79 and year 1870 to 1979; (*c*) as *Figure 1(b)*, but with 10 contour lines from 0.000667 to 0.195.

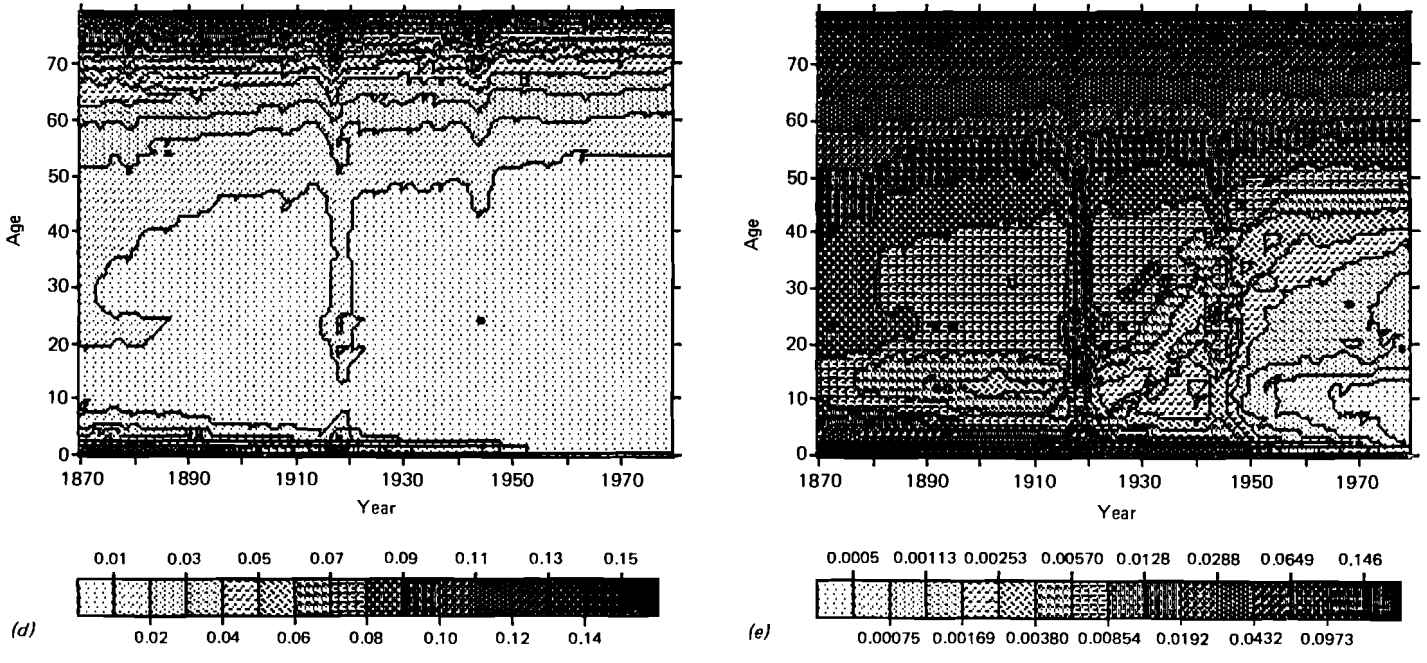

Figure 1. Italian male mortality rates: (*d*) as *Figure 1(b)*, but with evenly spaced contour lines from 0.01 to 0.15; (*e*) as *Figure 1(b)*, but with 15 contour lines starting at 0.0005.

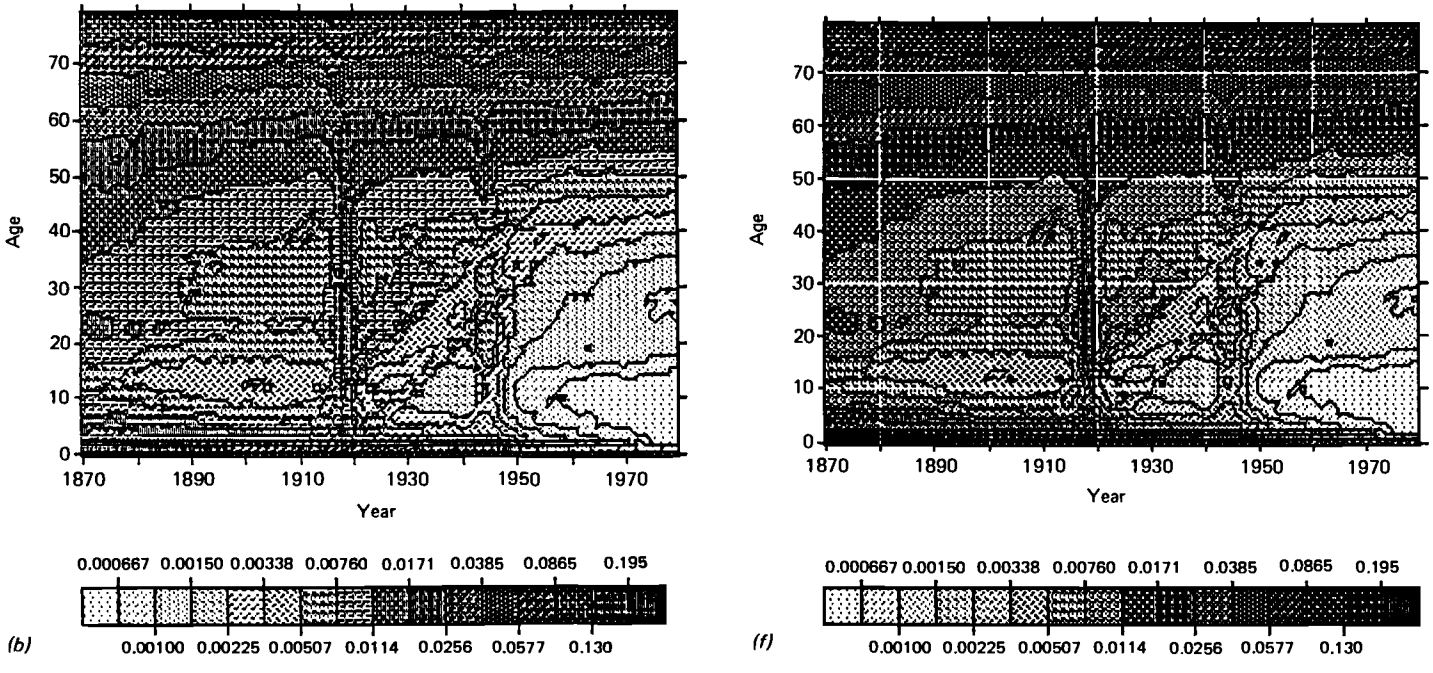

Figure 1. Italian male mortality rates: (*b*) (repeated) with contour lines from 0.000667 to 0.195 at multiples of 1.5, and from age 0 to 79 and year 1870 to 1979; (*f*) as *Figure 1(b)*, but with a grid.

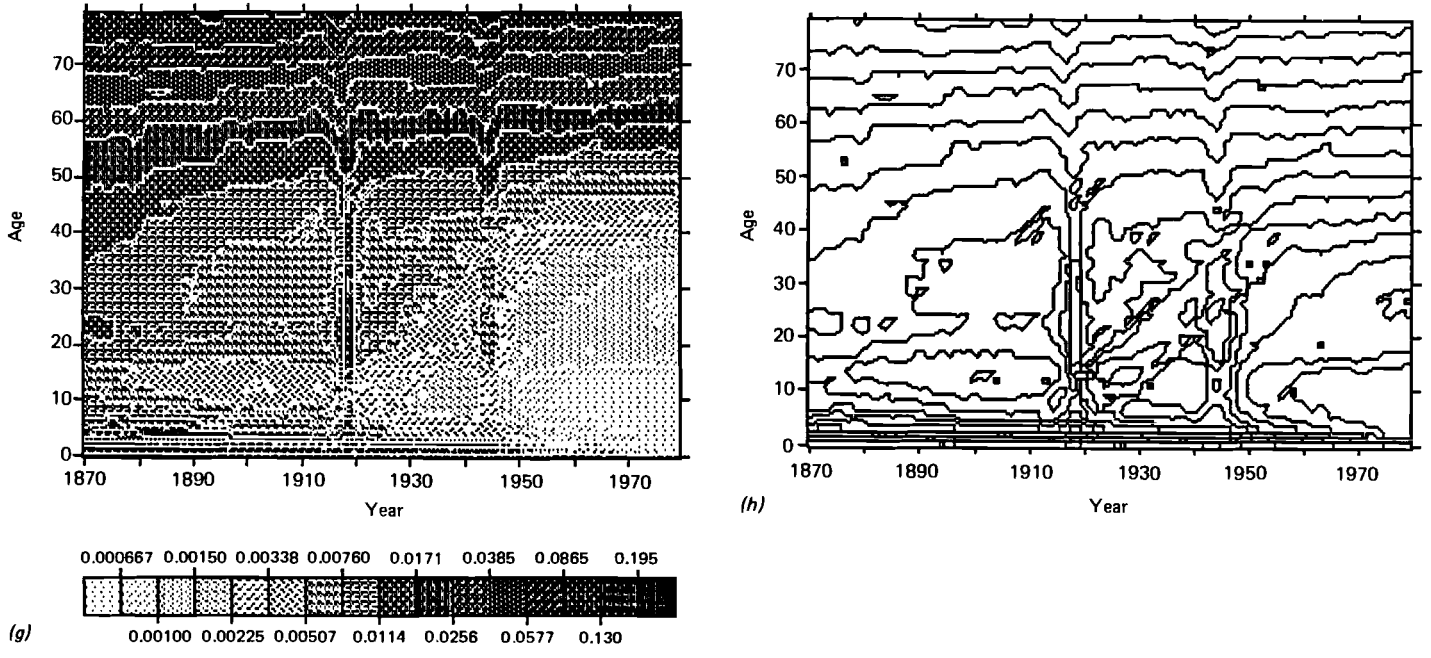

Figure 1. Italian male mortality rates: (*g*) as *Figure 1*(*b*), but without contour lines; (*h*) as *Figure 1*(*b*), but without shading.

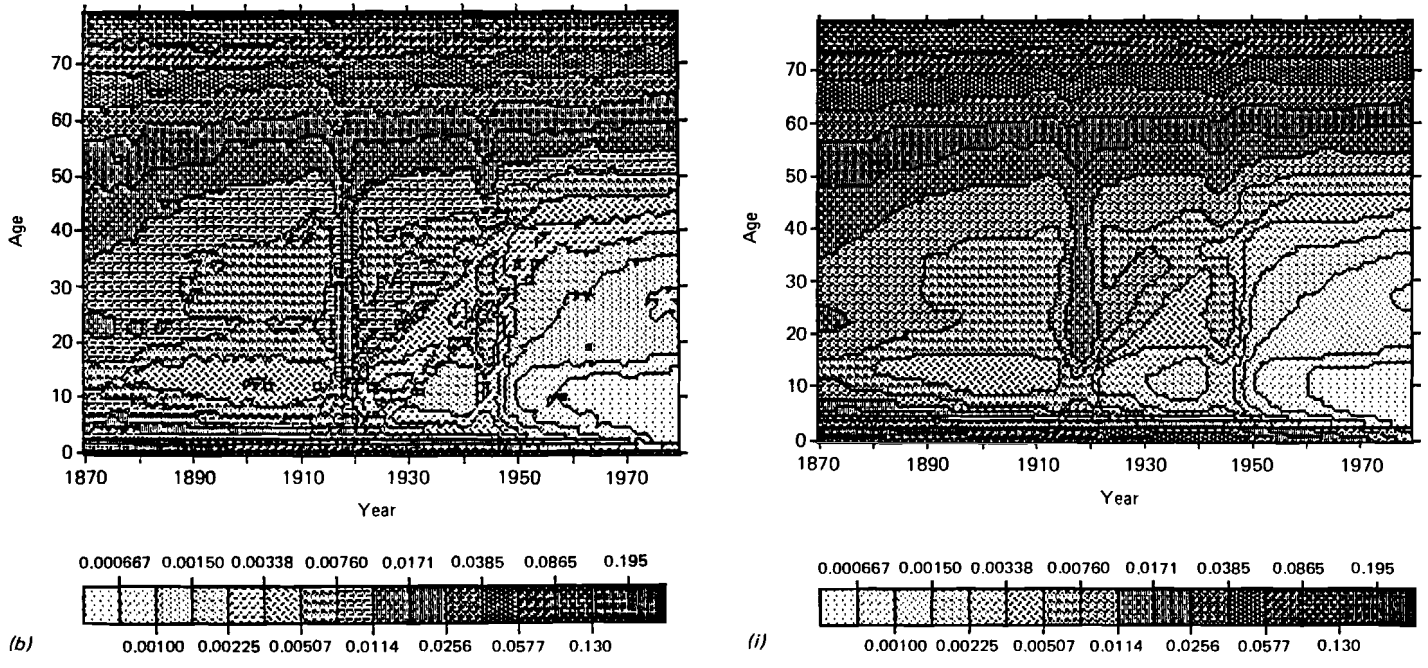

Figure 1. Italian male mortality rates: (*b*) (repeated) with contour lines from 0.000667 to 0.195 at multiples of 1.5, and from age 0 to 79 and year 1870 to 1979; (*i*) as *Figure 1(b)*, but smoothed on a 5 × 5 square.

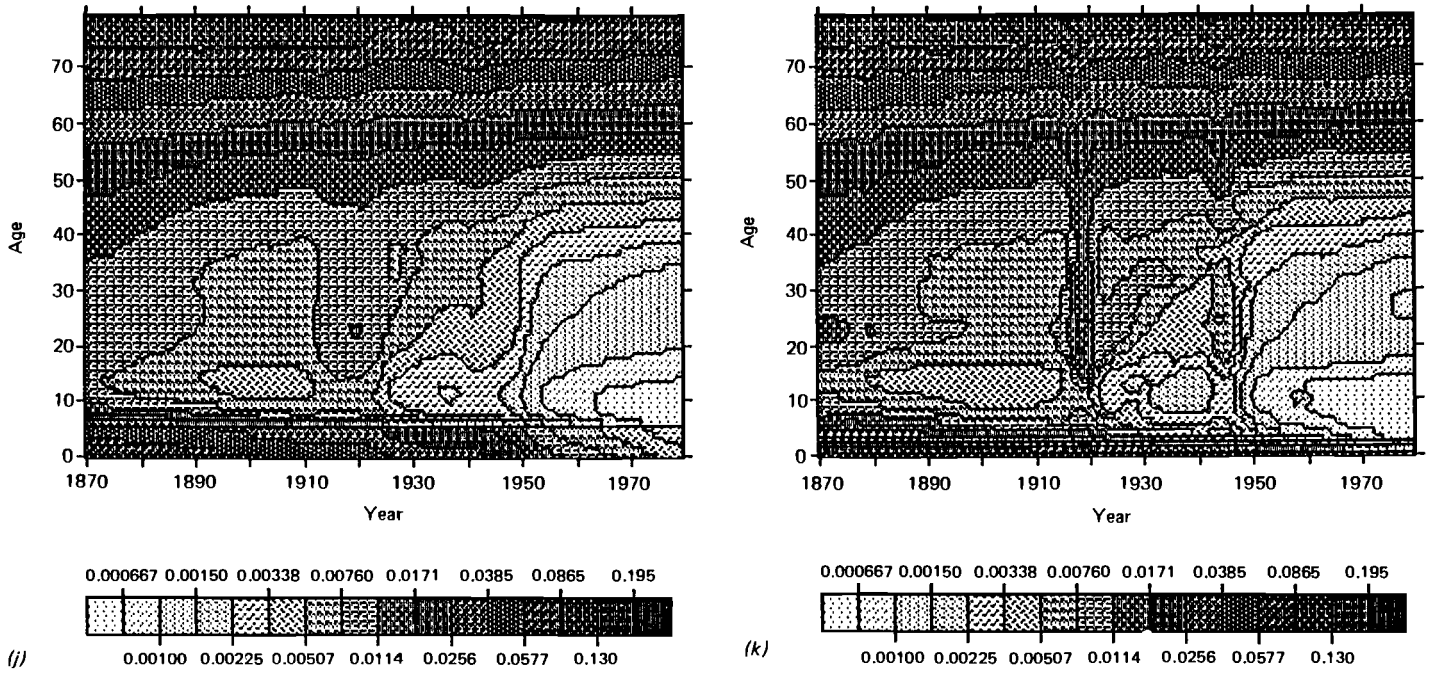

Figure 1. Italian male mortality rates: (*j*) as *Figure 1*(*b*), but smoothed on a 11 × 11 square; (*k*) as *Figure 1*(*b*), but smoothed on a weighted 5 × 5 square (Matrix 1).

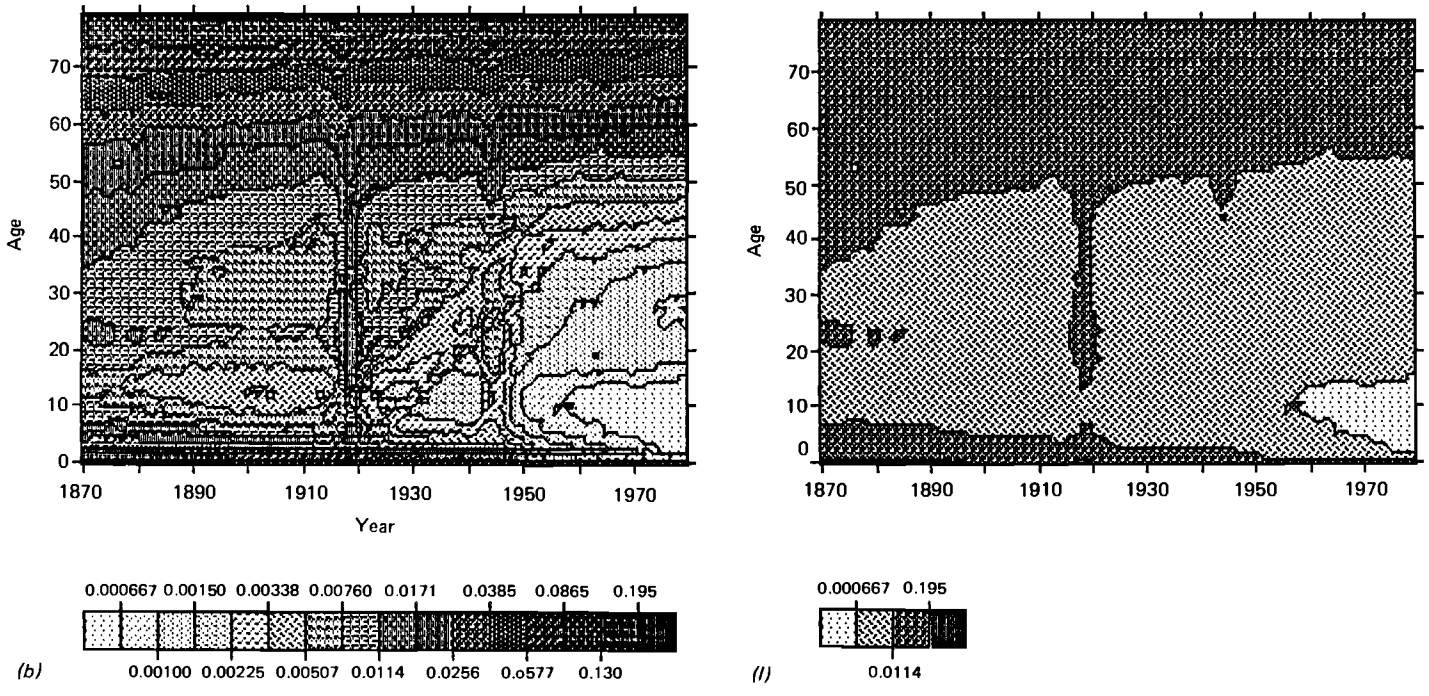

Figure 1. Italian male mortality rates: (*b*) (repeated) with contour lines from 0.000667 to 0.195 at multiples of 1.5, and from age 0 to 79 and year 1870 to 1979; (*l*) as *Figure 1*(*b*) but with only three contour lines.

square were proportional to Matrix 1. Thus, the points in the corners of the square were given weights of 1/256, whereas the point in the center received a weight of 36/256. The theoretical advantages of such weighted smoothing algorithms [see Tukey (1977) for an introductory discussion] have to be balanced against the conceptual simplicity and computational convenience of the kind of straightforward averaging illustrated in *Figures 1(j)* and *1(k)*.

1	4	6	4	1
4	16	24	16	4
6	24	36	24	6
4	16	24	16	4
1	4	6	4	1

Matrix 1.

By using fewer contour lines, a less busy and hence smoother-looking Lexis map can usually be produced. *Figure 1(l)* illustrates of an extreme example of this approach: Italian male mortality is represented on a Lexis map on which all but three of the contours (and four of the levels) have been suppressed. The map, in its simplicity, strikingly highlights the rapid progress against mortality at younger ages, especially after World War II, in contrast with the slow progress at older ages.

5. Close-Ups

As mentioned above and discussed by Caselli *et al.* (1985a), the patterns of male mortality in Italy from ages 10 to 49 for years 1910 to 1969 reveal some interesting cohort effects. *Figures 2(a)* and *2(b)* present Lexis maps of this restricted age and time area: the maps can be considered as enlargements or close-ups of a section of the map in *Figure 1(b)*. Thus, contour maps can be used both to display a large data array and also to focus on selected portions of the array. Note that, because in *Figure 2(a)* the contours are drawn at the same levels as in the original *Figure 1(b)*, only half of the possible levels are utilized. In *Figure 2(b)*, twice as many contours are drawn as in *Figure 2(a)*, every other contour in the second figure being at the same level as a contour in the first figure. Part of the advantage of a close-up is that if the height of the surface varies less in the restricted region being scrutinized, then the level lines can be located at closer intervals to reveal more local detail.

Figures 2(a) and *2(b)* make the diagonal patterns on *Figure 1(b)* more apparent; the added grid makes it clear that the patterns do, indeed, run along cohort lines. Consider one of the most striking differences on the map, the difference between the mortality rates suffered by the cohort born in 1903, which appears on the map at age 10 in the year 1914, and the cohort born in 1908, which appears on the map at age 10 in the year 1919. (Please see previous footnote for an explanation of why the year of birth is one less than the current year minus age.)

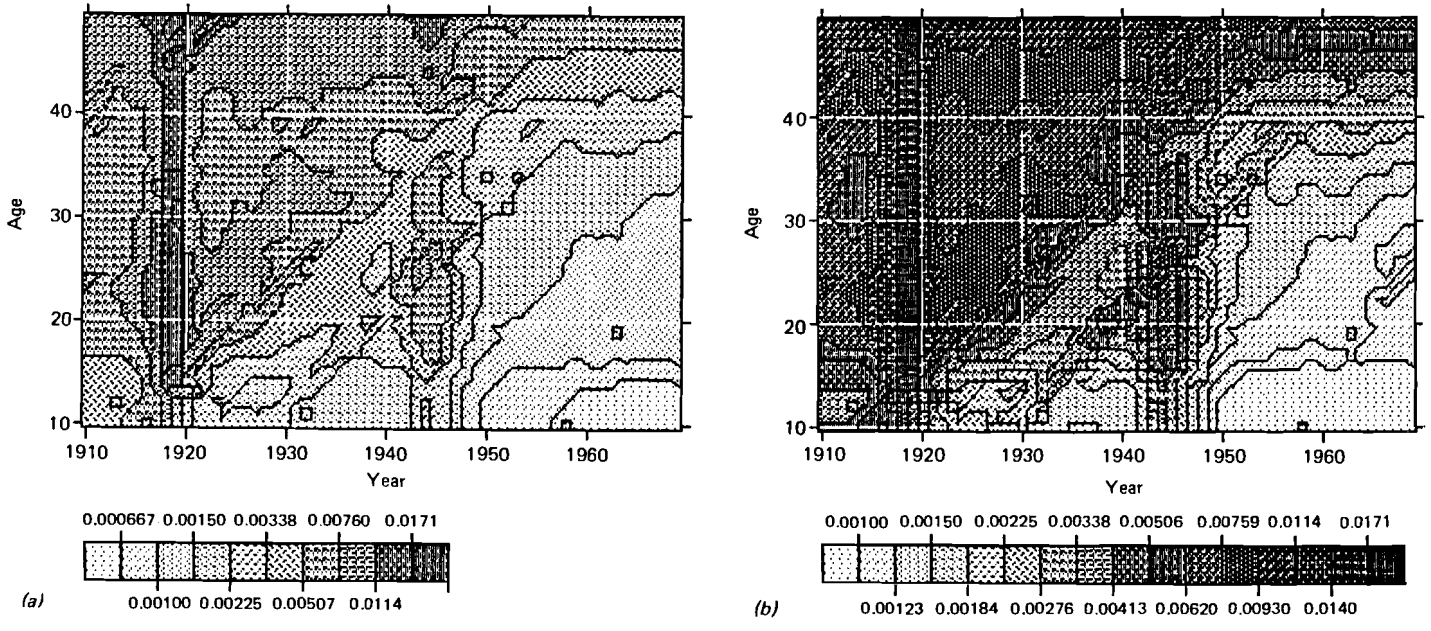

Figure 2. Italian male mortality rates: (*a*) with a grid, contour lines from 0.000667 to 0.0171 at multiples of 1.5, and from age 0 to 79 and year 1910 to 1969; (*b*) with a grid, contour lines from 0.00100 to 0.0171 at multiples of $1.5^{0.5}$, and from age 0 to 79 and year 1910 to 1969.

These two cohort diagonals are separated at most ages between 10 and 30 by two contour levels, indicating a rough mortality differential of about 50%; after age 30 the discrepancy appears to sharply diminish and then disappear.

To explore this intriguing differential and similar differentials among nearby cohorts, we produced *Figure 2(c)*, which plots contour lines of mortality for the cohorts born between 1894 and 1924; these cohorts are followed from age 0 to 54. Note that in *Figure 2(c)*, year of birth runs along the horizontal axis, not the current year. The figure reveals some strong cohort differences, especially among cohorts born between 1903 and 1909 and among cohorts born between 1917 and 1920. It is interesting to see how the period effects of World Wars I and II appear on this figure, as backward diagonals.

To more closely scrutinize the differences among the cohorts born between 1903 and 1909, we produced *Figure 2(d)*, which plots the contours of the mortality rates experienced by the 1904 to 1909 cohorts, from age 0 to age 54, relative to the mortality rates experienced by the 1903 cohort. Thus *Figure 2(d)* facilitates comparisons of the cohorts, with the 1903 cohort serving as the standard for comparison. In the case of the 1908 cohort, for instance, the map reveals that it suffered substantially higher mortality at all ages except ages 8, 9, and 10—the 1903 cohort experienced these ages just prior to World War I, whereas the 1908 cohort passed through these ages during the final years of the war and the Spanish influenza epidemic. At ages 14 and 15, which the 1903 cohort lived through from 1917 to 1919, the 1903 cohort experienced more than five times the mortality experienced at these same ages by the 1908 cohort. Rough calculations indicate that between ages 16 and 34, mortality rates for the 1908 cohort averaged about 50% of those for the 1908 cohort, and between ages 35 and 54 mortality rates were about 30% lower on average.

Thus, the general tendency was for the risk differential to diminish, but local fluctuations complicate the pattern. Careful scrutiny of the details of the pattern of mortality differential between the 1903 and 1908 cohorts, and of similar differentials between other cohorts, might lead to better understanding of the interaction of age, period, and cohort effects. More generally, our use of *Figures 1(b)* and *2(a)–2(d)* provides a suggestive illustration of the value of contour maps in exploratory analyses of population surfaces.

6. Maps from Interpolated Data

The mortality rates for Italian males used in *Figures 1* and *2* are available by single year of age and single year of time. Frequently demographers have to work with less finely-spaced data; mortality rates, for instance, may be available every decade or so, by five-year age classes. *Figure 3(a)* displays the evolution of Italian male mortality based on data published in Preston *et al.* (1972). Data sets from this source were available for 1881, 1891, 1901, 1910, 1921, 1931, 1960, and 1964. Death rates were given for five-year age categories from age 5 up to age 80, as well as for age 0 and the four-year category from age 1 to 5. We converted the n-year death rates into single-year death rates such that the resulting mortality curve followed a

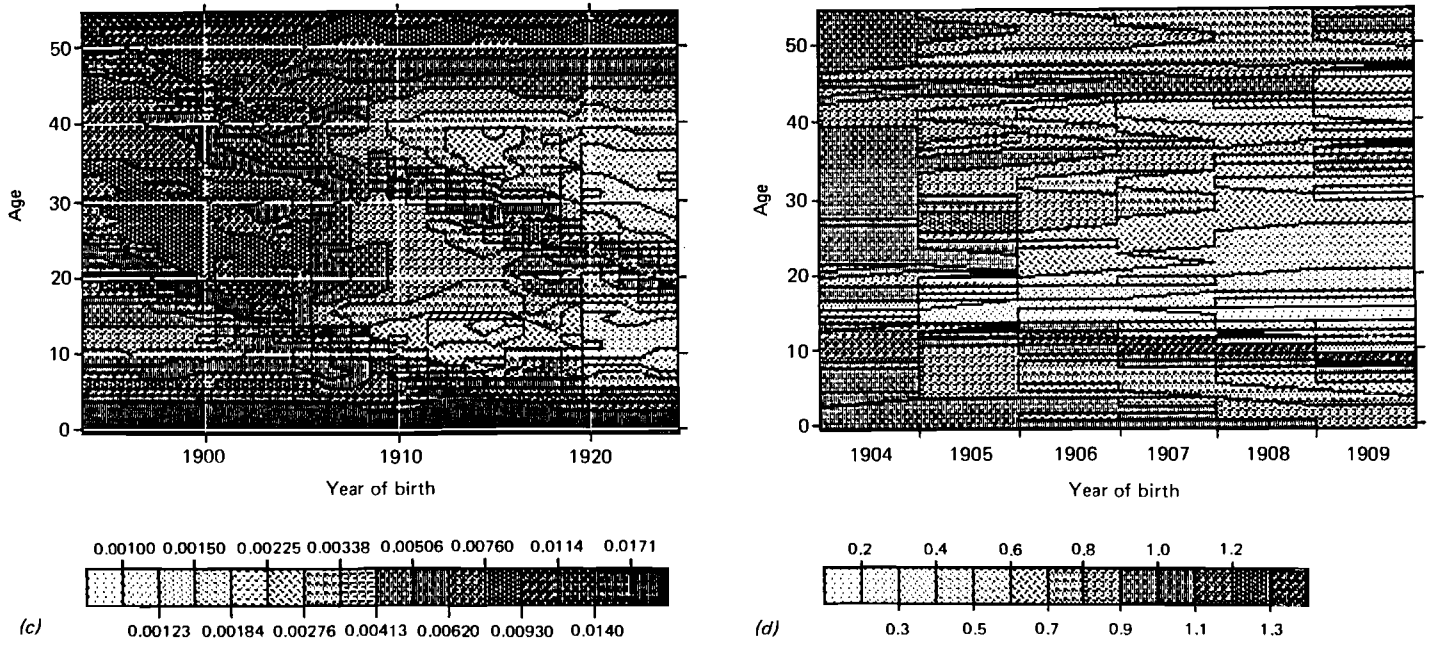

Figure 2. (*c*) Italian male cohort mortality rates, with a grid, contour lines from 0.00100 to 0.0171 at multiples of $1.5^{0.5}$, and from age 0 to 54 and year of birth 1894 to 1924. (*d*) Italian male mortality rates relative to 1903 cohort age-specific levels, with contour lines from 0.2 to 1.3 at intervals of 0.1, and from age 0 to 54 and year of birth 1904 to 1909.

piece-wise linear trajectory; we then used simple linear interpolation between the available data points over time to estimate the height of the mortality surface at intermediate points in time. Comparison of *Figures 3(a)* with *3(b)*, which presents single-year of age and time data at the same scale, reveals the difference between working with detailed data and interpolated data. The global patterns of mortality over age and time are apparent in *Figure 3(a)*, but all the interesting local features, including the effects of World Wars I and II, are lost.

The longest time series of mortality rates are available for Sweden. We used mortality rates based on interpolations made by Vaupel *et al.* (1979) and, for recent years, by ourselves, of data from Keyfitz and Flieger (1968) for 1778 to 1882 and from various editions of the *Swedish Statistical Yearbook* for 1881 through 1981. These data were available for the most part for five-year periods; before 1880 the data were given for five-year age categories but thereafter data by single-year of age were available. It is apparent from *Figure 4*, which shows the evolution of Swedish female mortality from 1779 to 1981, that systematic progress against mortality at all ages began in Sweden around 1830. A remarkable acceleration of progress, especially at younger ages, starts after 1920. In early years, strong fluctuations are evident, especially the destructive effects of the Swedish war with Russia in 1808–1809.

7. Maps of Female Fertility

Figure 5 displays the contours of US birth rates from 1917 to 1980 for women from age 14 to 49; the figure is based on data compiled by Heuser (1976, 1984). For comparison, two versions of the map are given, one in color (*a*) and the other in black and white (*b*). In the center of the baby boom, for women around age 23 around 1960, fully a quarter of women gave birth each year. The concentration of high birth rates among women in their early- and mid-20s and the cycles of high and low birth rates that characterize baby booms and busts are strikingly revealed on the map.

Figure 5 is a standard map in which current year runs along the horizontal axis and age along the vertical axis. Other coordinates help reveal cohort effects. In particular, because the eye can follow vertical and horizontal lines more easily than diagonals, it may be useful to twist a contour map so that year of birth, rather than current year, runs along the horizontal axis. *Figure 6* illustrates this approach. Alternatively, as shown in *Figure 7*, year of birth may run along the horizontal axis and current year along the vertical axis. We used only five contour lines on *Figure 7* because the lines were otherwise too closely spaced to be intelligible.

Taken together, *Figures 5*, *6*, and *7* indicate that the age effect in fertility is very strong, that period fluctuations are also strong, but that cohort effects appear to be much less prominent. Perhaps more refined methods of presentation will reveal persistent cohort patterns; some relevant analysis is presented later in this paper in conjunction with *Figures 10*, *11*, *15*, *18* through *20*, *27*, and *45*. Note that the period effects shown in *Figures 5*, *6*, and *7* can be separated into three parts. Before age 18 fertility rates have remained low and after age 35 or so there is a general pattern of declining fertility. It is between ages 18 and 35, and especially

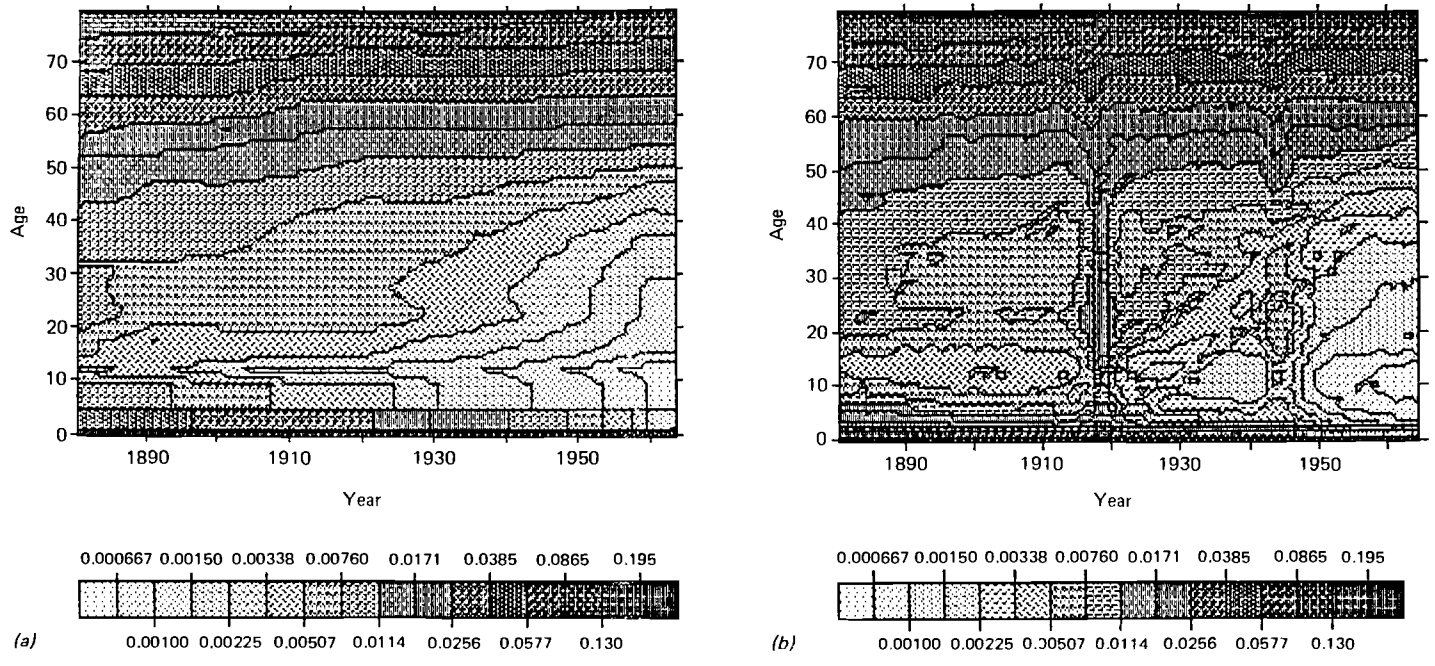

Figure 3. Italian male mortality rates with contour lines from 0.000667 to 0.195 at multiples of 1.5, and from age 0 to 79 and year 1881 to 1964: (*a*) interpolated data; (*b*) single-year-of-time-and-age data.

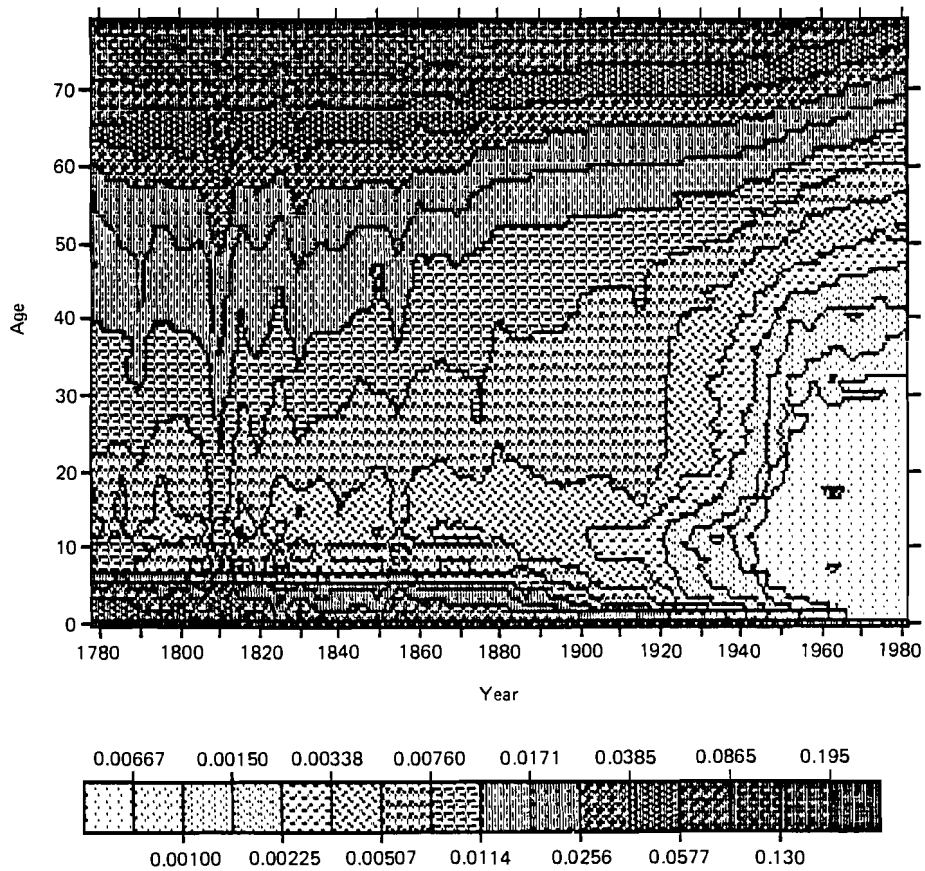

Figure 4. Swedish female mortality rates, with contour lines from 0.000667 to 0.195 at multiples of 1.5, and from age 0 to 79 and year 1778 to 1981.

around age 23, where the most dramatic absolute swings in fertility rates have occurred. In conjunction with *Figure 15*, we consider relative fluctuations in fertility rates, in contrast with the absolute fluctuations shown in *Figures 5*, *6*, and *7*.

Figure 8 presents a Lexis map of Chinese fertility rates by single year of age from 15 to 49 and single year of time from 1940 to 1981; the map is presented and discussed in Zeng *et al.* (1985). As discussed in that paper, the most striking feature of the map is the rapid decline in fertility after 1970. This decline is well known and often summarized by the dramatic drop in the total fertility rate: in 1970 the total fertility rate was 5.8; by 1981 it had fallen 55% to 2.6. What the map graphically reveals is the age pattern of decline. Consider the ages where the fertility rate exceeds 20%: in 1968, this period of high fertility stretched from age 20 through 37. By 1981, in contrast, the period of high fertility was concentrated from age 23 to 27. In 1968, more than 20% of 20-year-olds and more than 10% of 40-year-olds gave birth. By 1981, the fertility rate of 20-year-olds had fallen under

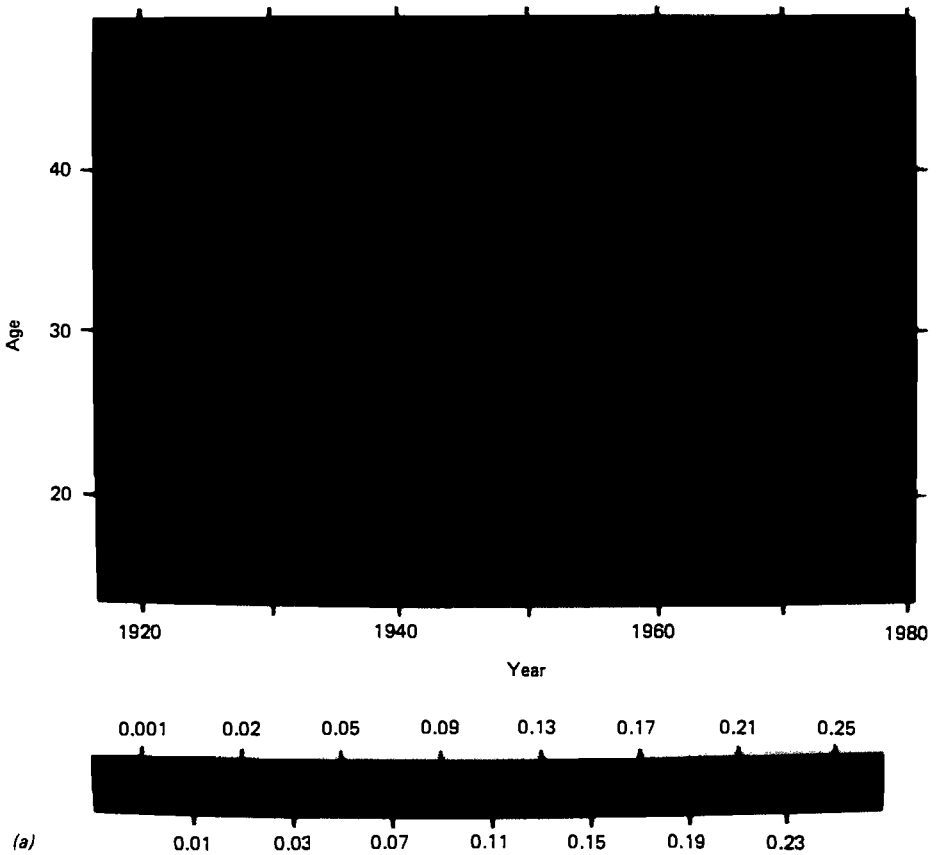

Figure 5(a). US fertility rates (in color), with contour lines selectively placed from 0.001 to 0.25, and from age 14 to 49 and year 1917 to 1980.

10% and the fertility rate of 40-year-olds had fallen under 2%. The precipitous decline in the fertility contours at older ages and the marked increase in the contours at younger ages reflect the success of Chinese birth control policy, including the increase in age of first marriage and, even more importantly, the widespread use of contraception.

The radical narrowing of the period of high fertility was slightly reversed in 1981 and there is some evidence of an increase in births among 25- and 26-year-old women. This is undoubtedly a result of the New Marriage Law, announced in 1980, and the concomitant boom in marriages, especially among women in their mid-20s.

The most conspicuous period disruption on the map is the trough in fertility in 1959–1961. This coincides with the Great Leap Forward and corresponds to a similar trough in marriage rates, except that marriage rates tended to be lowest in 1959 whereas fertility rates reached their low point in 1961. The recovery of fertility rates from their depressed level in 1961 was dramatic: during the prolific ages

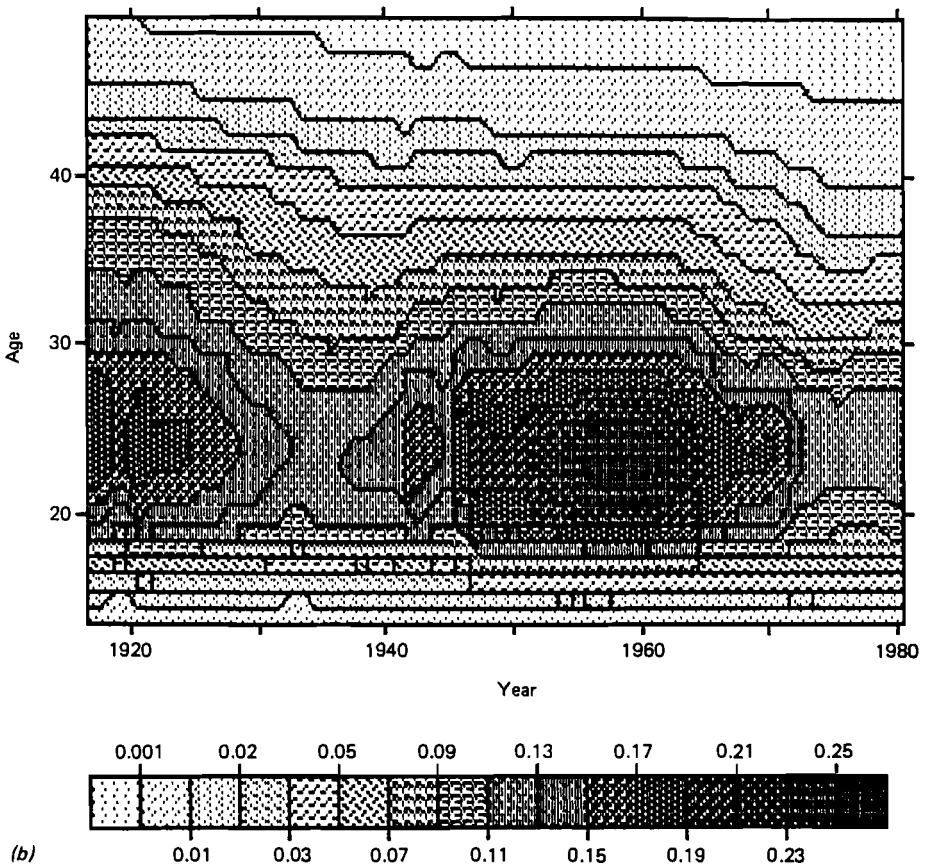

Figure 5(b). US fertility rates (in black and white), with contour lines selectively placed from 0.001 to 0.25, and from age 14 to 49 and year 1917 to 1980.

between 23 and 29, fertility rates rose from under 20% per year in 1961 to over 30% per year in 1962 and over 35% per year in 1962.

The fertility data pertaining to earlier years, especially the years before 1950, have to be interpreted with caution since they are reconstructions based on interviews taken in 1982. The general pattern seems reassuringly plausible: over the course of the 1940s and 1950s fertility rates were fairly stable, with some tendency toward increase. This is consistent with trends in improvements in living standards, and the absence of widespread contraception, during this period.

Figure 9 shows the fluctuating pattern of Finnish fertility since 1776; it is based on data supplied by Wolfgang Lutz. The various wars and famines that disrupted life in Finland are apparent on the map, as is the substantial decline in fertility after World War I, especially at older ages. Lutz also notes the decline in fertility apparent in the eighteenth century: this represents the culmination of a nuptiality transition starting about 1750.

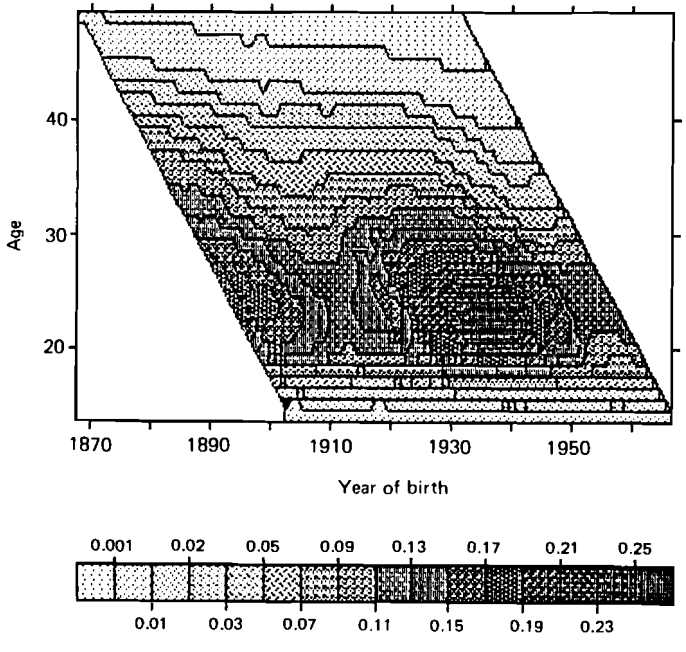

Figure 6. US cohort fertility rates, with contour lines selectively placed from 0.001 to 0.25, and from age 14 to 49 and year of birth 1868 to 1966.

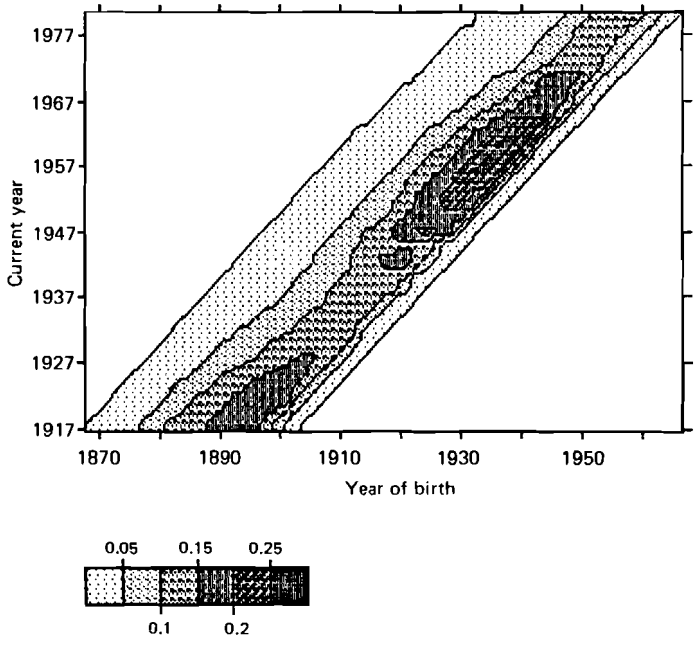

Figure 7. US fertility rates by current year and year of birth, with selected contour lines from 0.05 to 0.25, and from current year 1917 to 1980 and year of birth 1868 to 1966.

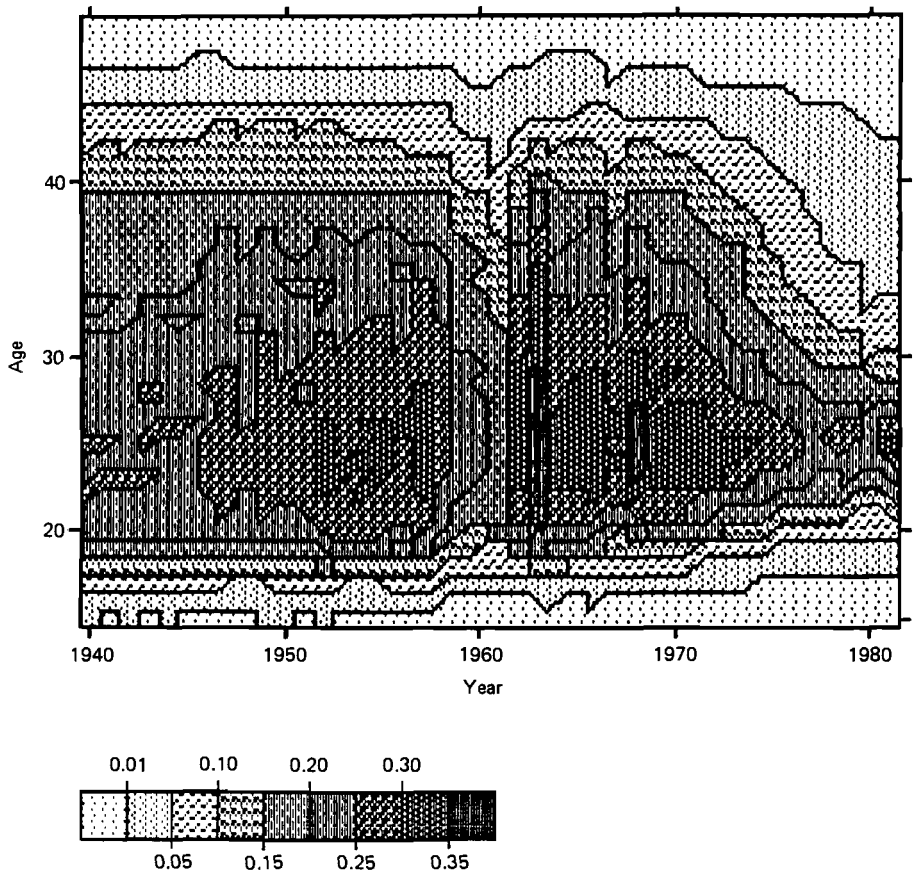

Figure 8. Chinese fertility rates, with contour lines selectively placed from 0.01 to 0.36, and from age 15 to 49 and year 1940 to 1981.

8. Alternative Graphic Displays of US Female Fertility

The most commonly used method for displaying demographic rates over age and time is to plot the rates over time for selected ages or over age for selected times. In *Figure 10*(*a*), for instance, US birth rates are plotted over time at ages 18, 23, and 28 and in *Figure 10*(*b*) the birth rates are plotted from age 14 to 49 for years 1920, 1950, and 1980. Comparison of *Figures 10*(*a*) and *10*(*b*) with the Lexis maps presented in *Figures 5*, *6*, and *7* reveals some of the strengths and weaknesses of these alternative graphic displays. The Lexis maps present far more information and give an overview of the entire surface. The plots over age and time focus attention on trends and fluctuations in those two directions. The Lexis maps might be compared to a lavish Chinese banquet, whereas the graphs over age and time are more like a delicate Japanese dinner.

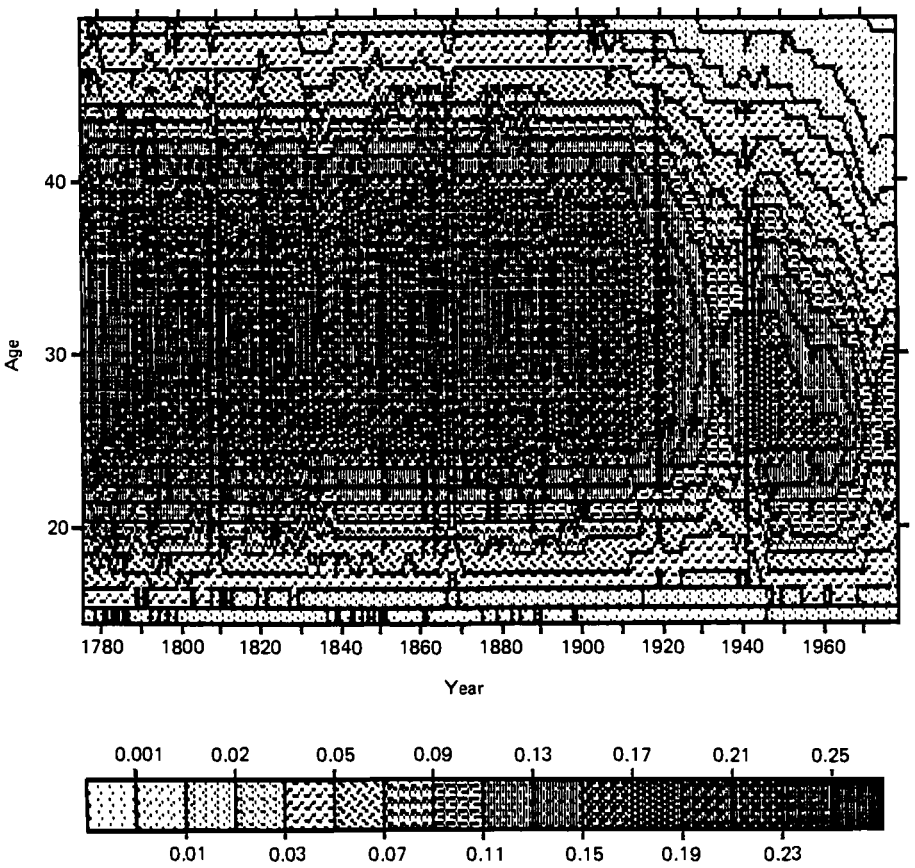

Figure 9. Finnish fertility rates, with contour lines selectively placed from 0.001 to 0.25, and from age 15 to 49 and year 1776 to 1978.

Figures 10(c) and *11* show two plots of the US birth rate data drawn from a three-dimensional perspective. *Figure 10(c)*, like all the Lexis maps in this *Report*, was produced using a simple IBM PC (with 128K of memory) and an inexpensive printer; *Figure 11* was drawn using a mainframe computer and high-quality plotter. With appropriate software, it is possible not only to produce, but also to rotate such three-dimensional pictures on a computer monitor so that they can be viewed from various angles: the three perspectives shown in *Figure 11* suggest how informative this kind of rotation can be. Clearly, three-dimensional plots will be an important tool for demographers.

Three-dimensional plots, however, will complement, and not supercede, contour plots. A three-dimensional plot sacrifices some of the richness of detail that is clearly portrayed on the corresponding contour map; furthermore, it is difficult on a three-dimensional plot to relate a point on the surface to the exact age and year underlying the point. Just as architects, surveyors, and engineers rely on contour

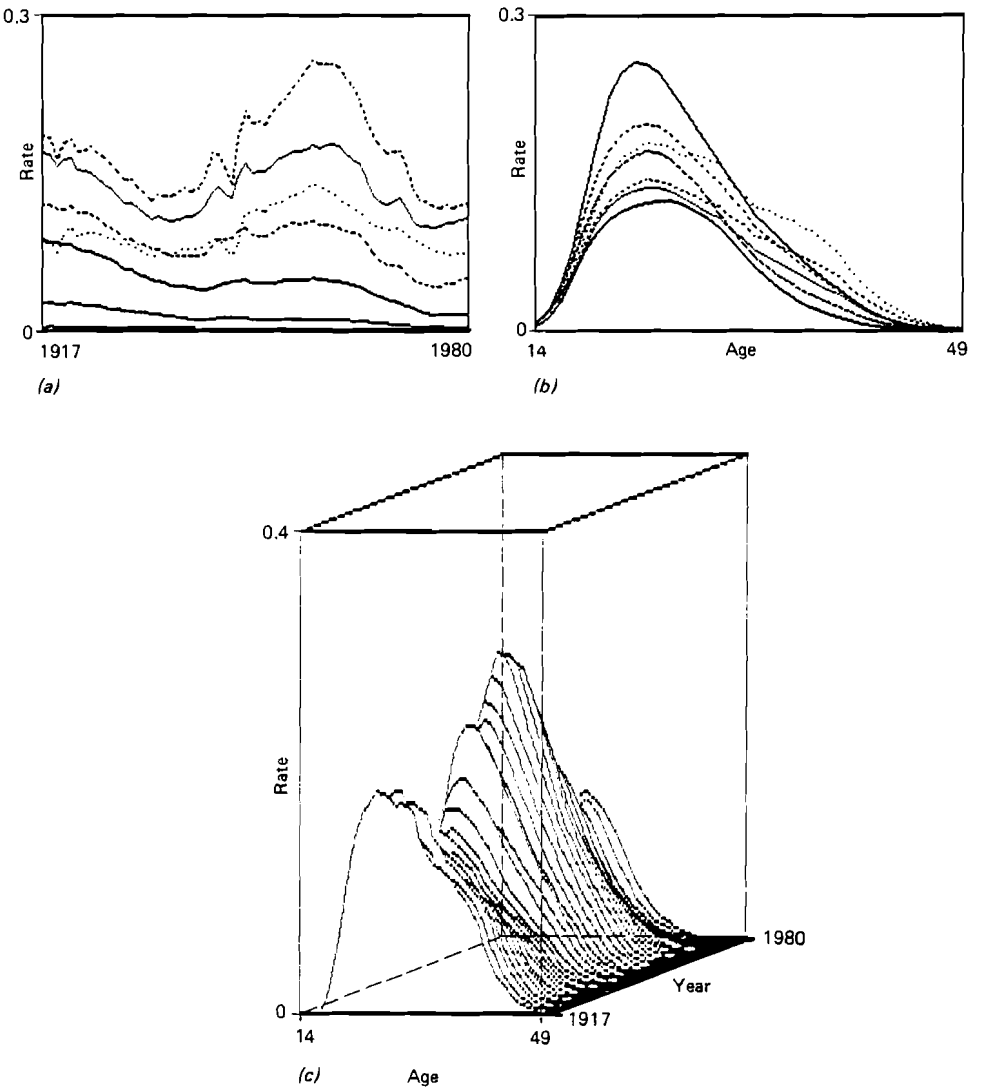

Figure 10. (*a*) US birth rates from year 1917 to 1980; (*b*) US birth rates from age 14 to 49; (*c*) Three-dimensional perspective of US fertility rates from age 14 to 49 and year 1917 to 1980.

maps for site planning and cartographers use contour and topographical maps in depicting a variety of terrains and surfaces, demographers will also undoubtedly find that for some purposes contour maps are the most appropriate means for representing a population surface. Fisher's (1982) comprehensive comparison of an array of different methods for "mapping information" reveals the relative advantages, for many purposes, of "the combined use of contour lines and tones".

Any graphical method has its strengths and weaknesses. Our point is simply that demographers should consider adding contour maps to their tool kit, to supplement graphs of rates over age and time, three-dimensional plots, age-distribution pyramids, and other techniques.

9. The Past Population of France and the Future Population of Sophia

Surfaces of population levels are especially important in the theory of population dynamics, as discussed by Arthur and Vaupel (1984). *Figure 12(a)* presents such a surface, of French population levels from birth to age 79 from years 1851 to 1965, based on interpolations of data in Keyfitz and Flieger (1968). Births run across the bottom of the map. As suggested by the figure, and confirmed by examining the underlying data values, the annual number of births in France has hovered around the level of three quarters of a million, with a low of under 600 000 000 and a peak of just over 850 000. Total population increased only by about 10% from 1851 to 1945, but then it jumped by 20% from 1945 to 1965; this again is suggested by the map and confirmed by examining Keyfitz and Flieger's tables.

In a population closed to migration, the surface has to continually fall off along any cohort line, as the members of the cohort die. A number of French cohorts, however, grew in size with age, not only because of the usual kind of in-migration, but also because of effective in-migration caused by the inclusion of Nice and Savoy (starting with the 1861 table) and the reinclusion of Alsace and Lorraine (starting with the 1920 table; Alsace and Lorraine were excluded in earlier tables, back through 1871). Note, in particular, the diagonal displaying the fluctuating population levels of the cohorts born between 1915 and 1920.

To depict the change that has occurred over time in age-specific population levels, or such other demographic statistics as fertility or mortality rates, it is useful to draw Lexis maps of relative surfaces on which the value of the statistic at each point is calculated relative to the value of the statistic in some base year. *Figure 12(b)*, for example, presents French population levels relative to the population level at the various ages in the first year, 1851. In conjunction with *Figure 12(a)*, this figure reveals the general trends in French population levels, as well as some interesting local fluctuations. The cycles in numbers of birth are apparent in *Figure 12(b)*, as is the great relative increase in population at the oldest ages, with about 3.5 times as many people age 79 in 1964 compared with the number of people at this age in 1851. Note the area of the map that has a value of about 1: this area shows the ages and times when the population was at the same level as it was at the corresponding age in 1851. Thus, for example, 24-year-olds were about as numerous in the mid-1960s as they were in the 1850s.

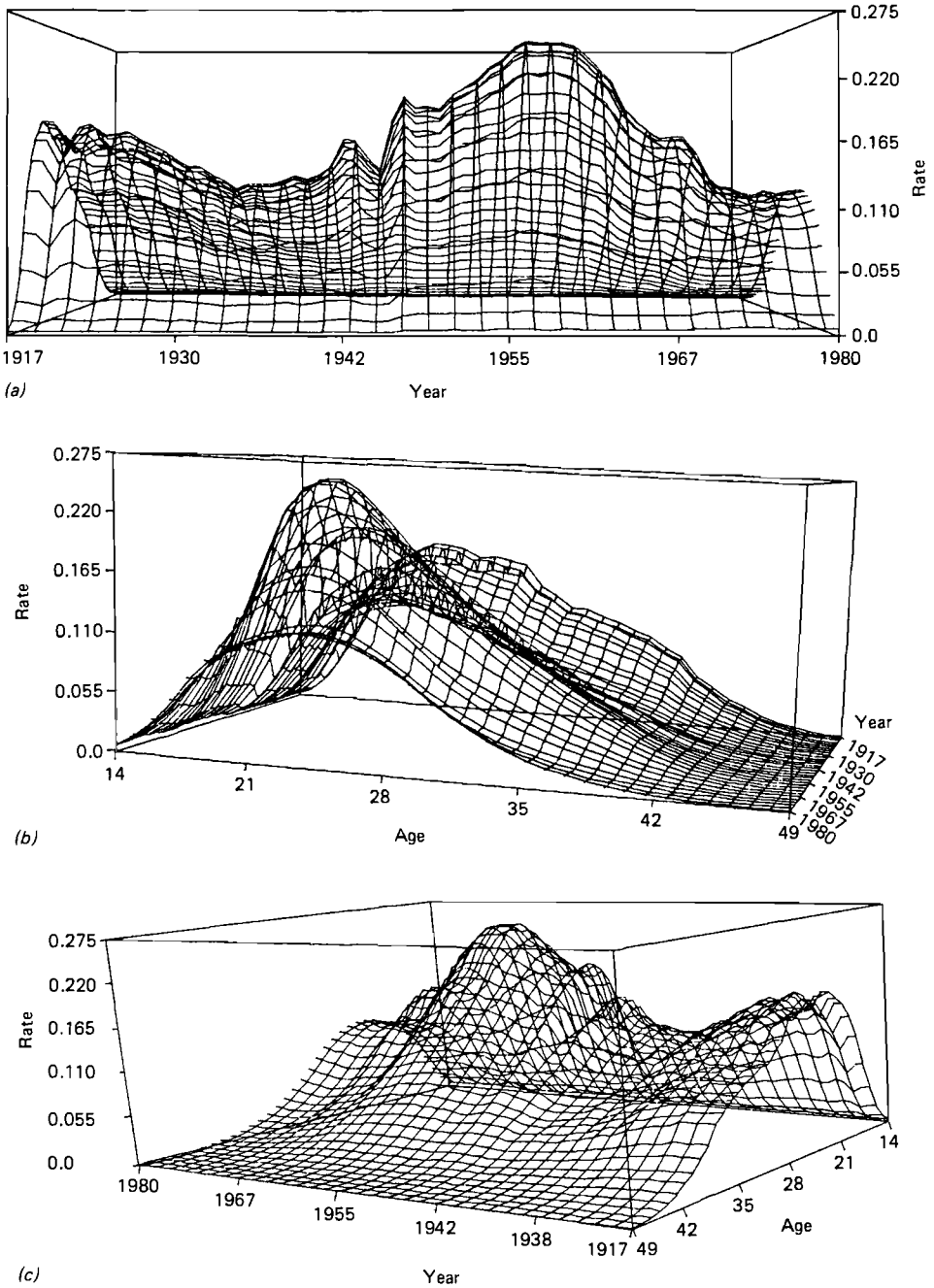

Figure 11. High-quality three-dimensional plots of US fertility rates.

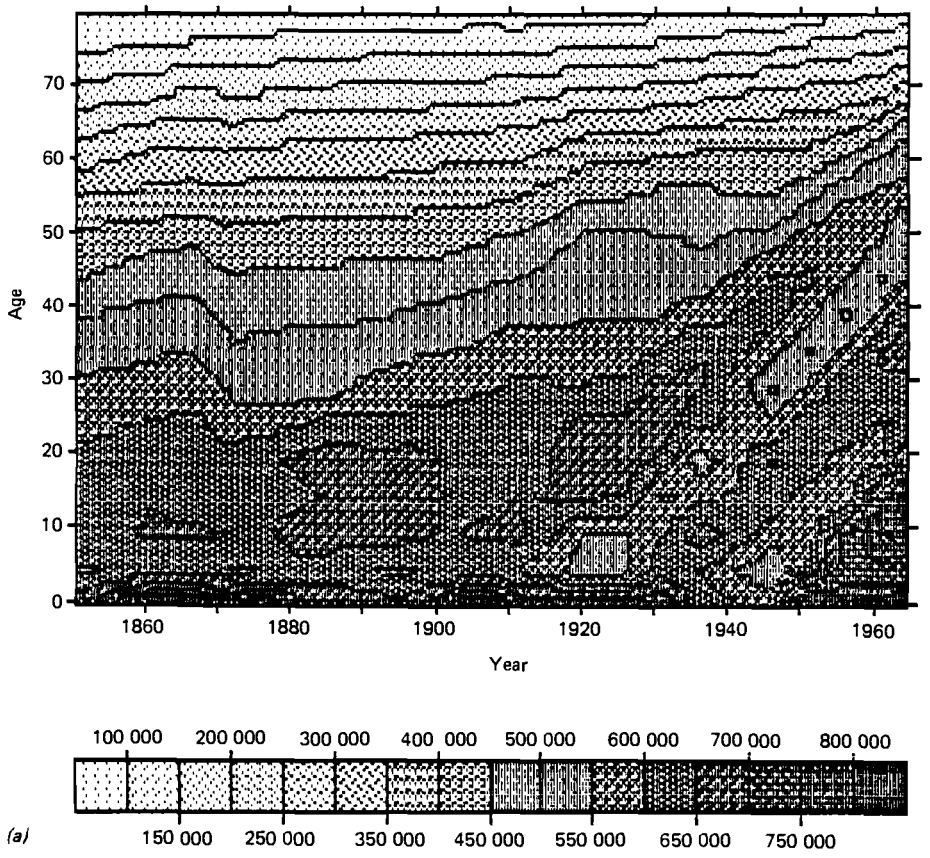

Figure 12(*a*). French population at each age and time, with contour lines from 100 000 to 800 000 at intervals of 50 000, and from age 0 to 79 and year 1851 to 1964.

Figure 13 presents a projection, from 1975 to 2049, of the age-specific population of Sophia, Bulgaria. Gateva (1985) from Bulgaria prepared the map, using a multiregional model for Bulgaria that included migration; she used a program developed by Scherbov *et al.* (1986), from the USSR, for the necessary calculations. The effects of strong in-migration, especially of people around age 20, are evident on the map, as are diagonal patterns resulting from fluctuations in the numbers of births. Projections of this type may be of considerable value to urban and regional planners, especially if alternative projections based on different scenarios and policy decisions are compared.

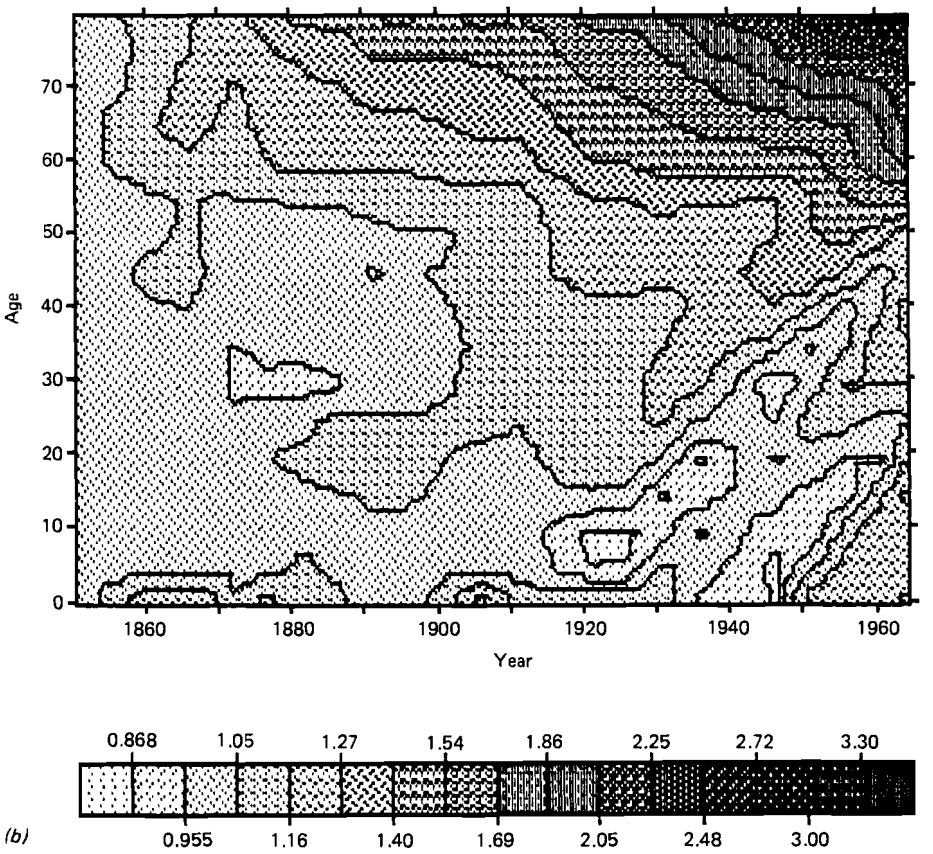

Figure 12(b). French male population relative to 1851 age-specific levels, with contour lines from 0.868 to 3.30 at multiples of 1.1, and from age 0 to 79 and year 1851 to 1964.

10. Relative Surfaces of Italian Mortality, US Fertility, and Belgian Population

Two applications of relative contour maps are shown in *Figures 14* and *15*. *Figure 14* displays age-specific mortality rates for Italian males relative to their levels in 1925, a year roughly halfway through the period studied. The map clearly reveals the great progress that has been made in reducing mortality at the youngest ages compared with the slow progress at the oldest ages. The map also puts the devastation of World War I into perspective: World War I essentially erased a half century of progress, but the setback was temporary and pre-World War I mortality rates at most ages were achieved and surpassed within a decade or so.

Figure 15 presents age-specific birth rates for US females relative to their level in the final year, 1980. The map highlights the dramatic reduction in birth rates above age 35, compared with the less radical (relative) changes at younger ages.

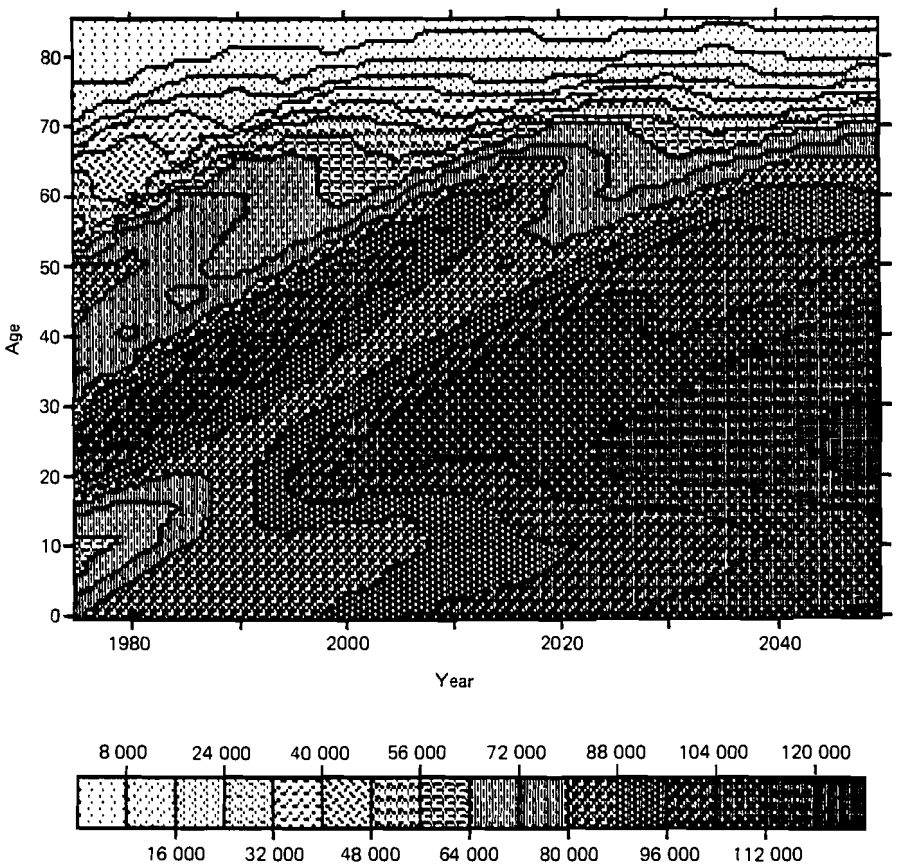

Figure 18. Population of Sophia, Bulgaria, with contour lines from 9 000 to 121 000 at intervals of 8 000, and from age 0 to 85, projected from 1975 to 2049.

Even the baby boom pales in significance when viewed from this perspective.

Instead of dividing a demographic array by the age-specific statistics for a particular year, the array could be divided by the period-specific statistics for a particular age. For example, *Figure 16* shows Italian male mortality rates at various ages relative to the infant mortality rate in the appropriate year. The falling contours on the top half of the map emphasize a trend that was less apparent in the original *Figure 1*(*b*), namely that progress against mortality at older ages has been slower than that at younger ages. In 1870 mortality rates at age 65 were roughly one fifth the level of infant mortality; a century later, mortality rates at age 65 were about one quarter higher than the prevailing infant rates.

Demographic statistics can also be expressed relative to some composite age-specific or period-specific measure. *Figures 17* and *18* provide two examples. To produce *Figure 17*, Belgian age-specific female population levels (from Veys, 1983) were divided by the total Belgian female population in each year. Thus, the map

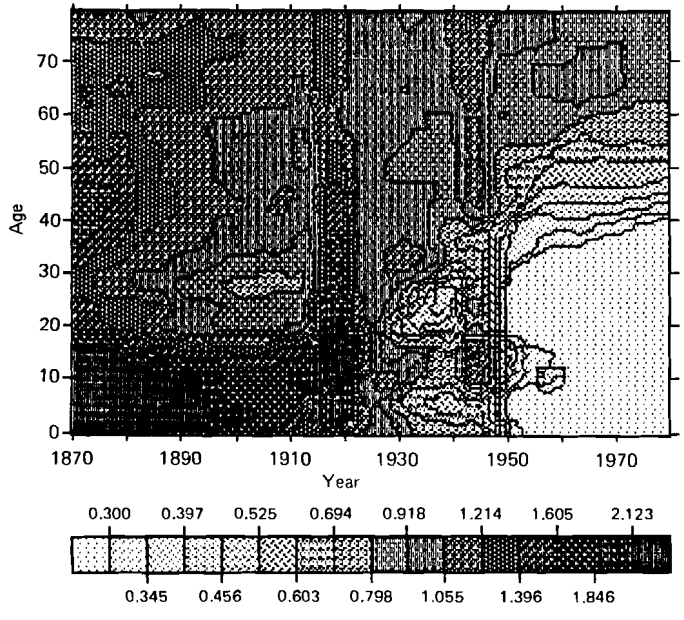

Figure 14. Italian male mortality rates relative to age-specific 1925 levels, with contour lines from 0.3 to 2.12 at multiples of 1.15, smoothed on a 5 × 5 square, and from age 0 to 79 and year 1870 to 1979.

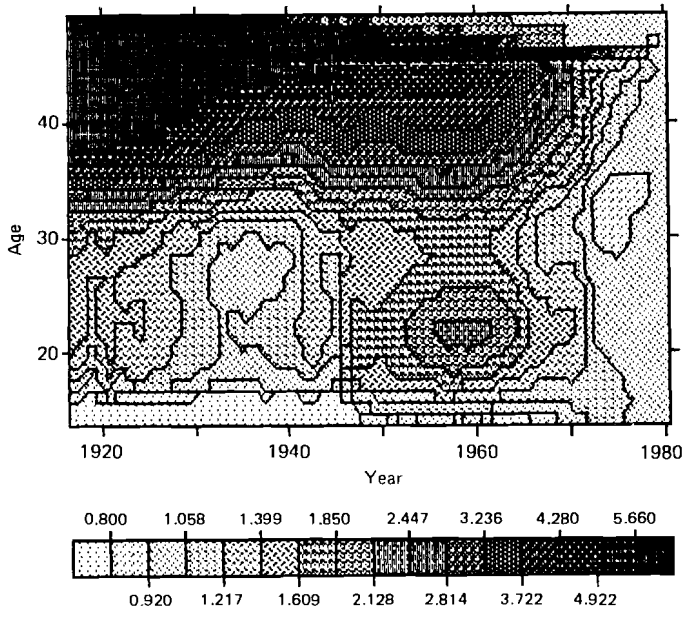

Figure 15. US birth rates relative to age-specific 1980 levels, with contour lines from 0.8 to 5.66 at multiples of 1.15, and from age 14 to 49 and year 1917 to 1980.

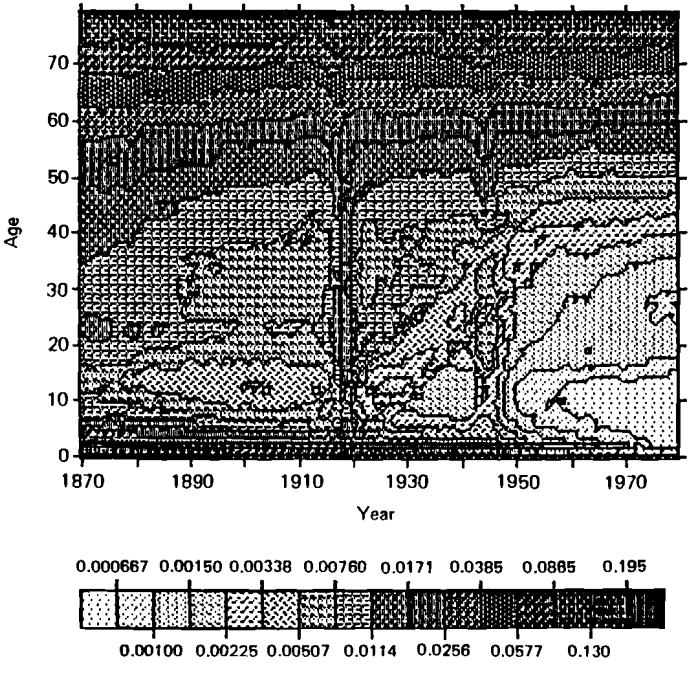

Figure 1(b). Italian male mortality rates (in black and white), with contour lines from 0.000667 to 0.195 at multiples of 1.5, and from age 0 to 79 and year 1870 to 1979.

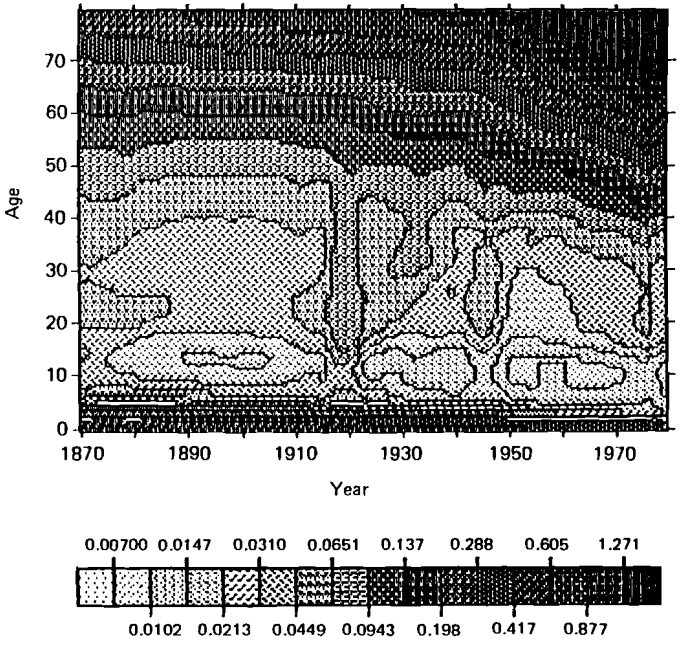

Figure 16. Italian male mortality rates relative to infant mortality, with contour lines from 0.007 to 1.27 at multiples of 1.5, smoothed on a 5 × 5 square, and from age 0 to 79 and year 1870 to 1979.

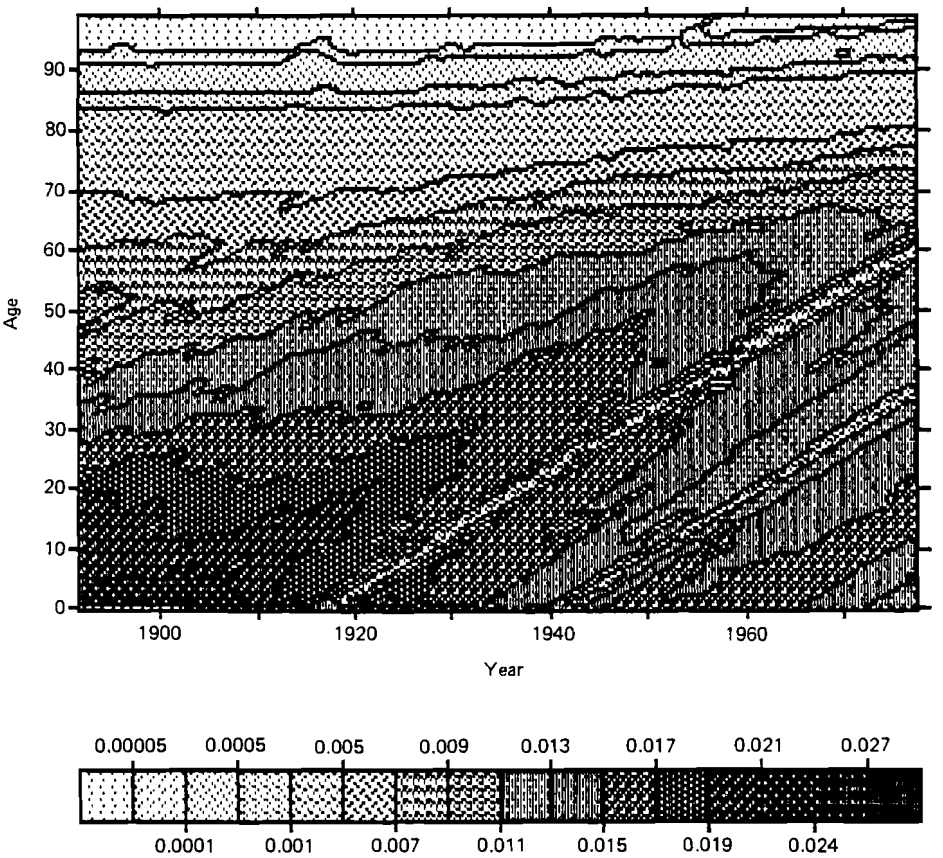

Figure 17. Age-distribution of Belgian female population, with contour lines selectively placed from 0.00005 to 0.027, and from age 0 to 99 and year 1892 to 1977.

gives contours of the age distribution of the population, i.e., the percentage of the population in each year that are at various ages. The diagonal traces of the small cohorts born during World Wars I and II are apparent, as is the general trend of the age composition of the population to shift upward to older ages. As a proportion of the population, 70-year-olds were as important in 1970 as 40-year-olds were in 1892.

Figure 18, which is based on US fertility data, is similar in nature except that the contours pertain to cumulative levels up through age 49 relative to the total level over all ages. The map can be interpreted as showing the proportion of all births in a given year that occurred to women of some age or less—in a synthetic population in which there were equal numbers of women at each age. The general trend is downward, especially at older ages: a greater cumulative proportion of children is being born each year to younger women. This trend runs through the periods of baby boom and bust.

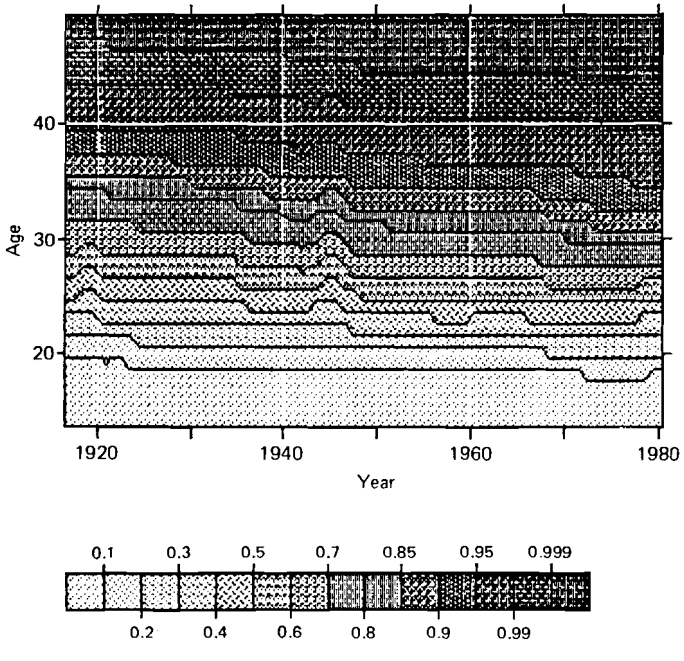

Figure 18. Cumulative distribution of US births by age of mother and year, with contour lines selectively placed from 0.1 to 0.999, and from age 14 to 49 and year 1917 to 1980.

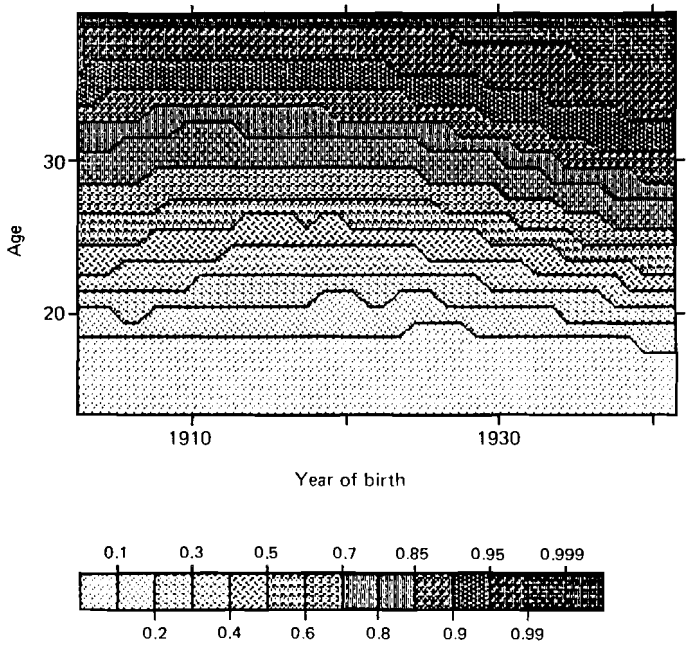

Figure 19. Cumulative distribution of US births by age and year of birth of mother, with contour lines selectively placed from 0.1 to 0.999, and from age 14 to 39 and year of birth 1903 to 1941.

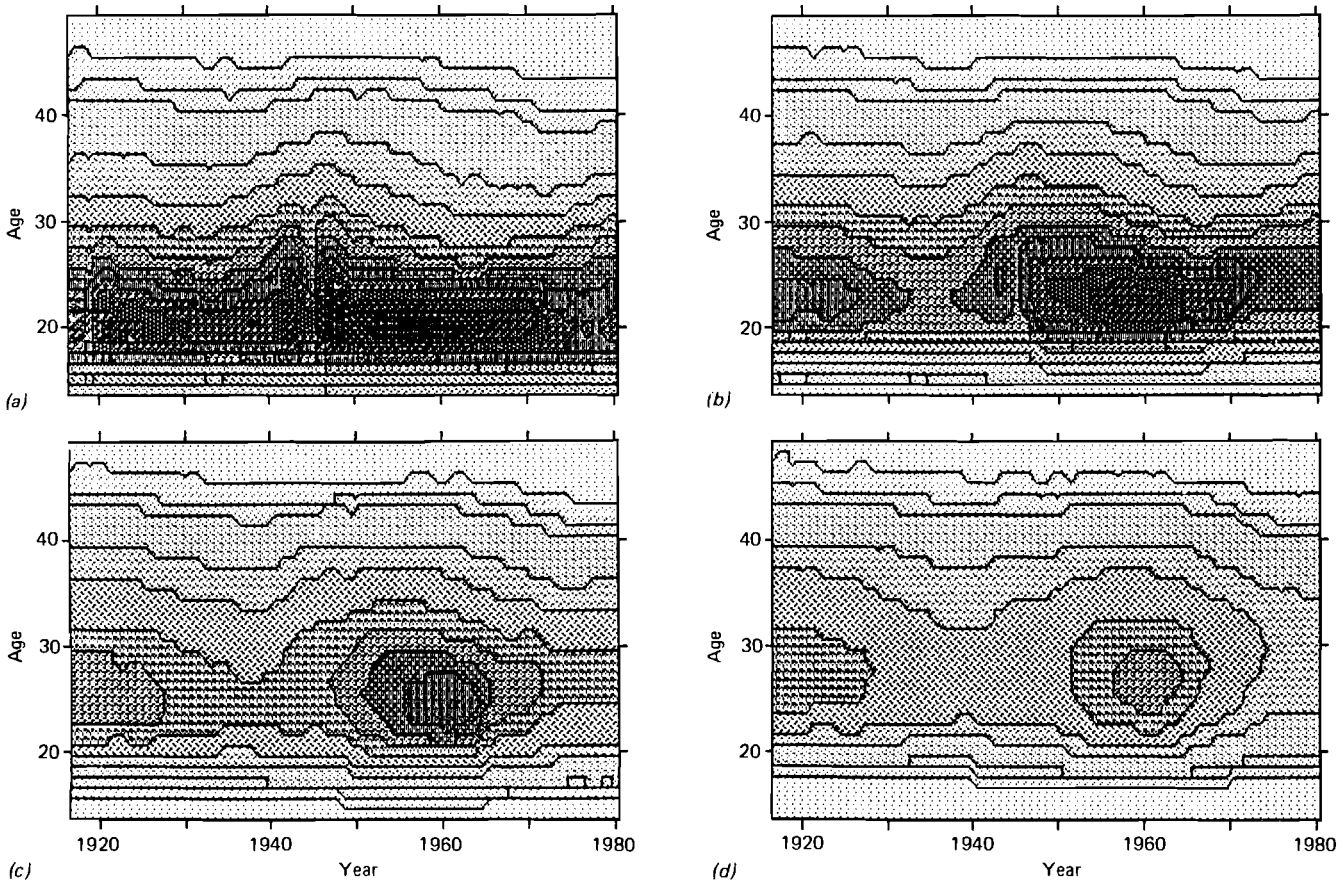

Figure 20. US birth rates with contour lines selectively placed from 0.0001 to 0.11, and from age 14 to 49 and year 1917 to 1980: (*a*) at parity 1; (*b*) at parity 2; (*c*) at parity 3; (*d*) at parity 4; (*e*) at parity 5; (*f*) at parity 6.

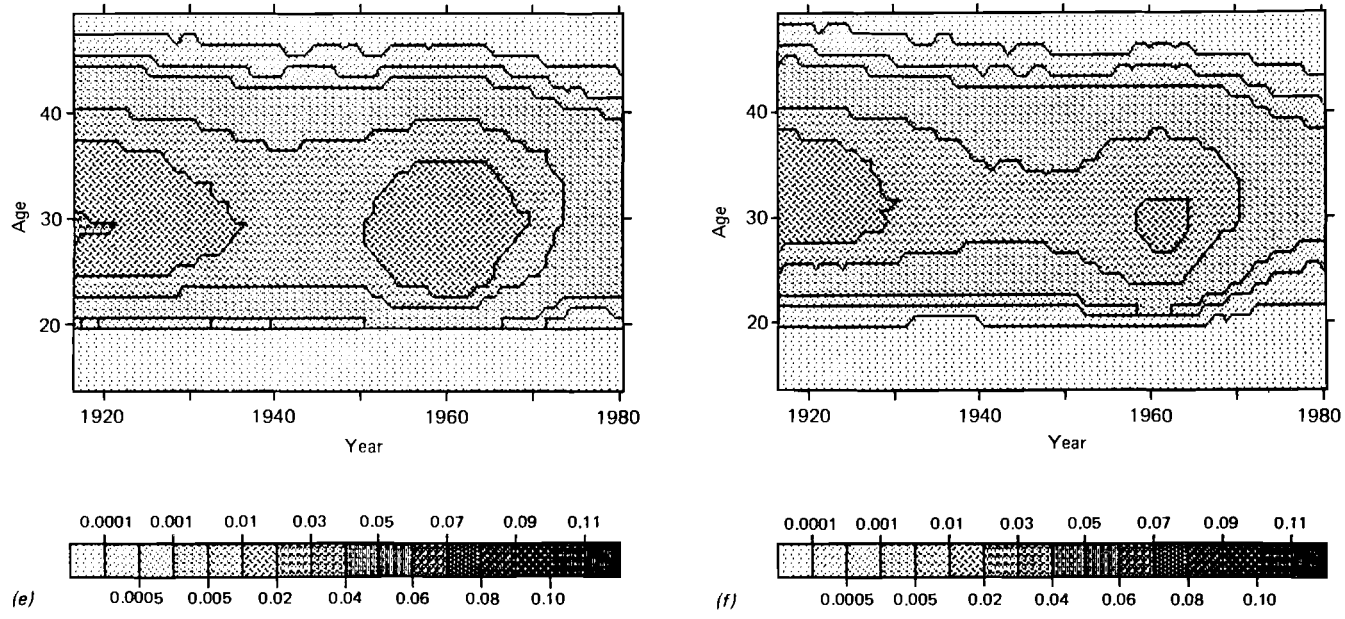

Figure 20 (continued)

Finally, it may sometimes be useful to examine Lexis maps based on statistics relative to a cohort-specific measure rather than either an age-specific or period-specific measure. Consider, for instance, *Figure 19*, which is similar to *Figure 18* except that cumulative fertility is computed relative to total *cohort* fertility up through age 39. Here, too, the general trend is downward: a greater cumulative proportion of the children born in each successive cohort is born to younger women. For the cohorts born around 1915, half the children were born by age 27, whereas for the 1940 and 1941 cohorts, half the children were born by age 23.

11. Small Multiples

To compare global patterns among several population surfaces it may be useful to shrink contour maps and present several of them on the same page: Tufte (1983) calls this the "small multiples" approach. *Figure 20* presents maps of US birth rates at various parities: in *Figure 20(a)*, first-birth rates (i.e., the proportion of all women of some age in some year who have their first child) are displayed; in *Figure 20(b)*, second-birth rates are displayed, and so on. In each of the small multiples, the same contour levels are used. Because the birth rates shown in these figures are all based on the same denominator at any particular age and time, namely, the total number of women of that age in that year, the maps can in effect be added together to approximate the total birth rate at any age and time; the result is approximate because seventh and higher birth orders are omitted. In other words, the maps decompose total fertility into the contribution made at different parities.

This decomposition indicates that the absolute fluctuations in numbers of first and second children were more significant, in creating the waves of baby booms and busts, than the absolute fluctuations in higher-order births: for both first and second children, fertility rates at the peak age (around 20 for first births and 22 for second births) were about 5% higher around 1960 than they were around 1935, whereas for fourth and higher birth orders, the absolute difference was only 1–2%. As shown in *Figure 5*, the absolute difference between the total fertility rates at age 22 in 1935 and 1960 was about 14%, so that the change in first and second birth rates accounted for roughly two thirds of the total change.

One aspect of the recent baby boom that is strikingly revealed by the maps in *Figure 20* is that the peak of the boom occurred around 1960 for all six parities, at ages that drift upward from about 20 in the case of first births to about 30 in the case of sixth births. The maps also show the recent trend toward greater first- and second-birth rates among women in their late 20s and in their 30s, although fourth- and higher-order birth rates for these women (as well as women at other ages) continue to decline. In general, the maps provide further evidence of the importance of age and period effects, but substantial cohort effects are not apparent.

The six small multiples shown in *Figure 20* are included on the computer diskette (see page 3), together with a program that displays the maps in sequence, either slowly or quickly, as a kind of demographic movie. The movie is not only visually striking, but also informative. In particular, movement in the cohort direction is apparent, as it should be since a woman cannot have her third child until after she has had her second child.

Figure 21 presents another illustration of the use of small multiples, this time to compare mortality rates from age 15 to 49 for years 1910 to 1965 for Italian, French, and Belgian males and females. The effects of World Wars I and II are most prominent in this period and for these ages; the maps graphically depict the different impact of the two wars among the two sexes in the three countries. The diagonal swath of high mortality for Italian males [*Figure 21*(*a*)] born around the turn of the century, discussed earlier, does not show up on any of the other maps in *Figure 21*. The prevalence of many small blocks on the Belgian maps [*Figure 21*(*c*) and *21*(*d*)] indicates some scattered noise or local fluctuations, perhaps attributable to the smaller size of the Belgian population compared with that of Italy or France or to irregularities in the available mortality data.

Figure 22 displays relative mortality rates for males and females in England and Wales, Sweden, and Italy from age 5 to 79 for years 1870 to 1978. In each case, the mortality rate for a given age is relative to the rate at that age in 1870. Thus, the maps provide a picture of the pattern of progress made in reducing mortality rates since 1870. They are analogous to the tables with rough contour lines in Kermack *et al.* (1934); Preston and van der Walle (1978) and Coale and Kisker (1985) present similar tables. These analysts ascribe the diagonal contours in their tables to cohort effects.

The maps in *Figure 22* provide a richer, more detailed picture of the various local and global patterns in the changes in mortality rates, in vertical, horizontal, and diagonal directions. Some diagonal trends are evident, especially for females in England and Wales [*Figure 21*(*f*)], but it is also evident that age and period effects play a substantial role in the evolution of mortality. The light rectangles in the lower right corners of all six maps show the rapid progress in reducing mortality at younger ages since World War II; the darkness of the remaining three quadrants of the maps displays the slow rate of progress at older ages and during earlier years. Note that the light rectangles in the lower right corners are divided, for males but not for females, by a a darker stripe, indicating relatively slow progress against mortality at, roughly, ages 16 to 20.

The maps in *Figure 22* for the three countries were produced using different kinds of data. As noted earlier, mortality rates for Italy were available for single years of time and age. For Sweden, the rates were generally available for five-year periods; before 1880 the rates were for five-year age categories and afterward for single years of age. Finally, for England and Wales, the rates were available for five-year age categories for single years of time about once per decade. Differences in the smoothness of the maps, especially for England and Wales compared with Italy, are probably largely attributable to these differences in data richness.

In the analyses of Kermack *et al.* (1934), Preston and van der Walle (1978), and Coale and Kisker (1985), Mortality rates were taken relative to a period earlier than 1870, the underlying assumption being that at an early enough period there would have been no systematic pattern of progress against mortality. *Figure 23* shows mortality rates for Swedish males (*a*) and females (*b*) relative to the average levels at each age in the period from 1778 to 1799. The figure reveals the fluctuating pattern of mortality before the middle of the nineteenth century and the general pattern of progress against mortality subsequently. The pattern is clearly more complex than a pure cohort-effect model would suggest.

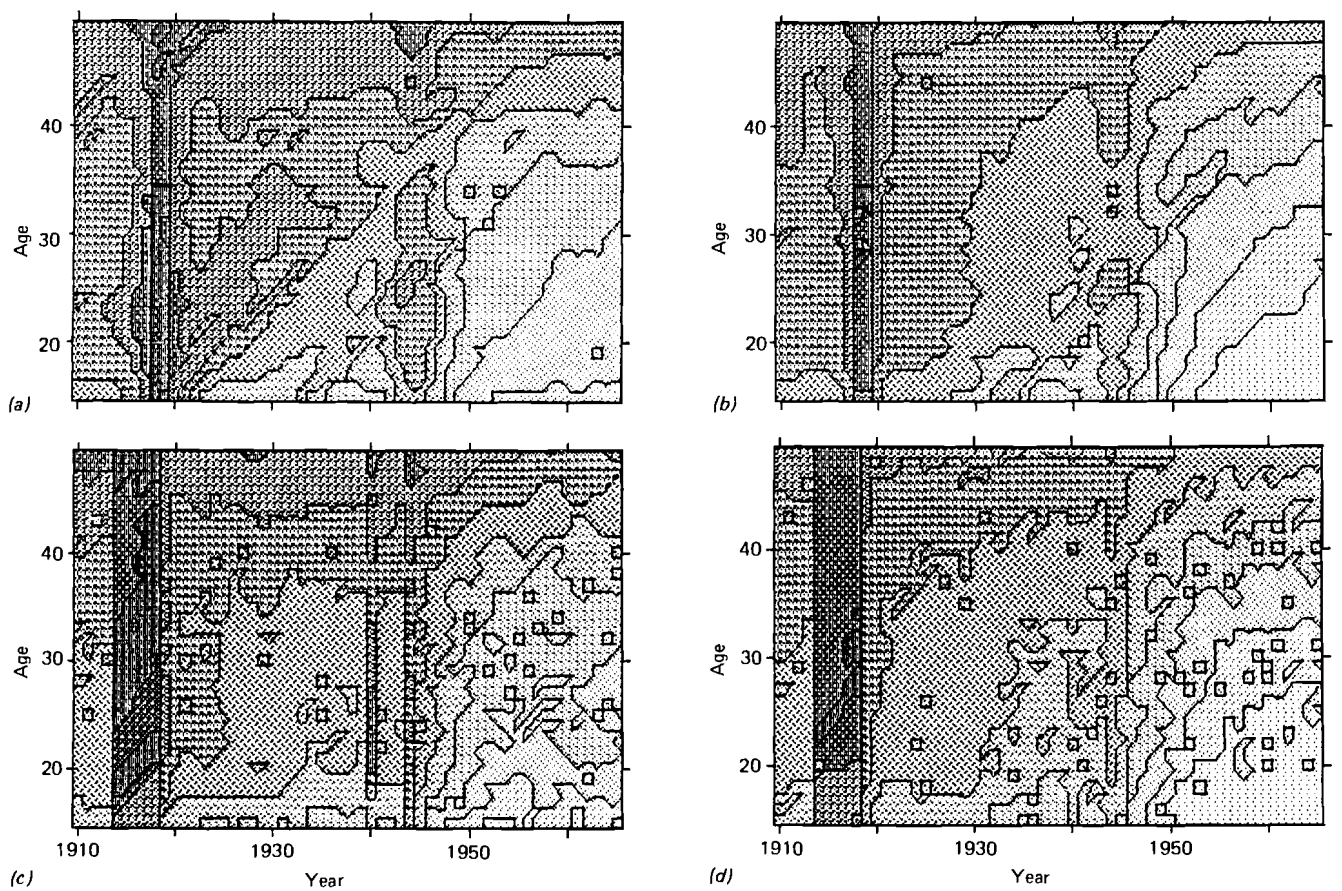

Figure 21. Mortality rates, with contour lines from 0.000667 to 0.195 at multiples of 1.5, and from age 15 to 49 and year 1910 to 1965: (*a*) Italian male; (*b*) Italian female; (*c*) Belgian male; (*d*) Belgian female; (*e*) French male; (*f*) French female.

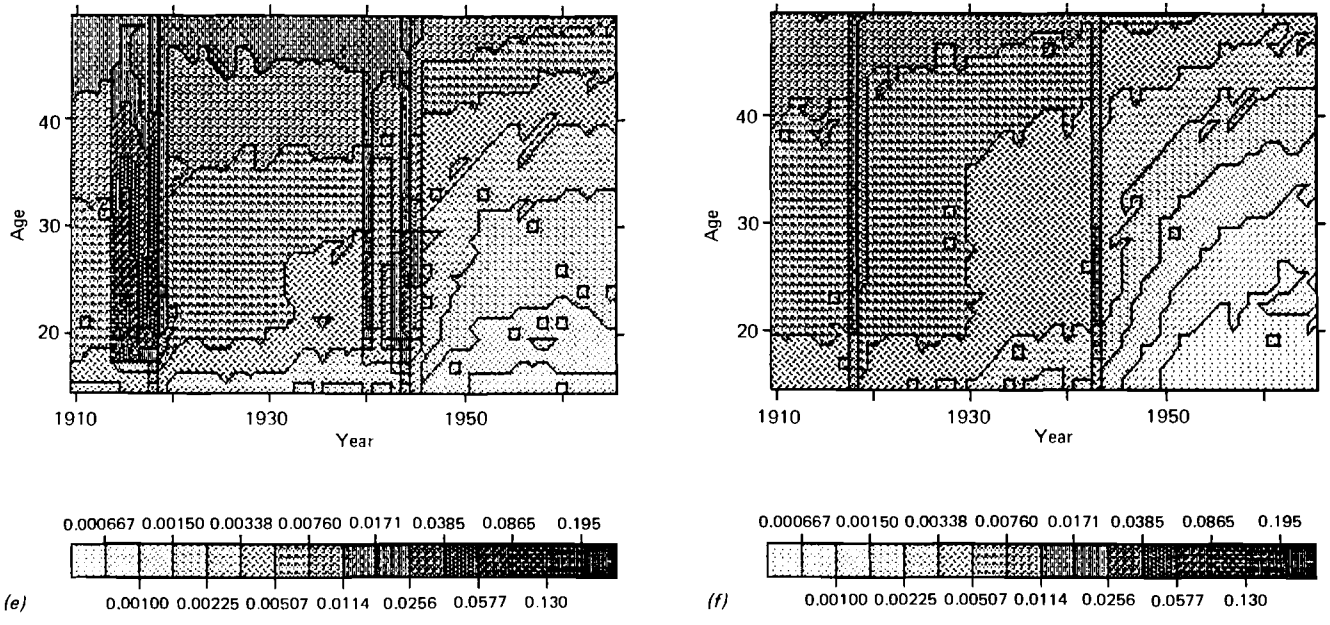

Figure 21 (continued)

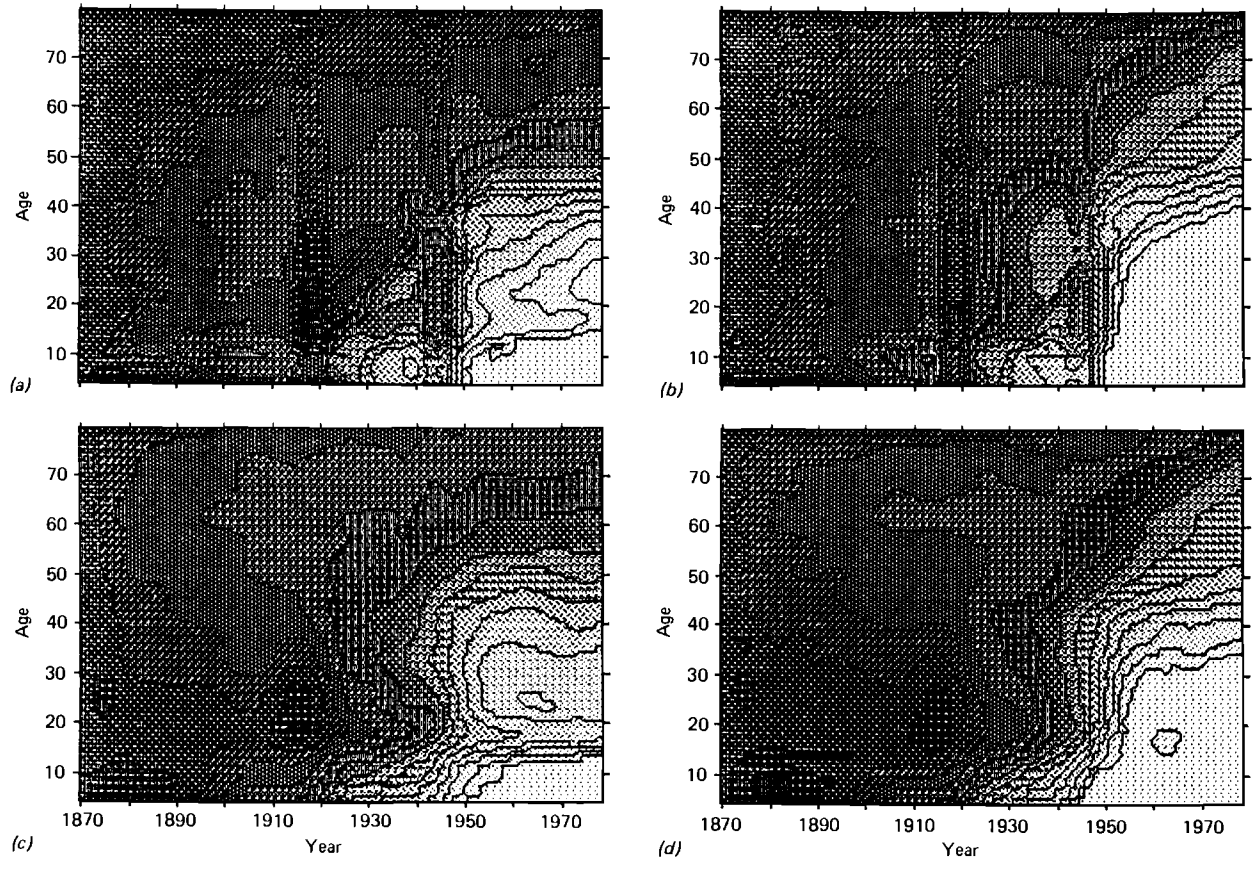

Figure 22. Mortality rates relative to 1870 age-specific levels, with contour lines from 0.100 to 1.284 at multiples of 1.2, smoothed on a 5 × 5 square, and from age 5 to 79 and year 1870 to 1978: (*a*) Italian male; (*b*) Italian female; (*c*) Swedish male; (*d*) Swedish female; (*e*) English and Welsh male; (*f*) English and Welsh female.

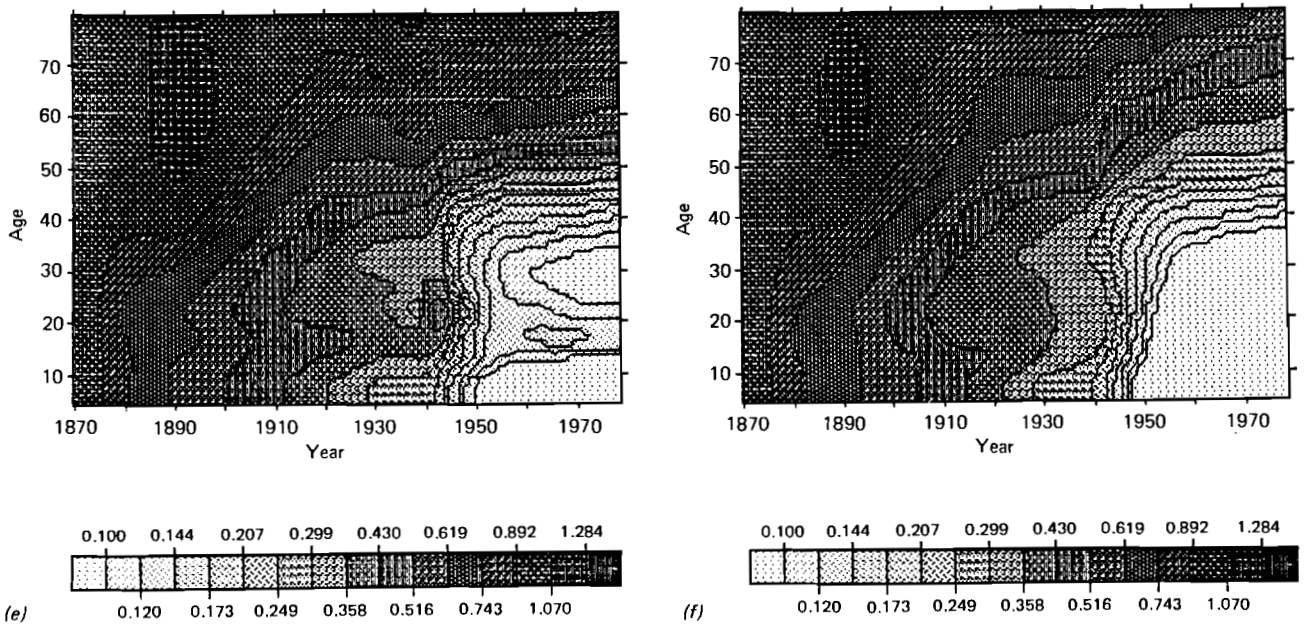

Figure 22 (continued)

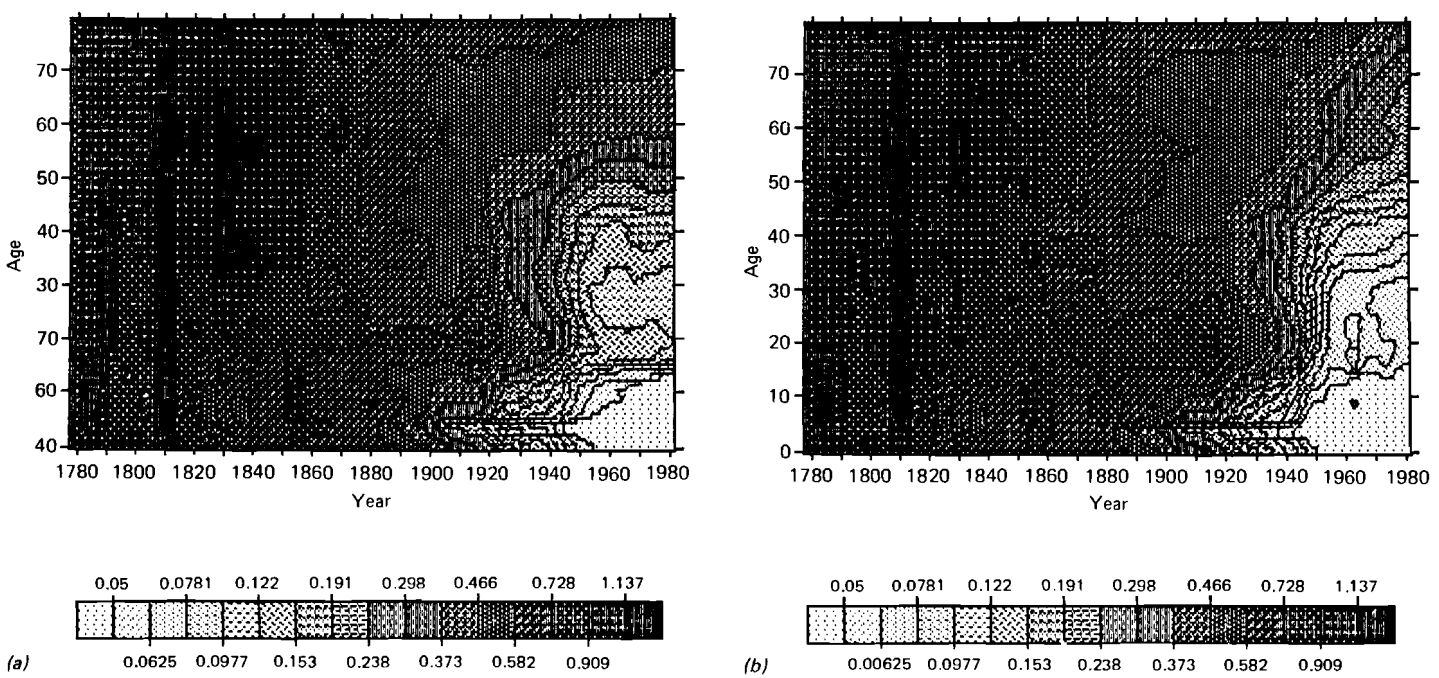

Figure 23. Swedish mortality rates relative to age-specific levels from 1778 to 1799, with contour lines from 0.05 to 1.137 at multiples of 1.15, smoothed on a 5 × 5 square, and from age 0 to 79 and year 1778 to 1981: (*a*) male; (*b*) female.

A direct way of considering the hypothesis that "a cohort carries its mortality level with it" is to examine mortality surfaces that are calculated relative to a cohort's mortality levels. In *Figure 24*, for instance, in each of the six surfaces shown the mortality rate at each age and year was divided by the mortality rate at that age for the cohort born in 1870. The pattern that emerges shows some strong diagonals, but it is apparent that there are also important effects in the horizontal and vertical directions. Interpretation of these and similar surfaces should also be tempered by the realization that diagonal patterns can emerge not only as a result of cohort effects, but also as the result of the interaction of period and age effects.

12. Ratio Surfaces

Instead of using small multiples or computer movies, another approach to comparing two or more demographic surfaces is to compute some new surfaces that represent at every point either the difference or the ratio of the height of one of the original surfaces to another. *Figure 25(a)*, for instance, shows the ratio of male to female mortality rates in Italy, smoothed on a 5 × 5 square. To highlight the ages and periods when Italian male and female mortality rates were roughly equal, *Figure 25(b)* presents a modified version of this map in which only three contour lines are drawn, for equal male and female death rates and for levels 10% above and below equality. The two figures reveal the worsening discrepancy between male and female mortality. In 1870, male and female mortality rates were roughly comparable at most ages, female mortality being somewhat more than 10% higher than male mortality around age 30 and male mortality being somewhat more than 10% higher than female mortality around age 50. By 1979, female mortality was substantially less than male mortality at all ages, being only half as high as male mortality between ages 15 and 30 and again between ages 40 and 70.

Two further ratio surfaces are presented in *Figures 26* and *27*. *Figure 26* displays the ratio of Italian male mortality to French male mortality from age 10 to 70 for years 1900 to 1960. The ratio fluctuates busily, producing the large number of contour lines shown in *Figure 26(a)*; in *Figure 26(b)* the surface is smoothed over weighted 5 × 5 squares. Like two hollow eyes in a skull, the black rectangles reveal the greater toll of death among young French males relative to young Italian males during World Wars I and II. The lighter shades on the bottom of the maps, under age 20 or so before World War I and after World War II, and under about age 35 between the wars, show when French males were experiencing less mortality than their Italian counterparts; at older ages, it is the Italians who have the advantage.

Figure 27 shows the difference, in the USA, between first and second birth rates, i.e., the proportion of all women of some age at some time who are having their first child minus the proportion who are having their second child. The most striking feature of the figure is the rapidity of the shift from the predominance of first births to the predominance of second births, as indicated by the dark horizontal swath giving way to a light swath. The midpoint of this shift is described by the contour at level zero running across the map at roughly age 25. The contour

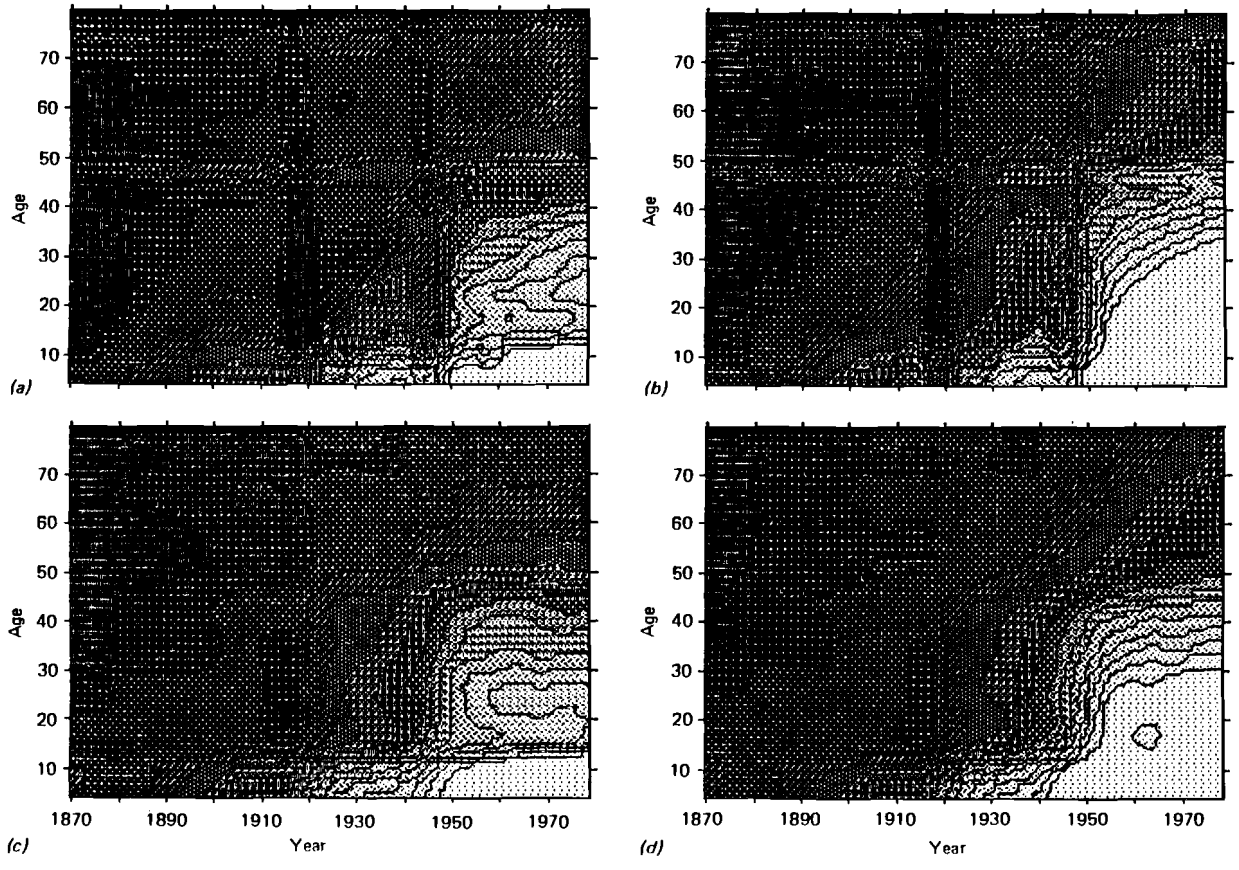

Figure 24. Mortality rates relative to 1870 age-specific cohort levels, with contour lines from 0.1 to 1.283 at multiples of 1.2, smoothed on a 5 × 5 square, and from age 5 to 79 and year 1870 to 1978: (*a*) Italian male; (*b*) Italian female; (*c*) Swedish male; (*d*) Swedish female; (*e*) English and Welsh male; (*f*) English and Welsh female.

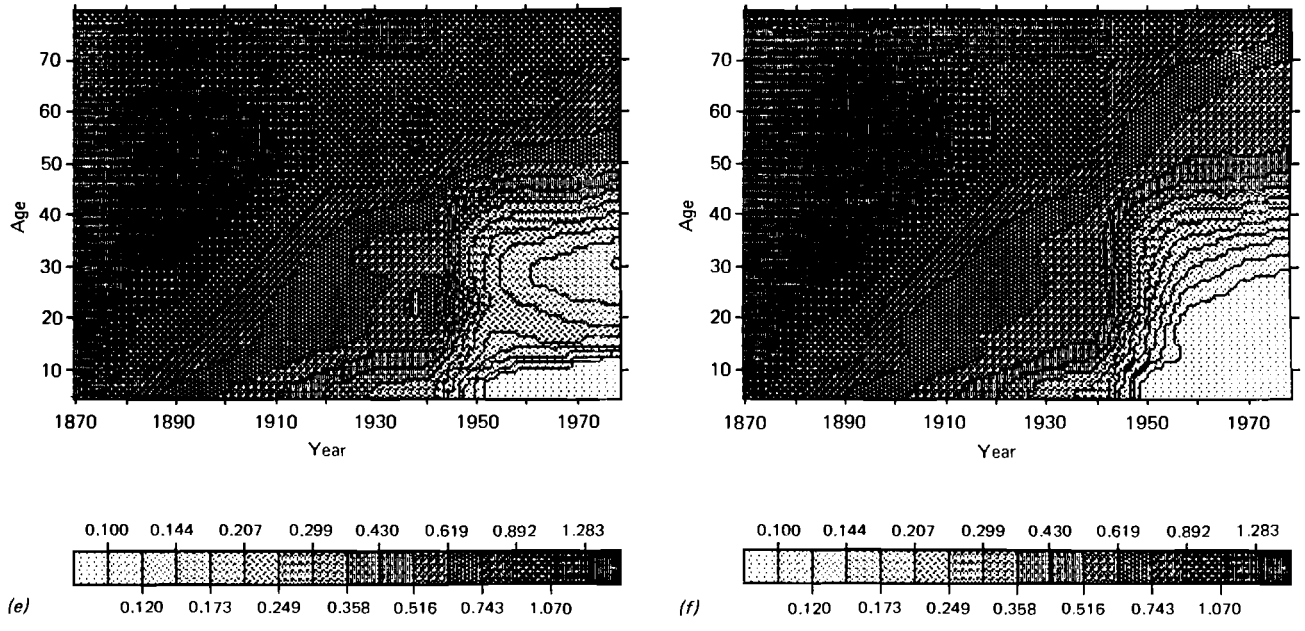

Figure 24 (continued)

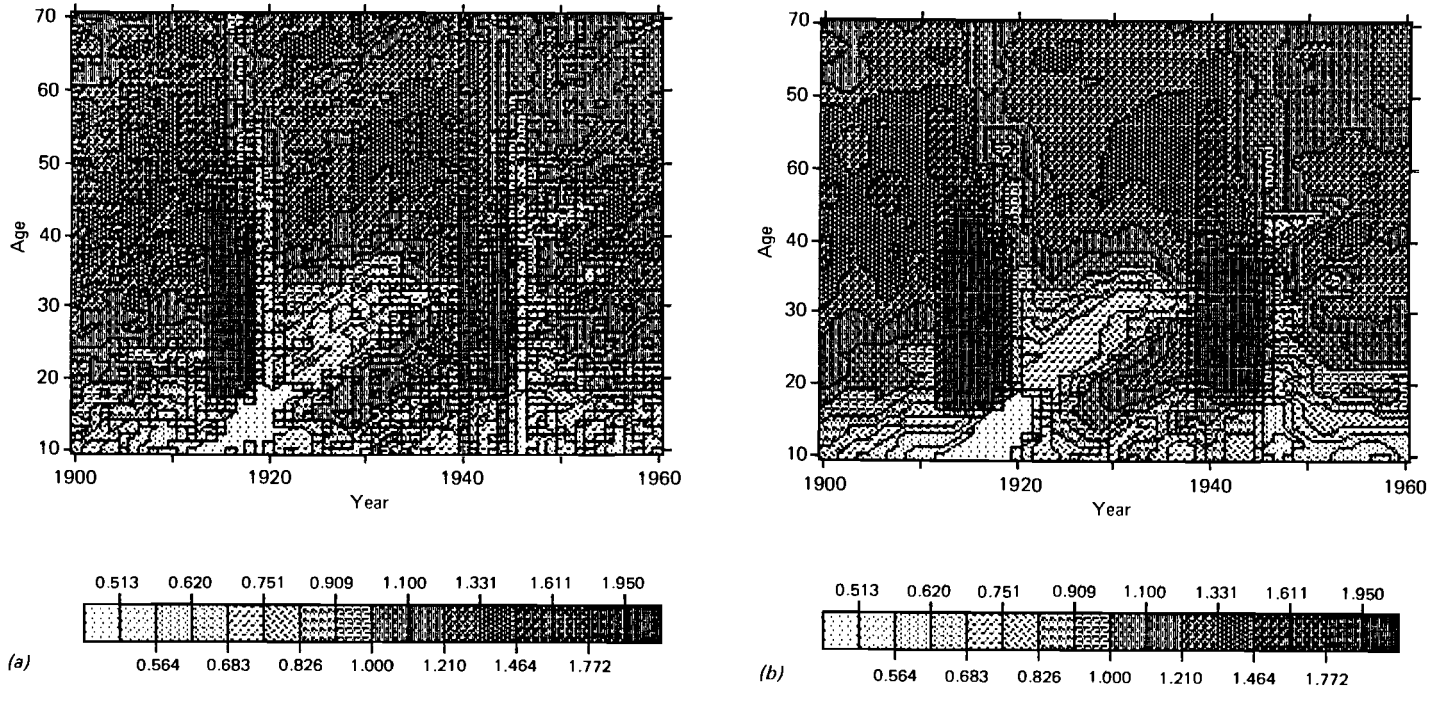

Figure 25. Italian female mortality rates divided by Italian male mortality rates, smoothed on a 5 × 5 square, and from age 0 to 79 and year 1870 to 1979: (*a*) with contour lines at multiples of 1.1 from 0.513 to 1.95; (*b*) with *selected* contour lines from 0.513 to 1.95.

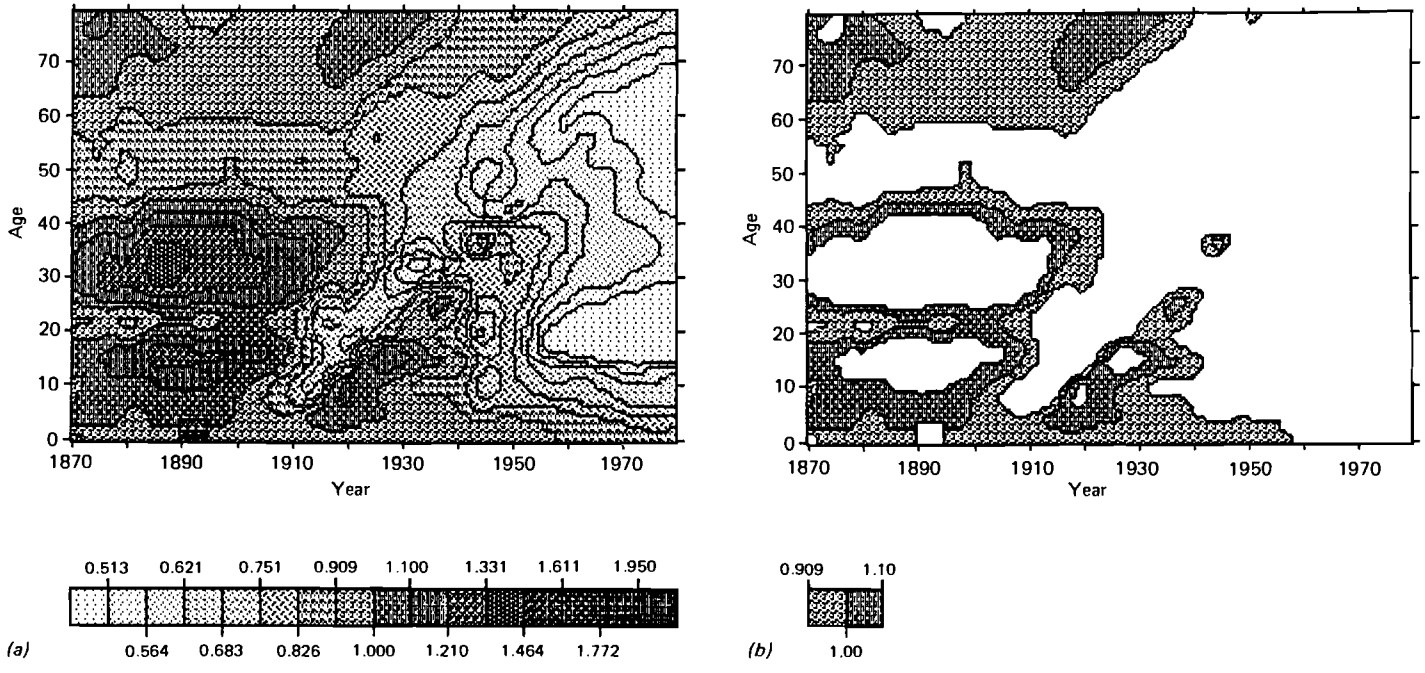

Figure 26. French male mortality rates divided by Italian male mortality rates: (*a*) with contour lines from 0.513 to 1.950 at multiples of 1.1, and from age 10 to 70 and year 1900 to 1960; (*b*) (*a*), but smoothed on a weighted 5 × 5 square.

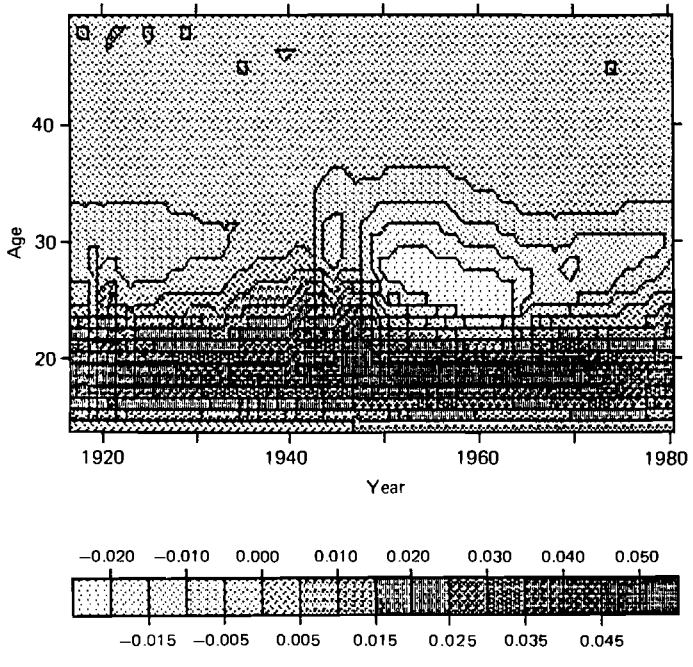

Figure 27. US fertility at parity 1 minus that at parity 2, with contour lines from −0.020 to 0.050 at intervals of 0.005, and from age 14 to 49 and year 1917 to 1980.

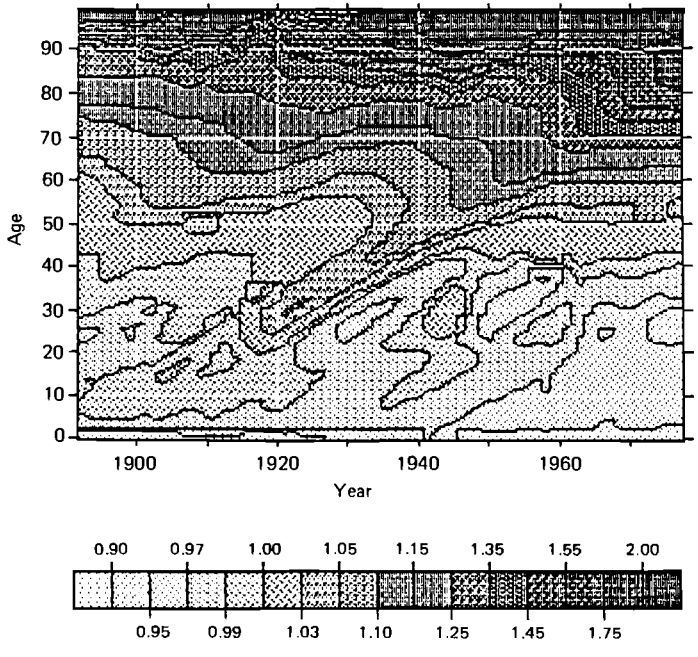

Figure 28. Belgian female population divided by Belgian male population, with contour lines selectively placed from 0.90 to 2.00, smoothed on a 5 × 5 square, with a grid, and from age 0 to 99 and year 1892 to 1977.

reaches a peak at age 30 in 1940 and falls to age 22 in 1960. In 1960, at the center of the baby boom, the shift from first births to second births is not only early, but also especially dramatic.

13. Sex Ratios, Nuptiality, and Cause-Specific Mortality

In addition to maps of death rates, birth rates, and population levels, contour maps can be drawn based on any other kind of data that is structured along two dimensions. *Figures 28*, *29*, and *30* suggest three possibilities. *Figure 28* displays the ratio of males to females in Belgium, based on Veys' (1983) data. An interesting contour to follow on the map is the contour at level 1: at ages below this line, males outnumber females, and at older ages females predominate. The line starts at age 43 in 1892, rapidly falls to age 20 during World War I, gradually rises back to age 43 or so by the mid-1940s, and then remains at roughly this age up through 1977. A striking feature of the map as a whole is the increasing predominance of females at older ages. Even in 1892, there were 25% more females than males at age 85, but by 1977 there were close to twice as many females than males at this age.

Figure 29 shows age-specific marriage rates for Chinese females, based on Zeng *et al.* (1985). The rates in *Figure 29(a)* give the proportion of women at different ages and times who marry; the denominator is not the number of unmarried women, but the total number of women. The rates in *Figure 29(b)*, on the other hand, are conditional first marriage rates: the denominator is the number of unmarried women. Since the conditional rates were somewhat noisy, we smoothed them on a weighted 3×3 square.

The most striking pattern on the Lexis map in *Figure 29(a)* is the shift upward in age of first marriage. It is apparent from the map that marriage in China is concentrated in a short period of age. Consider, for example, the ages when female first marriage rates exceed 10%. The period of high marriage rates shifted from ages 16 through 19 in the early 1950s, to ages 18 through 21 around 1970, and to ages 20 through 25 around 1980. As a result of this shift, the proportion of women who marry at age 17 fell from close to 20% in 1950 to about 2% around 1980, whereas the proportion who marry at age 23 rose from 2% to over 20%.

The darker areas on the map in *Figure 29(b)* represent ages and years when more than 40, 50, or even 60% of the unmarried women married. The tremendous spurt in marriages in 1980 and 1981 of women in their mid-20s who had delayed marriage is marked by a prominent black splotch. Among the cohort of women born in 1955, more than sixty percent of those who were still unmarried in 1980 (at age 25) married and more than 60% of the remainder married in 1981: more than 90% of the women who were not married at the start of the two-year period were married by the end of it.

Comparison of *Figures 29(a)* and *29(b)* reveals some interesting differences between the patterns of unconditional and conditional marriage rates. Since the conditional rates equal the unconditional rates divided by the proportion never married, the conditional rates have to be higher than the unconditional rates. Nonetheless, it is somewhat startling how much higher they are, especially at older

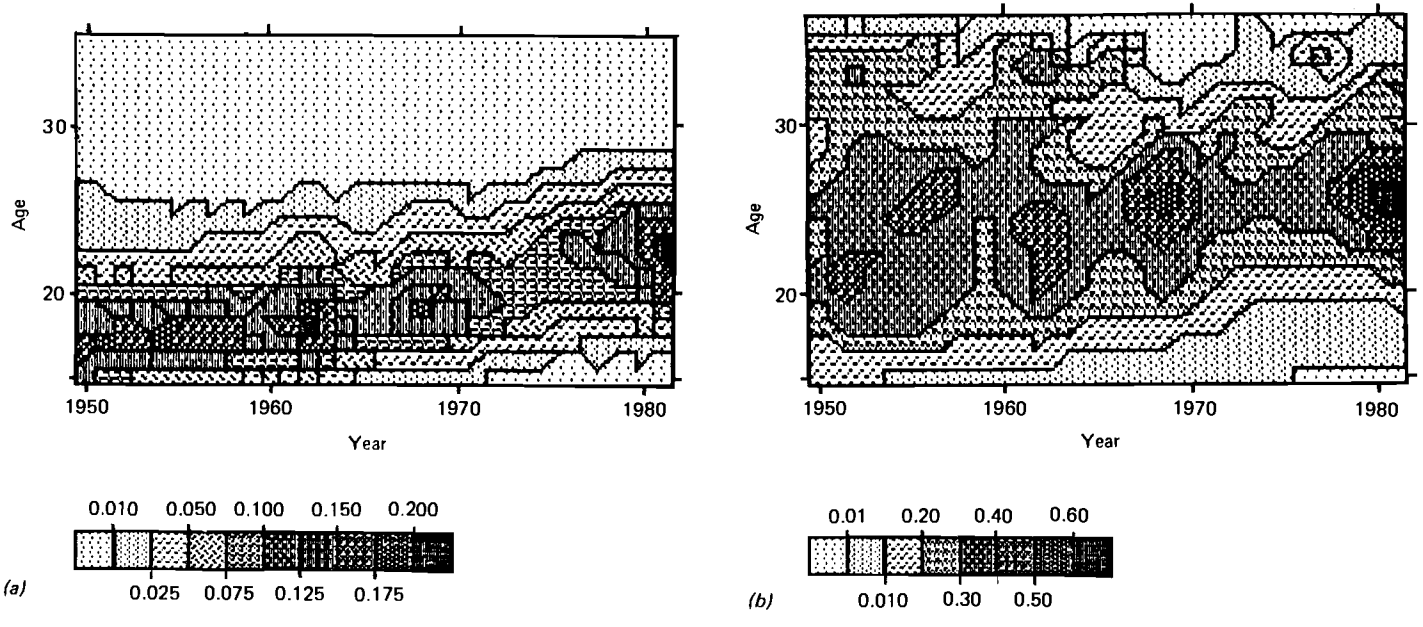

Figure 29. Chinese female first marriage rates: (*a*) from age 15 to 35 and year 1950 to 1981; (b) smoothed and conditional (see text).

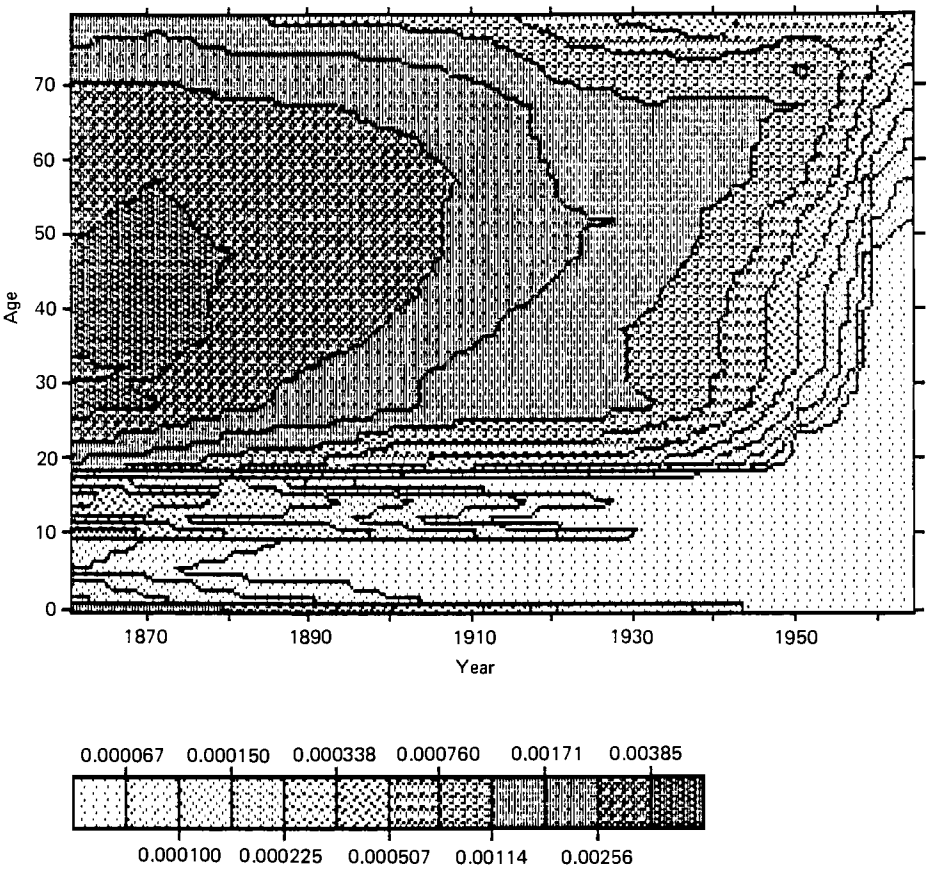

Figure 30. English and Welsh male tuberculosis mortality rates, with contour lines from 0.000067 to 0.00385 at multiples of 1.5, and from age 0 to 79 and year 1861 to 1964.

ages. The durable pattern of universal marriage in China implies that women in their late 20s who are not married as yet have a high chance of marrying. Consider age 25 through 28, for instance. A swath of dark shades runs across *Figure 29(b)*, indicating conditional marriage rates ranging from 20% to above 60%, averaging about 40% per year. For every cohort shown on the map, at least 90% of the women who were not married at age 25 marry by the end of age 28.

Contour maps can also be used to display surfaces of cause-specific mortality. In *Figure 30*, for instance, rates of male mortality in England and Wales from tuberculosis are displayed for 80 years of age over about a century of time; the map is based on interpolations of data from Keyfitz and Flieger (1968). The high toll of mortality exacted by tuberculosis in the middle ages of life, especially from 30 to 60, is apparent on the map, as is the acceleration of progress against tuberculosis after

World War II. Each contour line is 50% higher than the next, so this progress was very rapid indeed. Note also that there seems to be some evidence of cohort effects interacting with the period trend.

14. Life Table Statistics for Belgian Females

Life tables often provide statistics by age and over time on population size, number of deaths, death rates, period survivorship, period life expectancy, and sometimes cohort survivorship. All six of these statistics are available, for example, in Veys' (1983) compilation of Belgian life tables from age 0 to 99 for years 1892 to 1977. *Figures 31* through *36* use Veys' data for Belgian females to illustrate the different kinds of contour map patterns produced by different kinds of life table statistics. The differences in the patterns are quite striking, each kind of population statistic producing what might be called its characteristic pattern, its fingerprint:

(1) Lexis surfaces of population level (*Figure 31*) tend to show strong diagonals at younger ages, bending over toward horizontal lines at advanced ages.

(2) Surfaces of deaths (*Figure 32*) tend to be marked by two ridges running over time, one ridge (a cliff, really) highest in infancy, the other highest around age 70 or 80. As progress is made against mortality, the first ridge declines, but the second rises: deaths become increasingly concentrated around age 80. Perpendicular ridges mark periods of devastation, like World War I and its aftermath.

(3) Mortality rates (*Figure 33*) lie in a valley between two steep walls of high mortality in infancy and at advanced ages. Again, perpendicular ridges mark disasters. Over time, as progress is made against mortality, the valley slopes off, most rapidly at younger ages, producing contours that sometimes look like a flattened S and sometimes like a U turned sideways.

(4) Survivorship (*Figures 34* and *35*) and life expectancy (*Figure 36*) fall off with age, more slowly in recent years because of the progress that has been made against mortality. Depending on the axes, there are either strong diagonals, gradually becoming less steep with age [when cohort survivorship is plotted over current year, (*Figure 35(a)*], or flatter diagonals, again becoming even flatter with age. The maps of survivorship and life expectancy tend to be smoother than the maps of deaths and mortality rates, the life expectancy maps being the smoothest. This is to be expected: life expectancy can be considered a kind of average of survivorship figures, and survivorship an average of mortality rates. Moreover, the cohort maps tend to be smoother than the period maps, since the cohort maps average out period effects.

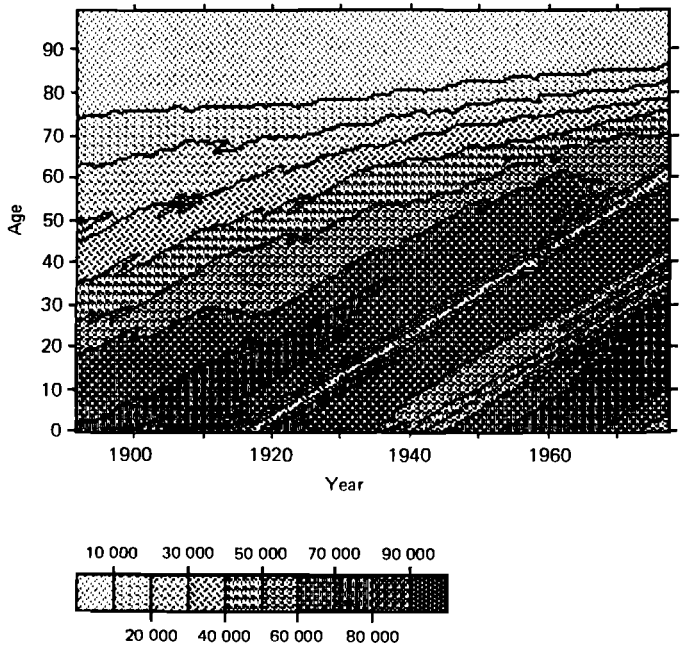

Figure 31. Belgian female population for single year of age and time, with contour lines from 10 000 to 90 000 at intervals of 10 000, and from age 0 to 99 and year 1892 to 1977.

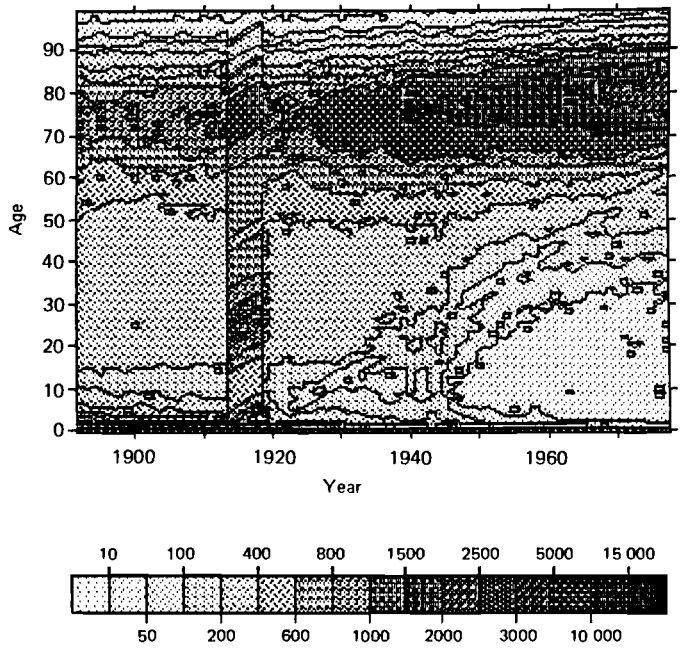

Figure 32. Belgian female deaths, with contour lines selectively placed from 10 to 15 000, and from age 0 to 99 and year 1892 to 1977.

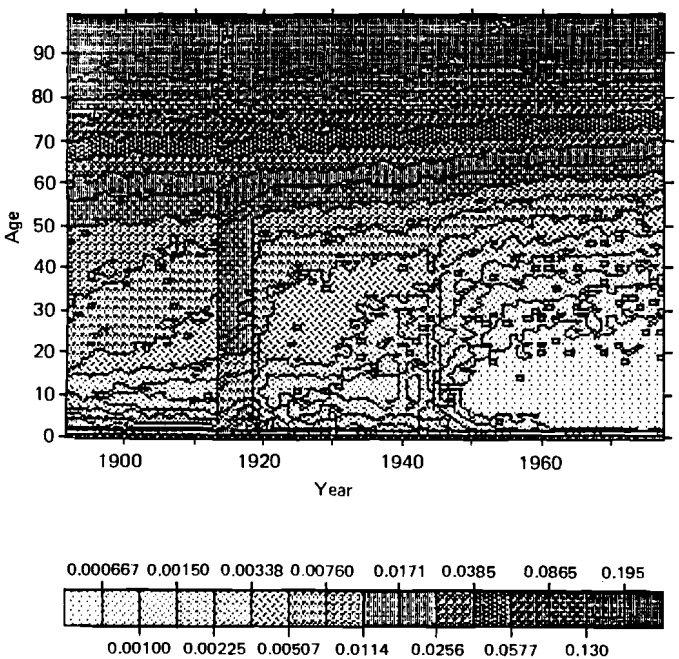

Figure 33. Belgian female mortality rates, with contour lines from 0.000667 to 0.195 at multiples of 1.5, and from age 0 to 99 and year 1892 to 1977.

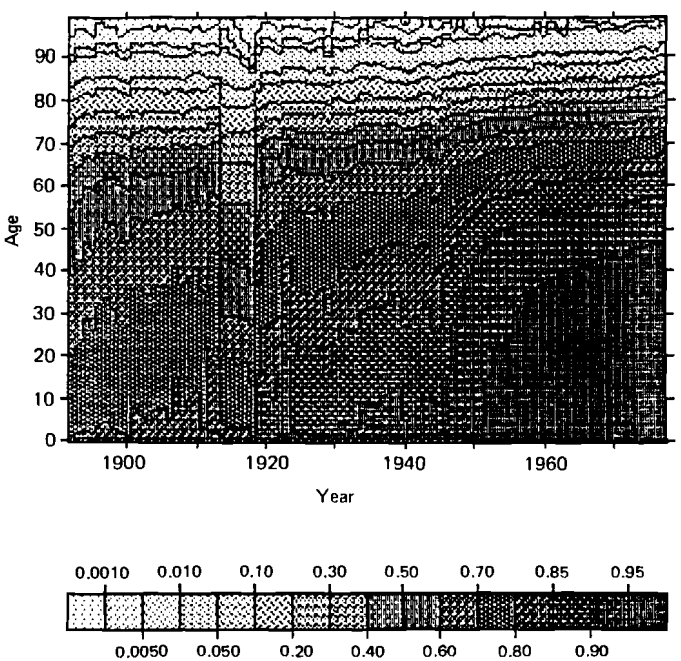

Figure 34. Belgian female period survivorship, with contour lines selectively placed from 0.001 to 0.95, and from age 0 to 99 and year 1892 to 1977.

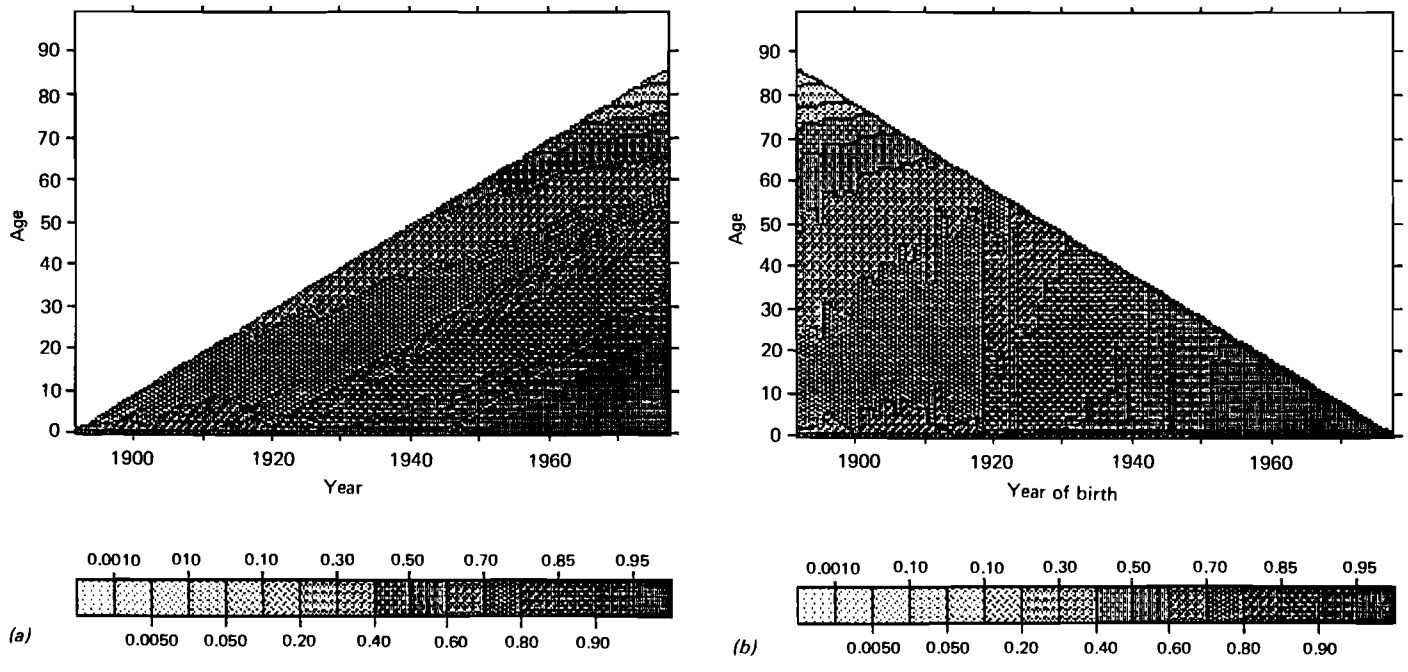

Figure 35. Belgian female cohort survivorship, with contour lines selectively placed from 0.001 to 0.95, and from age 0 to 99 and year 1892 to 1977: (*a*) by current year and age; (*b*) by year of birth and age.

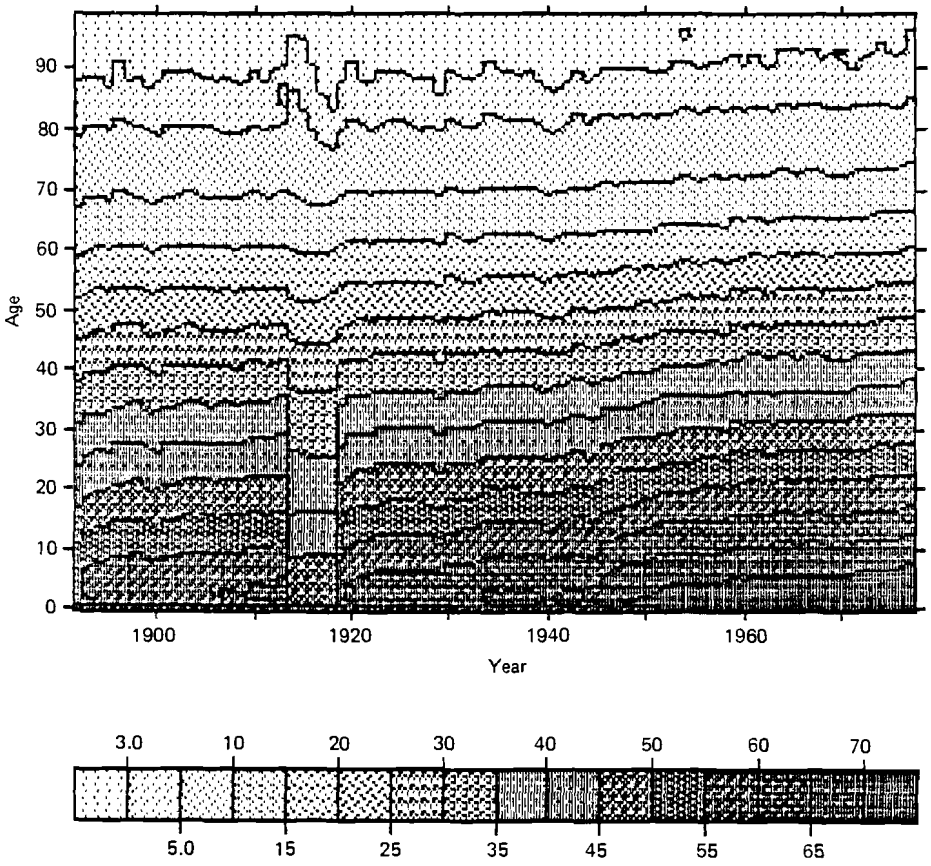

Figure 36. Belgian female period life expectancy, with contour lines selectively placed from 3 to 70, and from age 0 to 99 and year 1892 to 1977.

15. US Female Mortality Rates from 1900 to 2050

Faber (1982) published life tables for US males and females by single year of age from birth to 119 for every 10th year from 1900 through 2050. The mortality rates at advanced ages and after 1980 are based on extrapolations. *Figure 37(a)* displays the surface of the force of mortality for US females. Note that the Lexis map graphically reveals Faber's underlying assumption that progress against mortality will slow down in the future.

In *Figure 37(b)*, the Lexis map is suppressed after 1980, leaving a white area that the reader might wish to use to draw his or her own projections. Two sample results are shown in *Figures 37(c)* and *37(d)*: the map in *Figure 37(c)* was drawn by Yashin and the optimistic map in *Figure 37(d)* was drawn by Vaupel. Faber's projections imply a life expectancy for US females of 83.8 years at 2050 mortality rates. Rough calculations indicate that Yashin's projections imply a life expectancy of

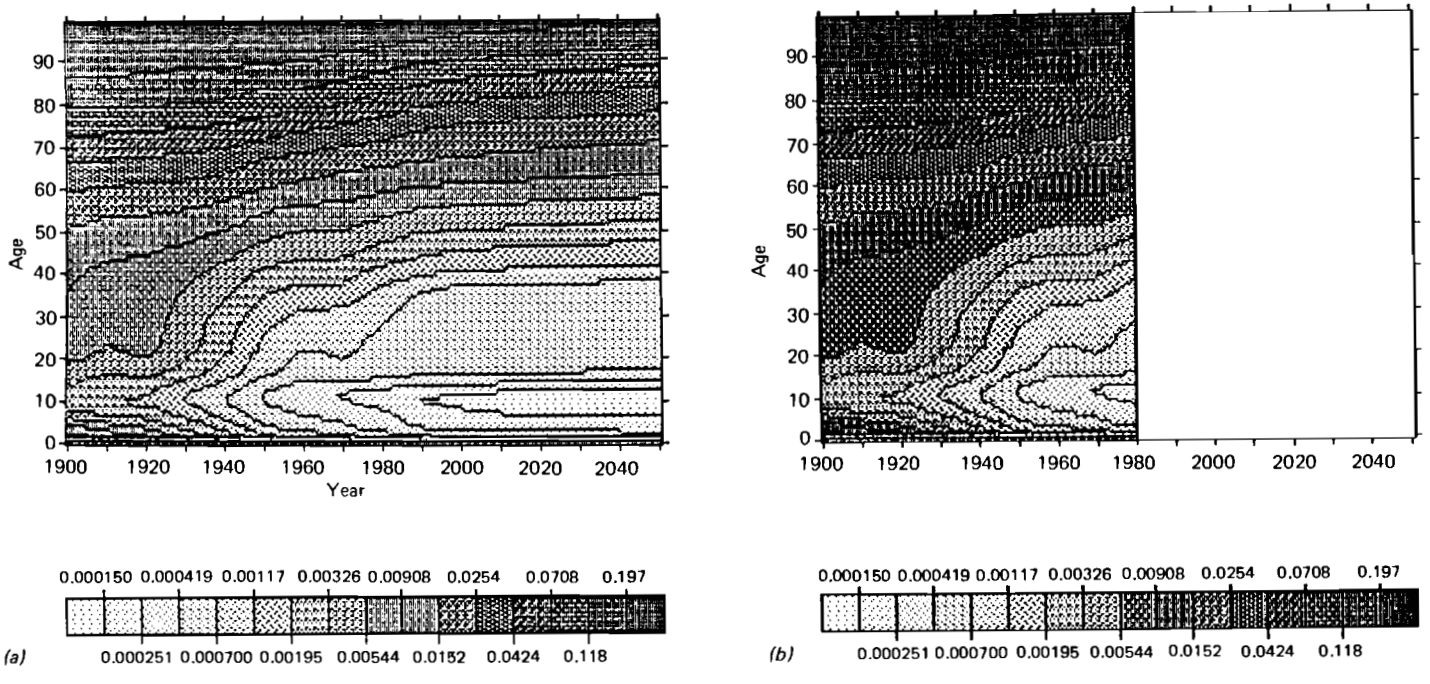

Figure 37. Force of mortality for US females based on Faber (1982) life tables (*a*) with contour lines from 0.000150 to 0.197 at multiples of 1.67, and from age 0 to 99 and year 1900 to 2050; (*b*) As (*a*), but from year 1980 to 2050 is left blank for the reader to draw her or his own projections.

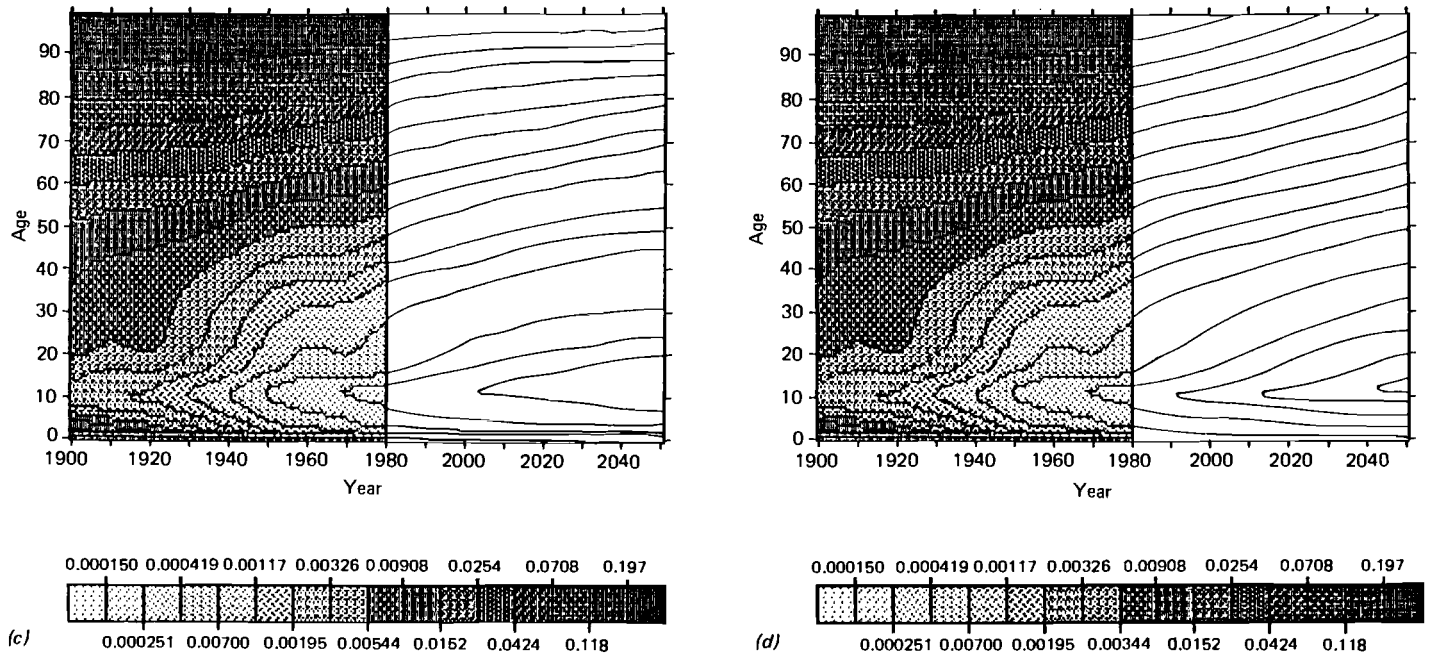

Figure 37. Force of mortality for US females based on Faber (1982) life tables, with contour lines from 0.000150 to 0.197 at multiples of 1.67, and from age 0 to 99 and year 1900 to 1980: (*c*) from year 1980 to 2050 are the projections of A. Yashin, (*d*) from year 1980 to 2050 are the projections of J. Vaupel.

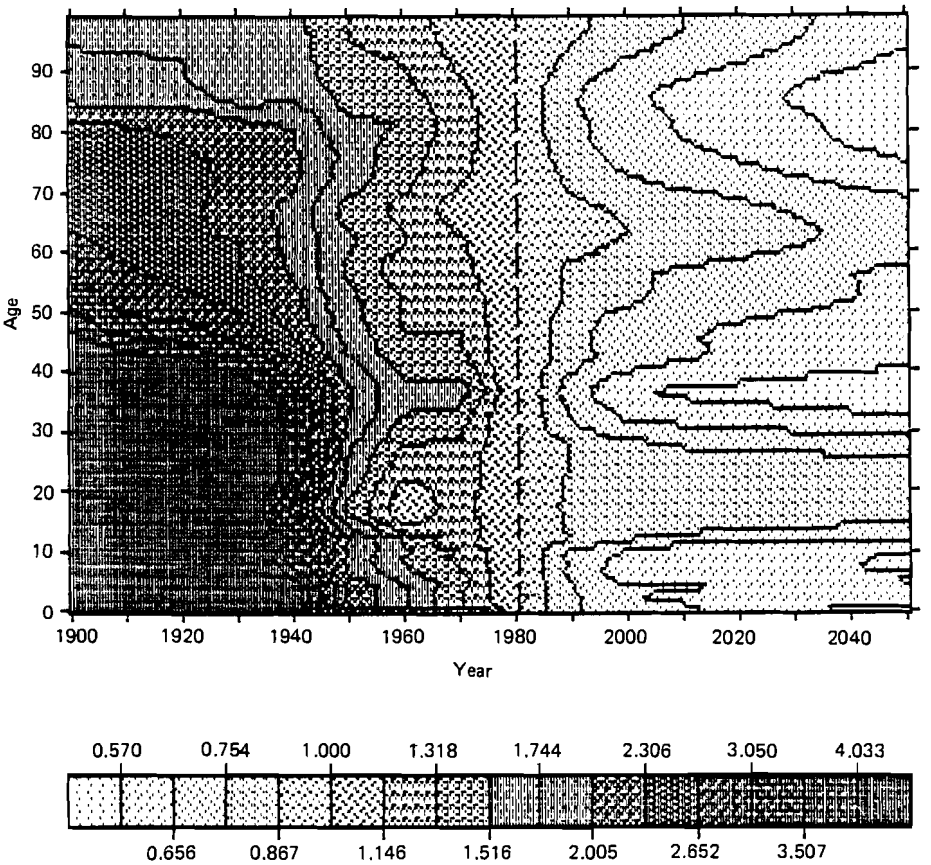

Figure 98. US mortality rates (Faber, 1982) relative to 1980 age-specific levels, with contour lines from 0.570 to 4.033 at multiples of 1.146, and from age 0 to 99 and year 1900 to 2050.

about 87 years, whereas Vaupel's projections imply a life expectancy of fully 98 years. [For some justification of this optimism, see Vaupel and Owen (1985) and Vaupel and Gowan (1986).]

The nature of the assumptions underlying Faber's projections, as given in *Figure 97(a)*, are presented clearly in *Figure 98*, which displays the force of mortality over age relative to the force of mortality in 1980. The right side of *Figure 98* is neither a mirror image of the left side nor a smooth continuation. The left side shows the rapid historical progress that has been achieved against mortality at most ages and the recent acceleration of progress at some ages, especially some of the older ages. The right side portrays a lackluster future, with slow and slowing rates of progress. Perhaps Faber's forecasts can be described as "conservative" in some sense, but they are certainly radically different from the performance of the past.

16. Model Life Tables

Demographers frequently make use of model life tables, especially those developed by Coale and Demeny (1984). In the Coale and Demeny tables, death rates in various age categories are given by the life expectancy of the population, for males and females, and for four different kinds of hypothetical populations, labeled East, West, North, and South. *Figure 39*(*a*)–(*b*) presents contour maps for females of two of these four types: East and West. Note that the horizontal axis gives life expectancy rather than time. Thus, *Figure 39* illustrates the use of a variable other than age or time as one of the dimensions on a contour map.

The most immediately striking feature of the two maps in *Figure 39*(*a*)–(*b*) is their similarity: the differences between the regions seem relatively small compared with the enormous difference resulting from change in life expectancy. It takes careful scrutiny of the maps to reveal the differences between the regions at the same level of life expectancy. But note that the contour lines are drawn at multiples of 1.5: mortality rates at some age and life expectancy on two maps that appear to be similar might differ by as much as 50%. As age increases from 10 to 99 and as life expectancy grows from 20 years to 80 years, mortality rates change by several factors of 1.5; indeed, the highest contour on each of the maps is almost 300 times greater than the lowest contour. For the two regions, at some specific age and life expectancy, mortality rates rarely differ by more than a single factor of 1.5. A factor of 1.5 looks small compared with a factor of 300; but, as users of the Coale and Demeny tables know, a factor of 1.5 may be of crucial significance.

Another approach to the construction of model life tables was developed by Brass (1971). In this approach, a standard trajectory of survivorship proportions, $p(x)$ where x stands for age, is modified by parameters a and b to produce alternative trajectories, $p'(x)$, such that

$$\text{logit}[p'(x)] = a + b\ \text{logit}[p(x)]$$

where the logit function is given by

$$\text{logit}(p) = 0.5\ \log[(1 - p)/p]$$

Given a trajectory of survivorship proportions, a trajectory of forces of mortality (and hence mortality rates) can be readily calculated. *Figure 40*(*a*)–(*d*) illustrates how the values of parameters a and b affect the resulting age-specific force of mortality: parameter a runs along the horizontal axis of each map and the four maps represent different values of b. The maps are consistent with the interpretation of a and b offered by Brass (1971); [see also Ewbank *et al.* (1983) and Zaba (1979)], namely that the parameter a essentially determines the level of mortality, whereas the parameter b changes the rate at which mortality increases with age: the higher b is, the sooner a particular level of mortality is reached (at any value of a).

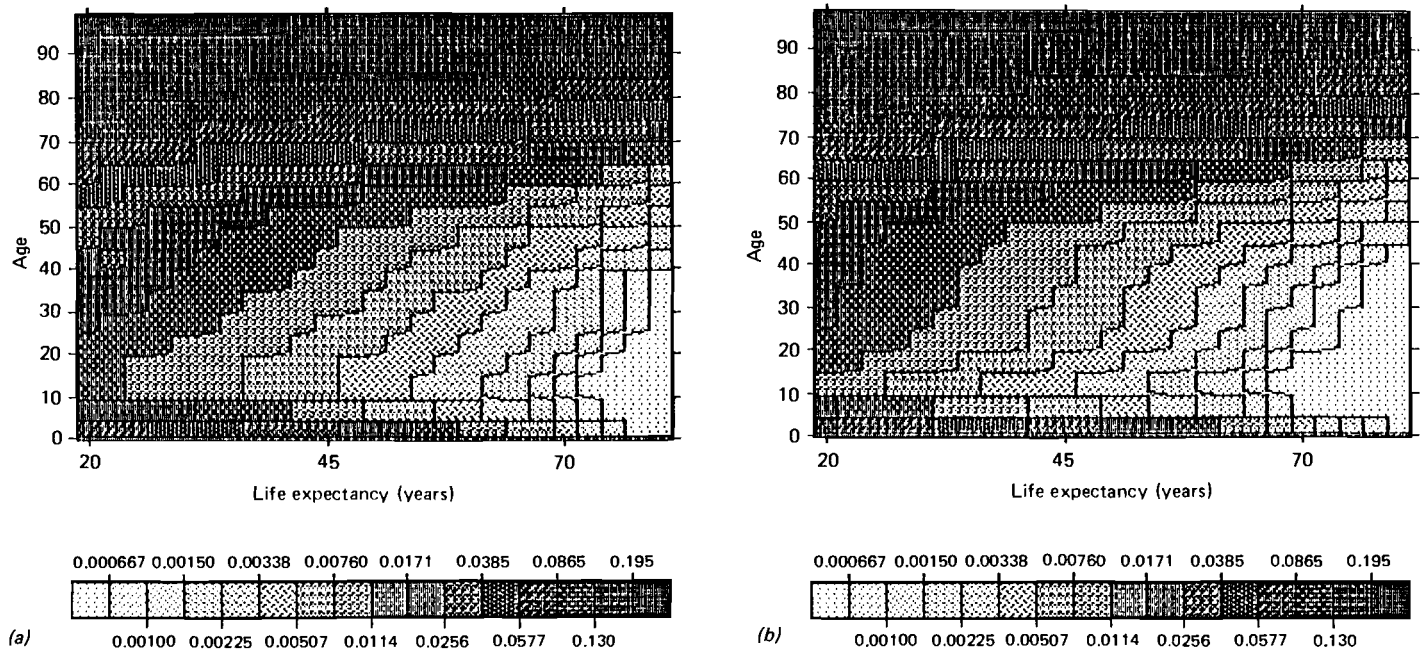

Figure 39. Death rates from the Coale and Demeny (1984) model data, with contour lines from 0.000667 to 0.195 at multiples of 1.5, and from age 0 to 99 and life expectancy 20 to 80: (*a*) hypothetical East region; (*b*) hypothetical West region.

17. Mapping Residuals to Show Goodness of Fit

How well does a model fit some empirical data? If the data are defined over two dimensions, then a contour map can be used to display the residuals, i.e., the differences between the actual values and the values predicted by the model. By scrutinizing the pattern of the residuals, an analyst may glean some clues as to how to improve the model. [Tukey (1977) and Mosteller and Tukey (1977) provide clear discussions of the use of residuals in data analysis and model building.]

As an illustration of this general method, *Figure 41*(*a*)–(*d*) show how well a modified form of Brass's (1971) model fits Italian female mortality data. The modification made involves the use of 1926 Italian female mortality rates as the standard rather than Brass's original standard; these mortality rates were used because 1926 seemed to be an average year, roughly halfway through the transition from high mortality to lower mortality. *Figure 41*(*a*) displays the actual values of Italian female mortality rates and *Figure 41*(*b*) displays the values estimated by the modified Brass model. *Figure 41*(*c*) displays the surface of residuals, i.e., the surface of d equal to $q - q'$, where q is the observed mortality rate and q' is the mortality rate predicted by the modified Brass model. Different values of a and b in the model were estimated for each year of time. The values used for a and b are displayed in *Figure 41*(*d*).

The values of a and b were calculated to minimize the sum of the squared deviations of Brass's model from the transformed data, using the logit formulas given above. As shown in *Figure 41*(*d*), the values of a have increased almost linearly over time, the trend being interrupted only during World Wars I and II. The values of b, on the other hand, were fairly stable until World War II, with a notable peak during World War I, and then increased substantially. The value of a, as indicated earlier in conjunction with *Figure 40*(*a*)–(*e*), can be interpreted as describing the overall level of mortality: as a increases, the level of mortality decreases. The value of b can be interpreted as determining the rate at which mortality increases with age: the higher is b, the higher are the mortality rates at later ages compared with the rates at younger ages. This interpretation of a and b is consistent with the pattern of Italian female mortality shown in *Figure 41*(*a*). Note in particular that after 1945 mortality rates at younger ages, age 30 say, increasingly diverge from mortality rates at advanced ages.

As shown in *Figure 41*(*c*), the residuals of the fitted model are in general fairly small, in nearly all cases between –0.005 and 0.005. The goodness of the fit can also be seen by comparing *Figures 41*(*a*) and *41*(*b*): the patterns of contours on the two maps are quite similar. Careful comparison of *Figures 41*(*a*) and *41*(*b*) reveals that even though the absolute deviations of the fitted model from the actual data are small, the relative deviations are sometimes sizeable, especially when mortality levels are low. For instance, the actual mortality rate at age 25 in 1965 is about 0.000667; the estimated mortality rate at this age and time, however, is about 0.00150, or more than twice the actual rate. To minimize different measures of goodness of fit, different estimation procedures could be used.

The pattern of residuals in *Figure 41*(*c*) provides some clues as to how to extend the model to fit the data better. After 1926 the estimated values tend to be too large at younger ages and too small at older ones. Before 1926 the picture is

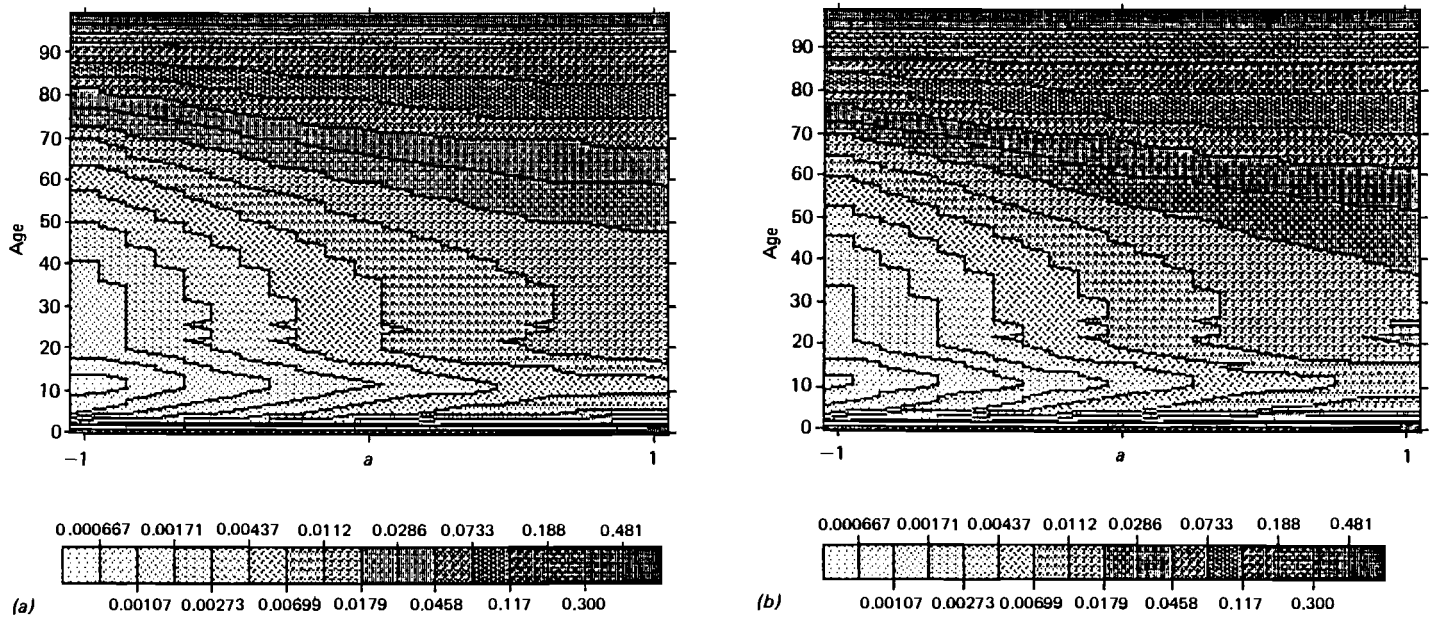

Figure 40. Force of mortality from Brass's (1971) model as a varies from −1 to +1 at intervals of 0.1, with contour lines from 0.000667 to 0.48 at multiples of 1.6 and from age 0 to 99: (*a*) $b = 0.6$; (*b*) $b = 0.8$.

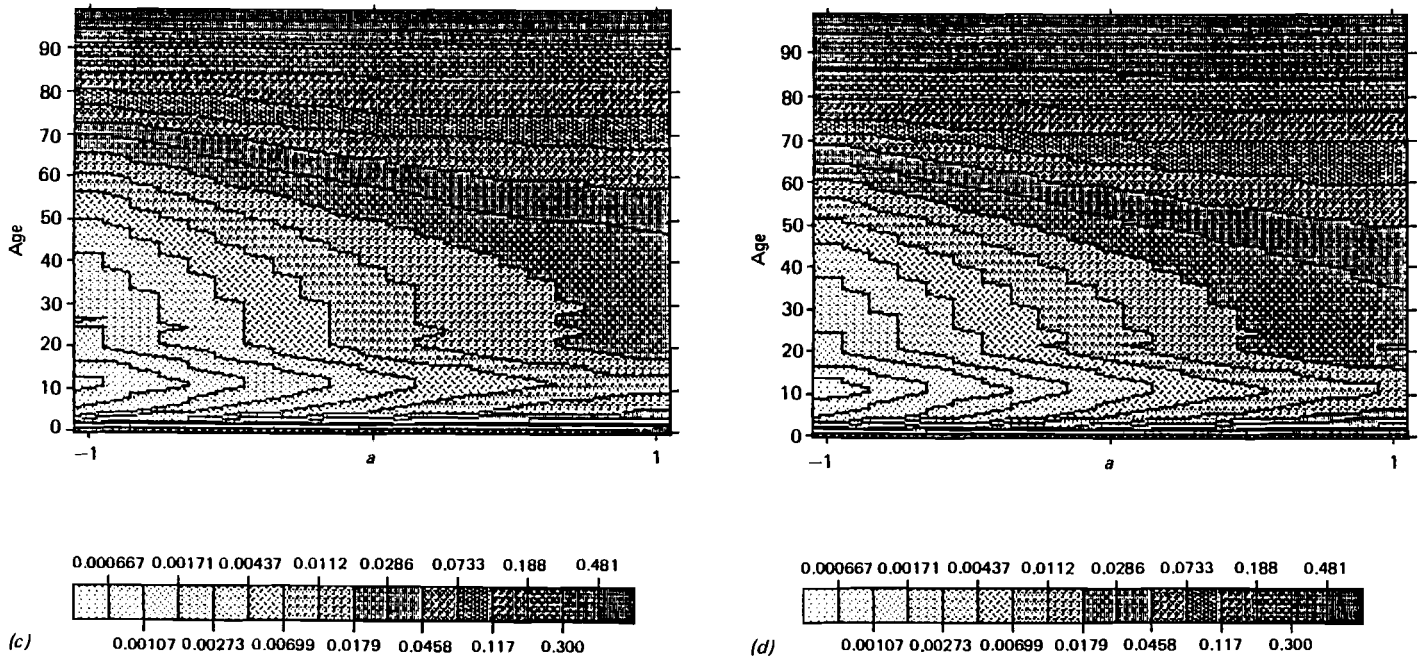

Figure 40. Force of mortality from Brass's (1971) model as a varies from −1 to +1 at intervals of 0.1, with contour lines from 0.000667 to 0.48 at multiples of 1.6 and from age 0 to 99: (*c*) $b = 1.0$; (*d*) $b = 1.2$.

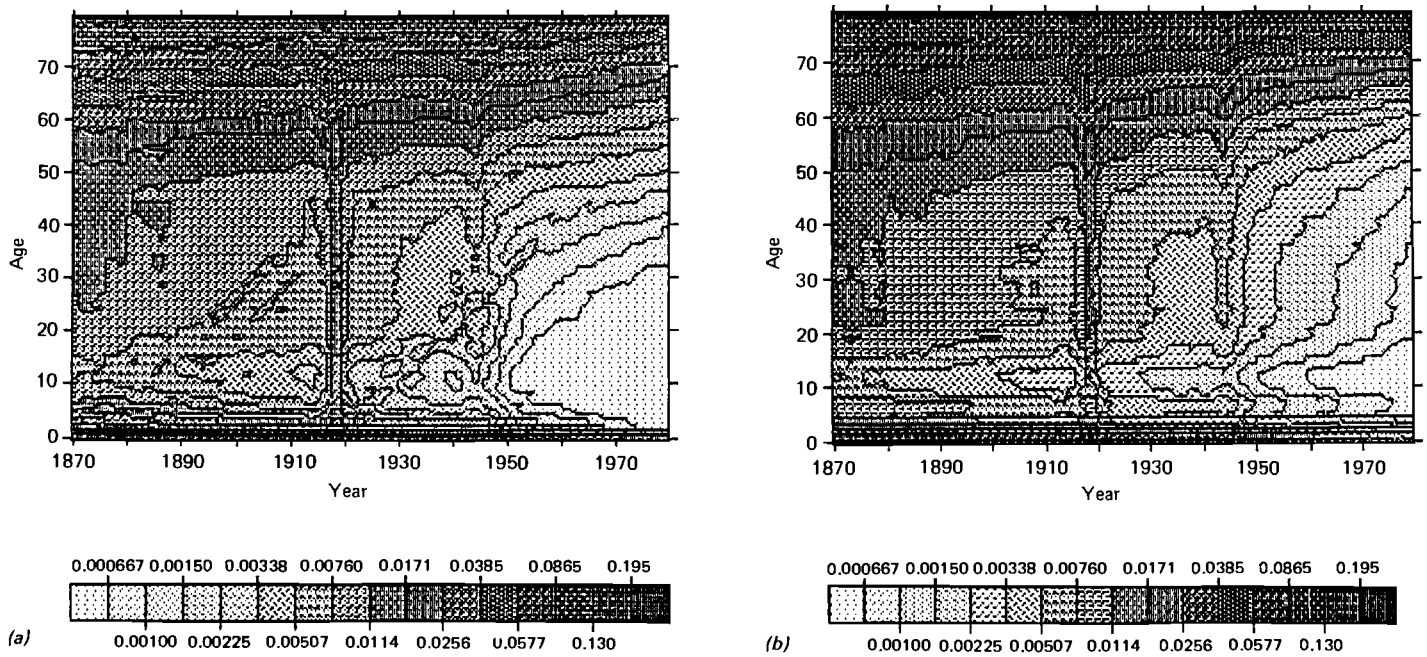

Figure 41. Italian female mortality rates: (*a*) with contour lines from 0.000667 to 0.195 at multiples of 1.5, and from age 0 to 79 and year 1870 to 1979; (*b*) as (*a*), but given by a modified Brass (1971) model.

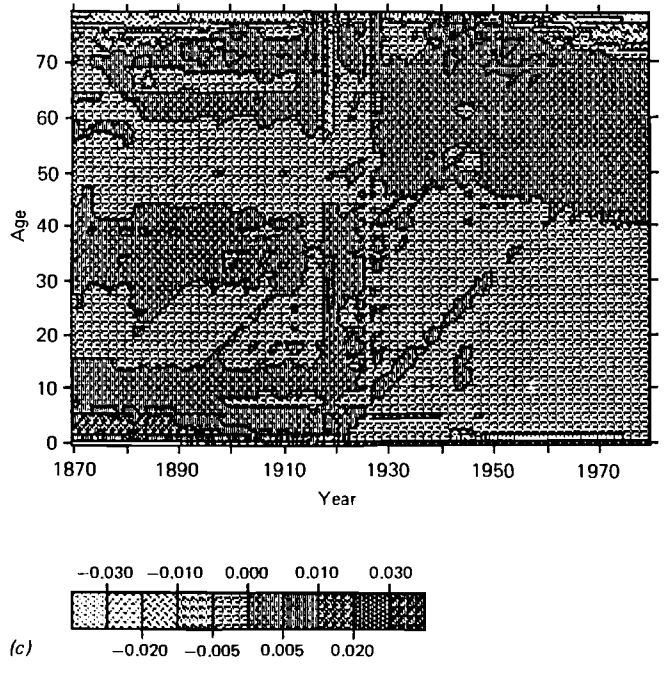

Figure 41(c). Residuals from a modified Brass (1971) model, with contour lines selectively placed from −0.03 to +0.03, and from age 0 to 79 and year 1870 to 1979.

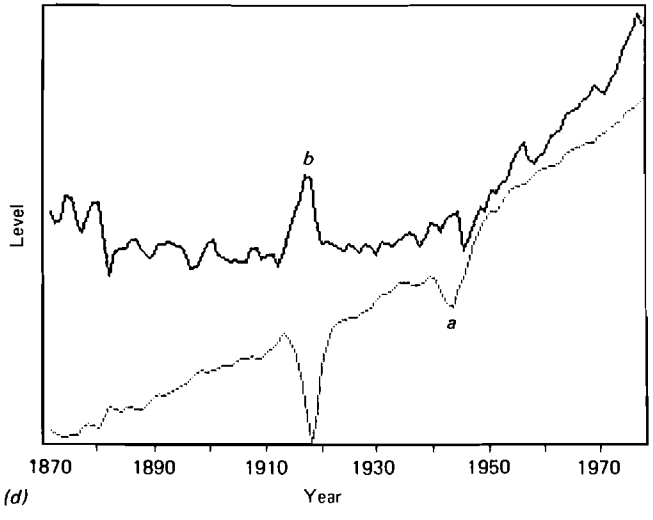

Figure 41(d). Plot of a and b used to produce Italian female mortality rates with the Brass model.

more complex, but there is some rough tendency toward the reverse pattern: the estimated values tend to be too small at younger ages and too large at older ones. Thus, there appears to be some interaction between the age and period effects on the map of residuals. Also note that between ages 15 and 25 there is a swath running across the map of residuals, which indicates the estimated values tend to be too large: the 1926 "standard" apparently does not appropriately reflect the general pattern of mortality between ages 15 and 25. Similarly, there is a darker swath, indicating underestimated values, running across the map between ages 60 and 70 or so. These systematic deviations suggest some ways the model might be improved.

The map of residuals includes several intriguing diagonal patterns, most notably two diagonals running between, roughly, ages 10 and 30, the first in the period 1890 to 1910 and the second in the period 1927 to 1950. The Brass model estimates "standard" age effects on a period by period basis; the residuals, by showing what is left after these effects are removed, provide some leads as to where cohort effects occur.

As a general strategy in exploratory data analysis and model building, it is often useful to remove age and period effects (or, more generally, the main effects along the x and y dimensions) from the data and then look at the residuals. One way of doing this is to fit a model, such as the Brass model or some other model of mortality, like the four-parameter extended Brass models proposed by Zaba (1979) and by Ewbank *et al.* (1983), or the eight-parameter model developed by Heligman and Pollard (1980). Another, more direct, approach is to simply subtract or divide out of a surface the average values for different ages and different years. Thus, the relative surfaces shown earlier in *Figures 13* through *18* can be interpreted as residual surfaces for which either a period effect or an age effect has been removed.

Figure 42(*a*)–(*d*) displays two surfaces of residuals calculated by removing both a period and an age effect: the original surface, which presents US fertility rates, was shown in *Figure 5*. *Figure 42*(*a*) shows the residuals when age and period effects are divided out; *Figure 42*(*b*) shows the residuals when these effects are subtracted out. In both cases, the period effect in any year was calculated as the average fertility rate in that year over the ages 14 through 49 (i.e., total fertility divided by 36) and the age effect was similarly calculated as the average fertility rate at some age over the period from 1917 through 1980. In the multiplicative model, estimated fertility rates are simply given by the product of the two effects, divided by the overall average fertility over all ages and years. In the additive model, the estimated fertility rates are given by the sum of the two effects, minus the overall average fertility. (The division and subtraction of overall average fertility normalizes the estimates so that the residuals center around one for the multiplicative model and around zero for the additive model.)

The residuals indicate that the multiplicative model is more informative than the additive model. The multiplicative model fits the data especially well during the ages, from 20 to 35, at which most births occur. The model also fits well during the period from about 1940 to 1955. The regular pattern of the residuals, indicating overestimates and underestimates in opposite corners, suggests that a simple extension of the model might substantially improve the fit. One way of adjusting the model to correct the errors in the corners would be to add an interaction effect

of age and time, given, say, by the product of age minus 30 and year minus 1940. Such an interaction term would have a positive value in the lower left and upper right corners and a negative one in the lower right and upper left corners.

The values of the age and period effects are shown in *Figures 42(c)* and *42(d)*. The age effect follows a remarkably regular pattern that looks much like the probability density function of the Gamma, Weibull, or log-normal distributions. Thus, it might be possible to closely fit this curve using a two-parameter function. The period effect shown in *Figure 42(d)* displays the waves of the baby booms and busts, as well as the historically low levels of fertility reached in the late 1970s. This curve is fairly regular and possibly might also be approximated by a two- or three-parameter function, perhaps one that incorporates information about prevailing social, economic, or demographic conditions.

18. Maps of Theoretical Demographical Models

To understand actual population phenomena, demographers often analyze simplified, theoretical models that capture some aspect of reality (Keyfitz, 1977). Contour maps can be used to show how some variable of interest in such models responds to changes in two of the parameters. *Figures 43* and *44* provide such illustrations.

Suppose mortality rates follow the female model West schedule of Coale and Demeny (1984). Further, suppose that a population is stable and is governed by these mortality trajectories (which can be classified by the single mortality measure $\mathring{e}_0$, life expectancy at birth) and by some growth rate r. What proportion of the population will be above age 65? The contour map in *Figure 43* displays the answer, for various values of $\mathring{e}_0$ and r; the jagged shape of the contours reflects the fact that $\mathring{e}_0$ is increased in steps of one year from 20 to 80. The two general effects are clear: the longer the life expectancy and the slower the rate of population growth, the more people above age 65. The map shows how these two effects interact. For instance, the map reveals that about 10% of a stable population will be above age 65 if either (1) life expectancy is about 23 years and the population is shrinking at 2% per year or (2) life expectancy is 80 years and the population is growing at 2% per year. If life expectancy is 80 years and the population is shrinking at 2% per year, then over a third of the population will be above 65.

As a second example, suppose that the force of mortality at any age is given by a Gompertz Curve such that $\mu(x) = ae^{bx}$. How will life expectancy at birth change as a and b vary? *Figure 44* graphically answers this question. Consider, for instance, the situation described on the middle of the right margin of the map when a is 0.00050 and b is 0.10, yielding a life expectancy of about 48 years. Cutting the mortality level by a factor of ten, i.e., reducing a to 0.00005, would increase life expectancy to 70 years. Alternatively, holding a constant but slowing the rate of aging by reducing b from 0.10 to 0.06 would have the same effect. Clearly, the effect on life expectancy of a small proportional change in the rate of mortality increase is much greater than a similar change in the level of mortality.

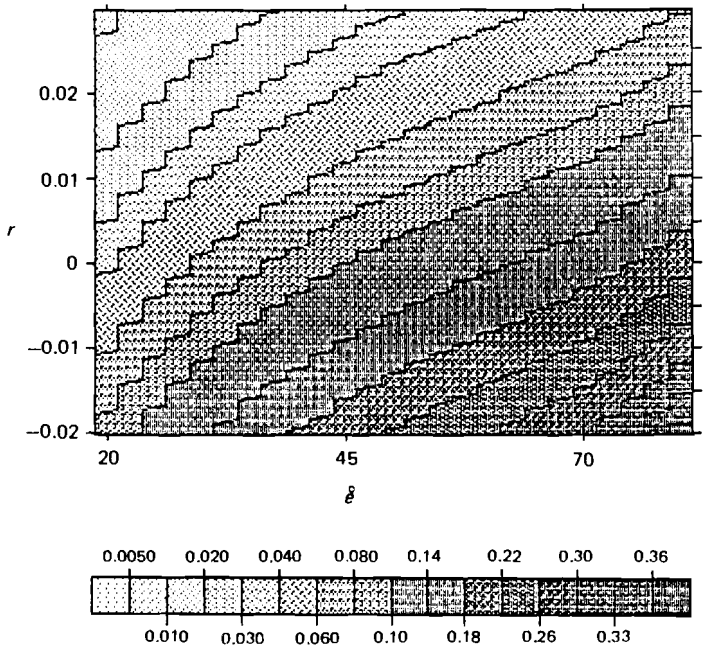

Figure 43. Proportion of people above age 65, with contour lines selectively placed from 0.005 to 0.36, and from $r = -0.02$ to 0.0295 and $\hat{e} = 20$ to 80.

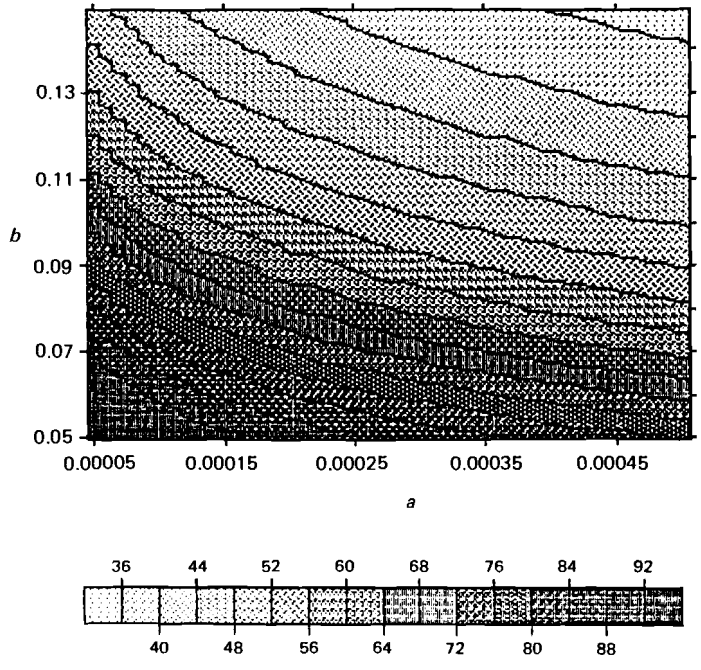

Figure 44. Changes in life expectancy at birth given by the Gompertz Curve as a and b vary, with contour lines selectively placed from 36 to 92 years of life expectancy and from $b = 0.05$ to 0.149 and $a = 0.00005$ to 0.00050.

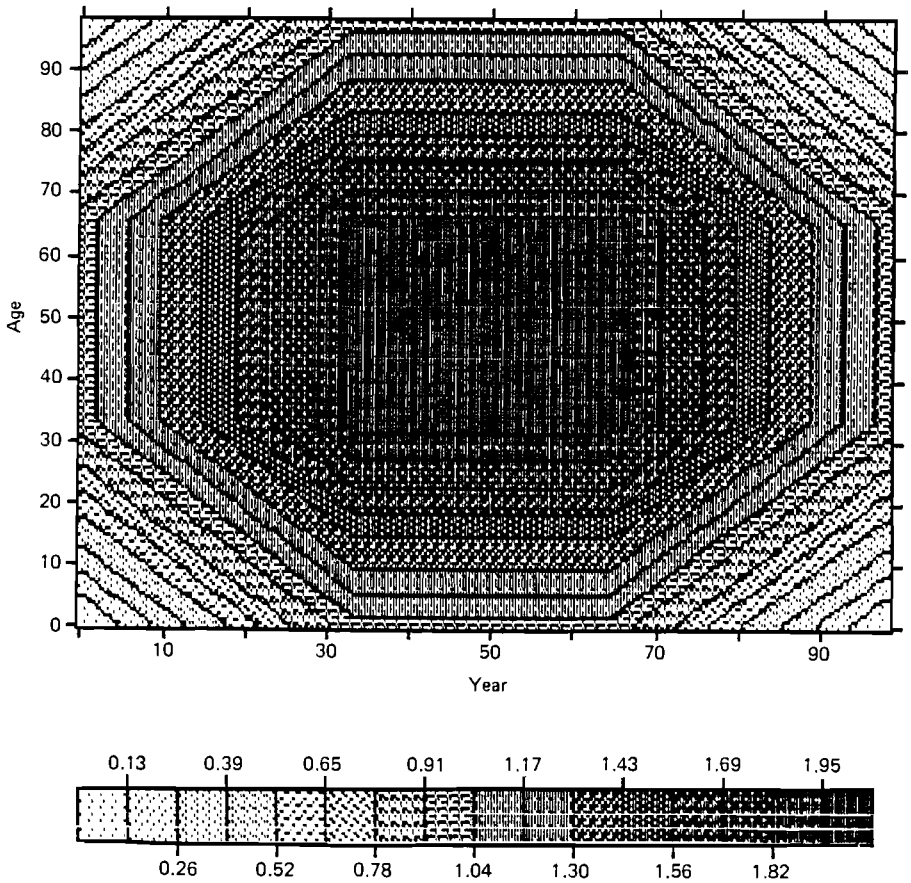

Figure 45. Interaction of age and period effects.

The maps in *Figures 45*, *46*, and *47*, which are also based on theoretical models, are designed to illustrate the contour patterns produced by the interaction of age, period, and cohort effects. Each of the three maps can be interpreted as consisting of nine separate maps. The height of the surface in *Figure 45* is simply $A + T$. A, the age effect, increases from 0 to 1 over the lowest third of the vertical axis, stays constant at 1 over the middle third, and decreases from 1 to 0 over the top third. Similarly, T, the time effect, increases from 0 to 1, stays at 1, and declines from 1 to 0 along the horizontal axis. Thus, in the center block the height of the surface is 2, as indicated by the uniform black rectangle.

The height of the surface in *Figure 46* is $A + T + C$, where C is a cohort effect that, within each of the nine blocks of the map, varies linearly from -1 to 1. For the earliest cohort in each block, which only appears in the upper left corner, the value of C is -1; for the latest cohort, which only appears in the lower right corner, the value of C is 1. Note that for the cohort born at the start of each block,

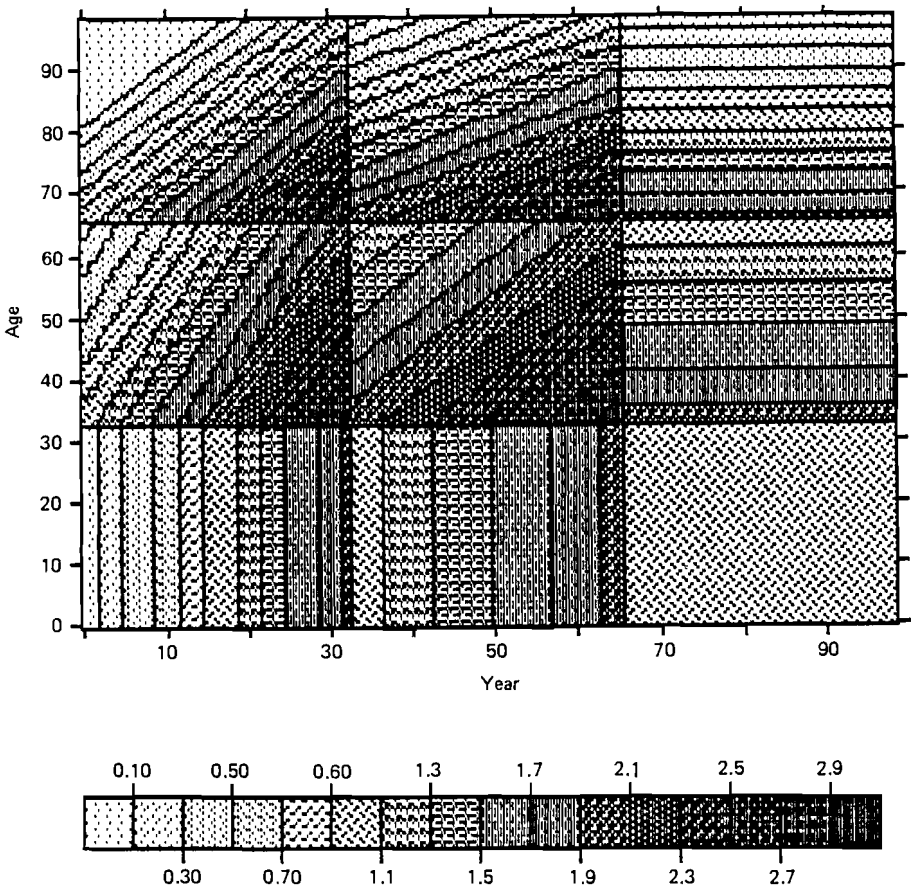

Figure 46. Interaction of age, period, and positive cohort effects.

in the lower left corner, which runs diagonally up to the upper right corner, the value of C is zero. The block in the lower right corner of the overall map has a uniform height of 1, produced by T declining from 1 to 0, A increasing from 0 to 1, and C increasing from -1 to 1: the strong age, period, and cohort effects cancel out.

The surface in *Figure 47* is similar, except that the height is now given by $A + T - C$.

The maps provide a clear, cautionary warning to demographers tempted to ascribe diagonal patterns to cohort effects, vertical patterns to period effects, and horizontal patterns to age effects. Note, for instance, that in *Figure 45*, the period–age interactions produce strong diagonals and that in *Figure 46*, the interaction of age and cohort effects with no period effect produces, in the lower central block, vertical lines, whereas the interaction of period and cohort effects with no age effect produces, in the right middle block, horizontal lines.

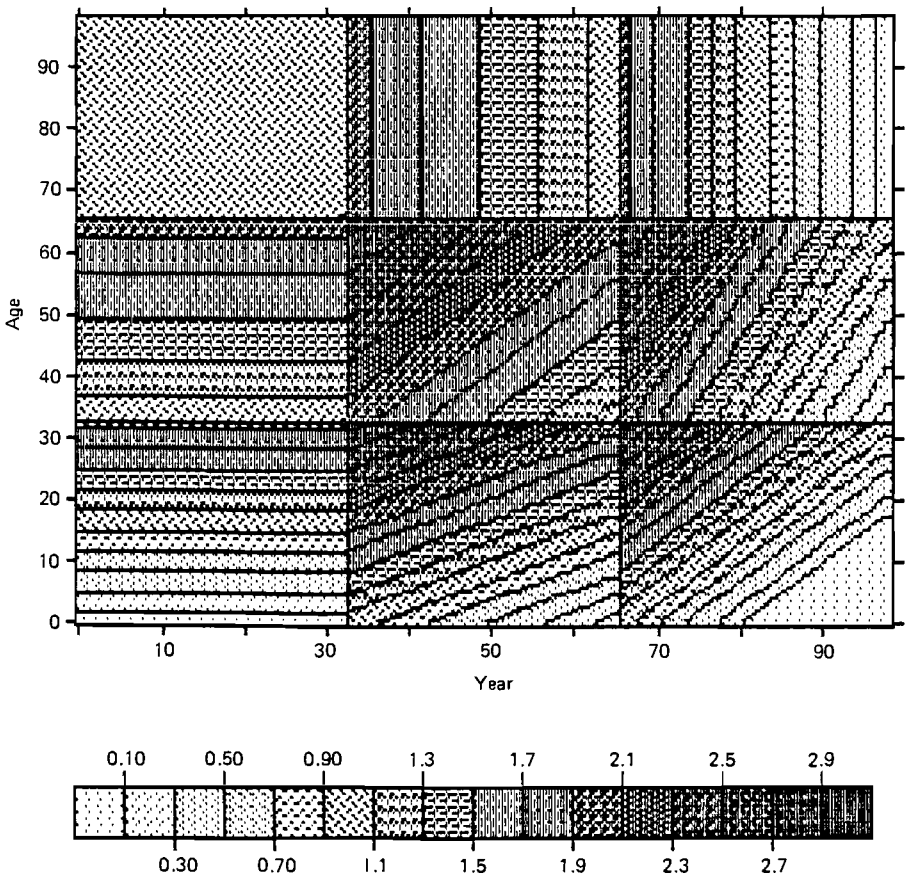

Figure 47. Interaction of age, period, and negative cohort effects.

19. Conclusion

The figures presented in this paper suggest just a few of the numerous ways that demographers can use contour maps to clearly, efficiently, and simultaneously display both persistent global and prominent local patterns in population rates or levels over two dimensions. In particular, contour maps can strikingly reveal the interaction between age, period, and cohort patterns. By using small multiples or computer movies, demographers can use the maps to gain access to several dimensions.

Even in cases where some demographic data already have been carefully scrutinized by perceptive analysts who have uncovered most of the interesting patterns, contour maps may be useful in highlighting these patterns. With contour maps, what was before understood can now be *seen*. Furthermore, the maps, by giving demographers a new perspective on data, may focus attention on some neglected aspects and patterns in even the thoroughly studied data.

Beyond efficient description, contour maps can help demographers with exploratory data analysis and with model building. Surfaces can be computed relative to some part of the surface or to another surface; and different surfaces can be placed next to each other and compared. The patterns produced by a model can be displayed as can the fit of the model to some empirical data.

The resulting contour maps can be displayed not only as printed output but also on a computer monitor. The shades used in most of the maps presented in this paper range from black to light grey, but the maps can be produced in glowing colors, on a color computer monitor or using a color printer, as illustrated by the two color maps included in this report and by the maps on the diskette available from IIASA: the effects are dramatic. Also impressive is the speed with which a computer can draw a map. A large computer is not needed—we have used a standard IBM PC with 128K of memory.

Tufte, in his lucid exposition of *The Visual Display of Quantitative Information* (1983), concludes that graphic designs should give "visual access to the subtle and difficult, that is, the revelation of the complex." Demographic surfaces can be particularly complex. A mortality surface, for example, might be defined over nearly a century of age and more than a century of time, comprising close to 10000 data points that may vary over four orders of magnitude. Contour maps are a striking, efficient, and clear means of giving demographers visual access to such surfaces.

William Playfair (1801), the pioneer of graphical methods for presenting statistical data, argued that with a good visual display "as much information may be obtained in five minutes as would require whole days to imprint on the memory, in a lasting manner, by a table of figures." The 80 or so Lexis maps in this research report summarize about half a million data points in a memorable, revealing manner.

References

Arthur, W.B. and Vaupel, J.W. (1984), Some general relationships in population dynamics, *Population Index*, **50**(2), 214–226.

Bennett, N.G. and Horiuchi, S. (1981), Estimating the completeness of death registration in a closed population, *Population Index*, **47**(2), 207–221.

Berg, F.T. (1860), *Befolknings Statistik 1856–1860* (Central Bureau of Statistics, Stockholm).

Brass, W. (1971), On the scale of mortality, in W. Brass (Ed), *Biological Aspects of Demography*, pp 69–110 (Taylor and Francis Ltd, London).

Caselli, G., Vaupel, J.W., and Yashin, A.I. (1985a), *Mortality in Italy: Contours of a Century of Evolution*, Collaborative Proceedings CP-85-24 (International Institute for Applied Systems Analysis, Laxenburg, Austria). Also in *Genus*, **41**(1–2), 39–55.

Caselli, G, Vallin J., Vaupel, J.W., and Yashin, A.I. (1985b), L'évolution de la structure par age de la mortalité en Italie et en France depuis 1900: effets de période et effets de génération. Forthcoming in *Espace Population et Société*.

Coale and Demeny (1984), Regional Model Life Tables and Stable Populations, 2nd edn (Academic Press).

Coale, A.J. and Kisker, E.E. (1985), *Mortality Crossovers: Reality or Bad Data?*, paper presented at the annual meeting of the Population Association of America, Boston.

Delaporte, P. (1941), *Evolution de la mortalité en Europe depuis l'origine des statistiques de l'Etat civil (Tables de mortalité de generations)* (Imprimerie Nationale,Paris).

Dupaquier, J. and Dupaquier, M. (1985), *Histoire de la Démographie*, pp. 388–389 (Perrin, Paris).

Ewbank, D.C., Gomez de Leon, J.C., and Stoto, M.A. (1983), A reducible four-parameter system of model life tables, *Population Studies*, **37**(1), 105–127.

Faber, J.F. (1982), *Life Tables for the United States: 1900–2050*, Actuarial Study No. 87, US Department of Health and Human Services, SSA Pub. No. 11-11534, September.

Federici, N. (1955), *Lezioni di Demografia*, 1 Edizione (De Santis, Roma).

Fisher, H.T. (1982), *Mapping Information: The Graphic Display of Quantitative Information* (Abt Books, Cambridge, MA).

Gateva, N. (1985), *Heterogeneity Dynamics of Spatial Population System*, Unpublished manuscript (International Institute for Applied Systems Analysis, Laxenburg, Austria).

Gambill, B.A., Vaupel, J.W., and Yashin, A.I.(1986), *The LEXIS Computer Program for Creating Shaded Contour Maps of Demographic Surfaces*, Working Paper WP-86-37 (International Institute for Applied Systems Analysis, Laxenburg, Austria).

Heligman, L. and Pollard, J.H. (1980), The age pattern of mortality, *Journal of the Institute of Actuaries*, **107**(I), 49–80.

Heuser, R.L. (1976), *Fertility Tables for Birth Cohorts by Color, United States, 1917–1973* (US Department of Health, Education, and Welfare, National Center for Health, Statistics, Washington).

Heuser, R.L. (1984), *Fertility Tables for Birth Cohorts by Color, United States, 1917–1980* (US Department of Health Education, and Welfare, National Center for Health Statistics, Washington).

Kermack, W., McKendrick, A., and McKinlay, P. (1934), Death-rates in Great Britain and Sweden: some general regularities and their significance, *The Lancet*, March 31, 698–703.

Keyfitz, N. (1977), *Applied Mathematical Demography* (John Wiley & Sons, New York).

Keyfitz, N. and Flieger, W. (1968), *World Population: An Analysis of Vital Data* (University of Chicago Press, Chicago).

Lexis, W. (1875), *Einleitung in die Theorie der Bevölkerungsstatistik* (Truebner, Strasbourg).

Lexis, W. (1880), La representation graphique de la mortalité au moyen de points mortuaires, *Annales de Démographie Internationale*, IV, 297–324.

Lotka, A.J. (1926), The progressive adjustment of age distribution to fecundity, *Journal of the Washington Academy of Sciences*, **16**, 317.

Lotka, A.J. (1931), The structure of a growing population, *Human Biology* **3**(4), 459–93.

Mosteller, F. and Tukey, J.W. (1977), *Data Analysis and Regression: A Second Course in Statistics* (Addison–Wesley, Reading, MA).

Natale, M. and Bernassola, A. (1973), *La mortalita per causa nelle regioni italiane, Tavole per contemporanei 1965–66 e per generazioni 1790–1969* n. 25 (Istituto di Demografia, Universita di Roma, Roma).

Perozzo, L. (1880), Della rappresentazione grafica di una collettivita di individui nella successione del Tempo, e in particolare dei diagrammi a tre coordinate, *Annali di Statistica*, Series 2a, Volume 12 (Ministry of Agriculture, Industry and Commerce, Rome).

Playfair, W. (1801), *The Commercial and Political Atlas*, 3rd ed, p. xii (J. Wallis, London). Quoted in Schmid, C.A. and Schmid, S.E. (1979), *Handbook of Graphic Presentation*, 2nd ed, New York).

Preston, S.H. and Coale, A.J. (1982), Age structure, growth, attrition, and accession: a new synthesis, *Population Index*, **48**(2), 217–259.

Preston, S.H. and van der Walle, E. (1978), Urban French mortality in the nineteenth century, *Population Studies*, **32**(2), 275–297.

Preston, S.H., Keyfitz, N., and Schoen, R. (1972), *Causes of Death: Life Tables for National Populations* (Seminar Press, New York).

Scherbov, S., Yashin, A.I., and Grechucha, V. (1986), *Dialog System for Modeling Multidimensional Demographic Processes*, Working Paper WP-86-29 (International Institute for Applied Systems Analysis, Laxenburg, Austria).

Statistics Sweden (1881–1981), *Swedish Statistical Yearbooks* (Stockholm, Sweden).

Tremblay, M. (1985), *Linguistic Mobility: Observation, Measurement and Mechanisms*, Unpublished manuscript (International Institute for Applied Systems Analysis, Laxenburg, Austria).

Tufte, E.R. (1983), *The Visual Display of Quantitative Information* (Graphica Press, Cheshire, CT).

Tukey, J.W. (1977), *Exploratory Data Analysis* (Addison-Wesley, Reading, MA).

Vallin, J. (1973), *La mortalité par generation en France, depuis 1899*, Travaux et Documents, Cahier n. 63 (Press Universitaires de France, Paris).

Vaupel, J.W. and Gowan, A.E. (1986), Passage to Methuselah: some demographic consequences of continued progress against mortality, *American Journal of Public Health*, **76**(4), 430–433.

Vaupel, J.W. and Owen, J.M. (1985), Anna's life expectancy, *American Demography*, **7**(11), 36–39.

Vaupel, J.W., Manton, K.G., and Stallard, E. (1979), The impact of heterogeneity in individual frailty on the dynamics of mortality, *Demography*, **16**(3), 439–454.

Veys, D. (1983), *Cohort Survival in Belgium in the Past 150 Years* (Catholic University of Leuven, Sociological Research Institute, Leuven, Belgium).

Wilmoth, J. (1985), *Identifiable Age, Period, and Cohort Effects: An Exploratory Approach Applied to Italian Female Mortality*, Working Paper WP-85-69 (International Institute for Applied Systems Analysis, Laxenburg, Austria).

Wunsch, G.J. and Termote, M.G. (1978), *Introduction to Demographic Analysis: Principles and Methods* (Plenum Press, New York and London).

Yi, Z., Vaupel, J.W., and Yashin, A.I. (1985), Marriage and fertility in China: a graphical analysis, *Population and Development Review*, **11**, 721–736.

Zaba, B. (1979), The four-parameter logit life-table system, *Population Studies*, **33**(1), 79–100.

About the Authors

James W. Vaupel and *Anatoli I. Yashin* are research scholars and *Bradley A. Gambill* is a research assistant in the Population Program, led by Nathan Keyfitz, at the International Institute for Applied Systems Analysis (IIASA) in Laxenburg, Austria. Vaupel is also Professor of Public Affairs and Planning at the University of Minnesota, USA; Yashin is a senior researcher at the Institute for Control Sciences in Moscow, USSR; and Gambill is a student at Duke University, USA.